AD-A086 948 JOHNS HOPKINS UNIV LAUREL MD APPLIED PHYSICS LAB F/G 5/2
INDIRECTLY FUNDED RESEARCH AND EXPLORATORY DEVELOPMENT AT THE A--ETC(U)
DEC 79 R W HART N00024-78-C-5384
UNCLASSIFIED JHU/APL/SR-79-2 NL

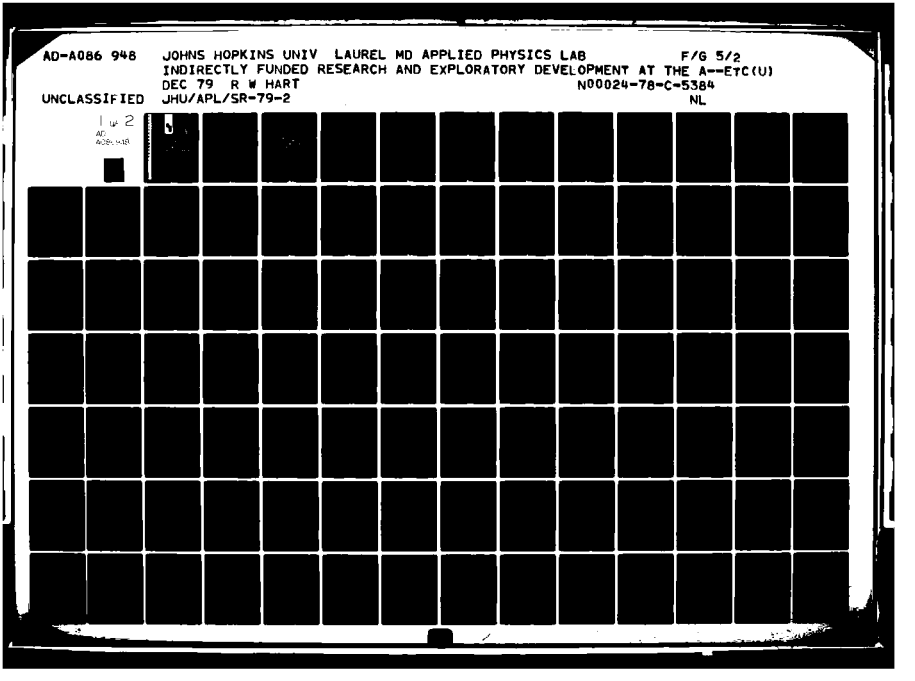

JHU/APL
SR 79-2
DECEMBER 1979

Special Reports

INDIRECTLY FUNDED RESEARCH AND EXPLORATORY DEVELOPMENT AT THE APPLIED PHYSICS LABORATORY

FISCAL YEAR 1978

THE JOHNS HOPKINS UNIVERSITY ■ APPLIED PHYSICS LABORATORY

Unclassified

SECURITY CLASSIFICATION OF THIS PAGE

PLEASE FOLD BACK IF NOT NEEDED FOR BIBLIOGRAPHIC PURPOSES

REPORT DOCUMENTATION PAGE

1. REPORT NUMBER	2. GOVT ACCESSION NO	3. RECIPIENT'S CATALOG NUMBER
JHU/APL/SR-79-2	AD-A086 948	

4. TITLE (and Subtitle)

INDIRECTLY FUNDED RESEARCH AND EXPLORATORY DEVELOPMENT AT THE APPLIED PHYSICS LABORATORY, FISCAL YEAR 1978.

A070 351

5. TYPE OF REPORT & PERIOD COVERED

Annual Report.
1 Jan - 31 Dec 78

6. PERFORMING ORG. REPORT NUMBER

7. AUTHOR(s)

R. W. Hart, Editor

8. CONTRACT OR GRANT NUMBER(s)

N00024-78-C-5384

9. PERFORMING ORGANIZATION NAME & ADDRESS

The Johns Hopkins University Applied Physics Laboratory
Johns Hopkins Rd.
Laurel, MD 20810

10. PROGRAM ELEMENT, PROJECT, TASK AREA & WORK UNIT NUMBERS

X8

11. CONTROLLING OFFICE NAME & ADDRESS

Naval Plant Representative Office
Johns Hopkins Rd.
Laurel, MD 20810

12. REPORT DATE

1 January - 31 December 1978

13. NUMBER OF PAGES

170

14. MONITORING AGENCY NAME & ADDRESS

Naval Plant Representative Office
Johns Hopkins Rd.
Laurel, MD 20810

11 Dec 78

15. SECURITY CLASS. (of this report)

Unclassified

15a. DECLASSIFICATION/DOWNGRADING SCHEDULE

NA

16. DISTRIBUTION STATEMENT (of this Report)

Approved for public release; distribution unlimited.

12 167

17. DISTRIBUTION STATEMENT (of the abstract entered in Block 20, if different from Report)

18. SUPPLEMENTARY NOTES

19. KEY WORDS (Continue on reverse side if necessary and identify by block number)

Basic research
Fundamental research
Indirectly funded research
Research Center annual report

20. ABSTRACT (Continue on reverse side if necessary and identify by block number)

This report summarizes the Indirectly Funded Research and Exploratory Development activities of The Johns Hopkins University Applied Physics Laboratory during fiscal year 1978 (1 January - 31 December 1978).

DD FORM 1 JAN 73 1473

Unclassified

SECURITY CLASSIFICATION OF THIS PAGE

JHU/APL
SR 79-2
DECEMBER 1979

Special Reports

INDIRECTLY FUNDED RESEARCH AND EXPLORATORY DEVELOPMENT AT THE APPLIED PHYSICS LABORATORY

FISCAL YEAR 1978

R. W. HART, Editor

THE JOHNS HOPKINS UNIVERSITY ■ APPLIED PHYSICS LABORATORY
Johns Hopkins Road, Laurel, Maryland 20810
Operating under Contract N00024-78-C-5384 with the Department of the Navy

ABSTRACT

This report summarizes the Indirectly Funded Research and Exploratory Development activities of The Johns Hopkins University Applied Physics Laboratory for fiscal year 1978 (1 January 1978 — 31 December 1978).

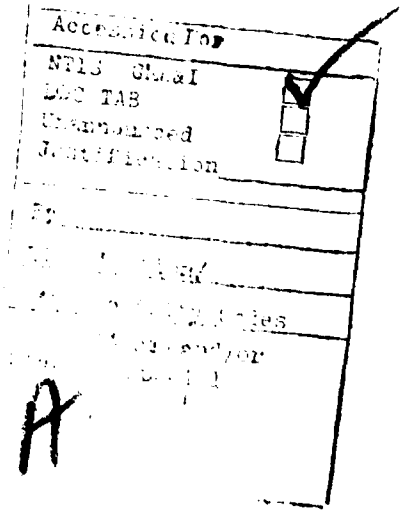

CONTENTS

INTRODUCTION

This section is a brief explanation of the compilation of this report, the purpose of the Indirectly Funded Research and Development (IR&D) Program, and the relationships of that program to the administrative structure of the Laboratory.

ORGANIZATION OF THE REPORT

The report is organized in two parts. The first part summarizes the IR&D work of the Research Center, which is the Division of the Laboratory devoted primarily to long-term scientific research. The second part summarizes the IR&D activities carried out in other, generally more applications-oriented, groups of the Laboratory.

PURPOSE OF THE IR&D PROGRAM

The Trustees of the University have summarized the role of APL as follows:

> "The general purpose of The Johns Hopkins University is public service through education, research, and the application of knowledge to human affairs. As part of the University, the Applied Physics Laboratory shares this purpose through the application of science to the enhancement of the security of the United States and basic research to which its facilities can make an especially favorable contribution."

The manner and extent to which the Laboratory fulfills this purpose are determined largely by the capabilities of the staff and the tasks that funding agencies support. Most of the Laboratory's activities are devoted to applications-oriented engineering research and development tasks. However, such tasks do not generally provide the means either to develop new capabilities in frontier areas of technology or to pursue basic research. The central purpose of the IR&D Program at APL is to support these capabilities, thereby enhancing the ability of the Laboratory to fulfill its purpose.

Since the support of national defense objectives is the major concern of the Laboratory, the central purpose of the IR&D Program is in accord with the primary aim of IR&D/B&P programs as stated in DoD Directive 5100.66, i.e., to assure the creation of an environment that encourages the development of innovative concepts for defense systems and equipment that complement and broaden the spectrum of concepts developed internally by DoD.

At the research level, military and civilian problem areas frequently overlap; thus, in accordance with its dedication to the application of science to areas where its facilities can make an especially favorable contribution, APL works for civilian as well as military agencies. These include the National Aeronautics and Space Administration (NASA), the National Institutes of Health (NIH), the Departments of Energy, Commerce, Transportation, and Interior, the Veterans Administration (VA), and the State of Maryland.

RELATIONSHIPS TO ADMINISTRATIVE STRUCTURE

The Director of the Laboratory defines the general objectives of the IR&D Program, authorizes the overall level of effort, establishes the relative levels of Research Center and Laboratory-wide efforts, and approves the program plan. The Research Center is an administrative division that has been devoted to scientific research since it was formed in 1947. Its IR&D Program is administered by the Chairman of the Research Center, who is responsible directly to the Director of the Laboratory for the planning and execution of the center's activities. The remaining, Laboratory-wide component is administered by the Assistant Director for Exploratory Development (currently also the Chairman of the Research Center). He is responsible to the Director and is assisted by an Oversight Committee comprised of high-level representatives of major administrative units of APL to assure that the activities are responsive to the needs of the Laboratory and that necessary staff and facility commitments can and will be made.

INDIRECTLY FUNDED RESEARCH AND DEVELOPMENT IN THE RESEARCH CENTER

The Research Center is a window into science for the Laboratory and thereby develops in-depth understanding in fields of concern to the Laboratory.

The IR&D Program, at a level of effort of about 29 man-years/year, is an integral part of the Research Center's activities. The Research Center maintains a permanent staff of 54, augmented by several postdoctoral appointees and graduate students, and also by many collaborators at other institutions. Results are disseminated primarily by the publication of scientific papers in the professional literature, by participation in regional, national, and international meetings, workshops, and symposia, and by internal seminars and reports. During the present fiscal year, 50 papers appeared in refereed journals or books and 25 others were accepted for publication.

Several nontechnical facets of the Research Center's activities during the present reporting period are of special interest. In the area of applied mathematics, the work on eigenvalue approximation has stimulated wide interest. Dr. D. W. Fox, Supervisor of the Research Center's Applied Mathematics Group, was invited to participate in the Conference on Mathematical Properties of Wave Functions, held at the University of Bielfield, Bielfield, Federal Republic of Germany, where he gave an invited address on 30 November, "Lower Bounds for Energy Levels of Atoms;" he also gave five invited talks at other European universities. Also, Dr. J. C. W. Rogers was invited to spend a month at the Institut de Recherche d'Informatique et d'Automatique where he presented several talks that are to be published in the journal, Analyse et Contrôle des Systèmes.

The work in chemical physics also has continued to evoke wide interest. In the area of theory of molecular structure and reactivity, eight investigators at other institutions contributed their efforts, collaborating primarily with Dr. D. M. Silver (Supervisor of the Chemical Physics Group) in work described in a dozen joint papers that were published during the fiscal year. Dr. Josef Stricker of the Technion Israel Institute of Technology spent his sabbatical term investigating excited oxygen with Dr. J. G. Parker of the Chemical Physics Group.

With respect to the topics of optical physics and chemistry, in the molecular photophysics area, Dr. F. J. Adrian (Supervisor of the Microwave Physics Group) was cochairman, along with Professor J. K. S. Wan of Queen's University, Kingston, Canada, of an International Workshop in Chemically Induced Magnetic Polarization held 7-10 June 1978 in the Chemistry Department of Queen's

University. He also presented one of the plenary lectures and is guest editor of a special edition of Reviews of Chemical Intermediates devoted to the workshop. Dr. J. C. Murphy (of the Microwave Physics Group) was one of four specially selected and invited speakers for the Opto/Photoacoustic Spectroscopy and Detection Conference to be held August 1979 at the Iowa State University, and the University of Sheffield (United Kingdom) has arranged to send a graduate student here next year on a several months' fellowship to work under Dr. Murphy and Dr. L. C. Aamodt.

In the area of solid-state physics, the organic and electrolyte work led to Navy/Army-funded materials projects, and the silicon film semiconductor work led to a DOE-funded solar cell project. Dr. G. Jones, from the University of Lancaster, England, spent the year with the Research Center's Solid-State Physics Group as a postdoctoral fellow working on transition metal boride layers.

With respect to wave propagations, Dr. R. A. Farrell (Supervisor of the Theoretical Problems Group) and Mr. R. McCally were invited by the International Society for Eye Research to describe their recent work on depolarized corneal light scattering to the Third International Congress of Eye Research held in Osaka, Japan.

It is also noteworthy that Dr. V. O'Brien (Theoretical Problems Group) served as an advisor to the postdoctoral research associates program of the National Research Council. She served on the panel for engineering and applied sciences, on the review board, and on the site evaluation committee for the program at the Aberdeen Proving Ground (APG) Ballistic Research Laboratory. Mr. B. F. Hochheimer (Excitation Mechanisms Group) participated in and presented an invited lecture to the National Research Council's Committee on Vision Workshop on Ocular Safety and Eye Care.

Three doctoral dissertations were completed this year under the supervision of Research Center researchers. Dr. J. A. Krill (APL Fleet Systems Department) completed his Ph.D. dissertation in Electrical Engineering at the University of Maryland as part of the Research Center's wave propagation project under Dr. Farrell. Dr. R. E. Terry (graduate student at The Johns Hopkins University) completed his dissertation in plasma physics under the supervison of Dr. E. P. Gray. Dr. G. W. Turner (a former APL graduate fellow) completed his Ph.D. dissertation in electronic and optical properties of amorphous boride thin films as part of the Research Center's semiconductor physics program.

MATHEMATICAL SCIENCES

APPLIED MATHEMATICS

In the field of applied mathematics, significant results are obtained for the temporal decay of solutions of the Navier-Stokes equation in cylindrical channels and for perturbations of eigenvalues of Hemitian matrices (Refs. 1 and 2). The two investigations are discussed in the following articles.

TEMPORAL DECAY OF NAVIER-STOKES FLOW IN CYLINDRICAL CHANNELS

Problem

The problem of entry flow development at the inlet region of channels or pipes is a classic problem of flow theory that has received much attention in the past. However, most of the previous work involved some degree of simplification either in flow geometry or in the governing equations. We treat the problem within the general framework of the Navier-Stokes equations governing the time-dependent flow of an incompressible viscous fluid in a cylindrical channel of arbitrary cross section. This estimate tells how fast (at the least) the energy of a disturbance at the inlet of a pipe decays. For steady-state laminar flows, the estimate leads to an upper bound on the "entrance length," which is defined as the distance through which an entrance flow develops a profile that differs from the fully developed profile by no more than 1%.

Objective

The objective was to develop an expression for the exponential decay of an energy functional of solutions of the time-dependent Navier-Stokes equations in cylindrical channels. The decay function is in terms of the distance from a fixed reference plane at the channel inlet. Since we assume that the initial velocity is 0 and that the velocity vanishes on the boundary of the flow region except on the intersection of the region with the reference plane, our result gives information on the downstream decay of the effect of a disturbance at the inlet region in the rest state. The decay constant depends only on the geometry of the flow region, although in a somewhat complicated manner.

Approach

The technique used here was used by Edelstein (Ref. 3) and Sigillito (Ref. 4) to study the spatial decay of solutions of the heat equation. The general approach is to derive a first-order differential inequality, with initial conditions, that is satisfied by the energy function. Solution of this differential inequality yields the exponential decay function. In the present work, substantial technical complications arose due to the necessity of estimating an integral of the pressure. We found a device first introduced by Payne (Ref. 5) to be very useful in dealing with this question.

Program

Consider the Navier-Stokes equations,

$$\dot{\underline{u}} \equiv \underline{u}_t + \underline{u} \cdot \text{grad } \underline{u} = \nu \Delta \underline{u} - \rho^{-1} \text{ grad } p$$

$$\text{div } \underline{u} = 0$$

where $\underline{u}$ is the velocity vector, p is the pressure, ρ is the density, and ν is the kinematic viscosity. We will consider the solutions of these equations in $R_o X[0,T]$ where R_o (see below) is a three-dimensional region bounded in part by a planar region C_o. Suppose that C_s is the intersection with R_o of the plane parallel to C_o and at a distance S from C_o. Define the energy-like functional

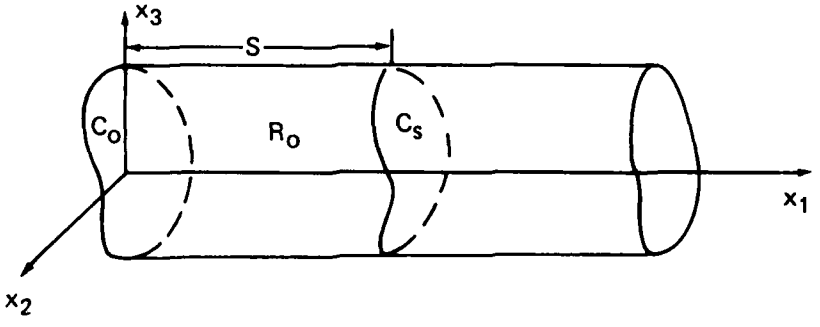

$$U(s,t) = \int_0^t \int_{R_s} (\rho|\dot{\underline{u}}|^2 + \mu|\text{grad } \underline{u}|^2)\,dV d\tau ,$$

then our result shows that there is a positive constant $K = K(R_o,\rho,\mu)$ such that

$$U(s,T) \leq U(o,t)e^{-Ks} \qquad (0 \leq t \leq T).$$

PERTURBATIONS OF HERMITIAN MATRICES AND THEIR EIGENVALUES

Problem

Suppose A and B are the Hermitian matrices on a complex space X and the eigenvalue problem $Ax - \lambda Bx = 0$ makes good sense, as for instance when B is positive-definite. An important problem in computational matrix algebra is to find estimates for the changes in the eigenvalues when A changes by δA and B by δB, where δA and δB are Hermitian.

Objective

The purpose of this study is to improve the methods and the understanding of the nature of the bounds by finding the quantities that are of intrinsic importance. Here these turn out to be relative changes in the quadratic forms of the matrices.

Approach

In discussing this question, the Hermitian forms $A(x,y) = \langle Ax,y\rangle$, $B(x,y) = \langle Bx,y\rangle$, and the inner product $\langle x,y\rangle$ arise naturally. However, the estimates that we obtained are expressed in terms of the forms A, B, δA, and δB alone, and so it has seemed appropriate to formulate the analysis mainly in terms of these forms.

Progress

We introduce the idea of a quasi-definite pair of Hermitian forms and then show (a) that this property is equivalent in finite dimensional spaces to that of <u>definiteness</u> used by Crawford (Ref. 6) and Stewart (Ref. 7) for relative matrix eigenvalue problems and (b) that it ensures that the finite dimensional problems make sense.

A central device in this work is the use of angles to characterize eigenvalues and the maximum-minimum and minimum-maximum characterization of these angles.

The principal results are summarized by the following proposition:

> Let $\overline{A} = \underline{A} + \delta A$ and $\overline{B} = B + \delta B$. If $[A,B]$ is definite, then $[\overline{A},\overline{B}]$ is also quasi-definite provided $D(X) < 1$.

Theorem: Assume $[\underline{A},\underline{B}]$ is quasi-definite and $D(X) < 1$. Then the following bounds hold for the eigenvalues:

$$\delta\theta_i = \tan^{-1}\overline{\lambda}_i - \tan^{-1}\lambda_i - \sin^{-1}D(Y_{n-i+1})$$

$$\leq \delta\theta_i \leq \sin^{-1}D(X_i), \quad i = 1,2,\ldots,n,$$

where Y_{n-i+1} and X_i are minimizing and maximizing subspaces in the classical minimum-maximum and maximum-minimum characterization of eigenvalues.

A weaker but simpler result is given by the corollary:

$$|\delta\theta_i| \leq \max_{x\in X} \left(\frac{[\delta A(x)]^2 + [\delta B(x)]^2}{[A(x)]^2 + [B(x)]^2} \right)^{\frac{1}{2}}.$$

These estimates for the perturbations of eigenvalues are "best possible" and improve those of Stewart (Ref. 7).

Principal Investigators: Dr. D. W. Fox, Supervisor, and Dr. V. G. Sigillito, senior mathematician, the Applied Mathematics Group of the Research Center; Prof. A. R. Elcrat, Department of Mathematics, Wichita State University. Dr. Elcrat is not funded by the IR&D Program.

References

1. A. R. Elcrat and V. G. Sigillito, "A Spatial Decay Estimate for the Navier-Stokes Equations," J. Appl. Math. Anal. (to be published).

2. D. W. Fox, "Changes in Relative Matrix Eigenvalues," Proc. Symp. Inf. Linkage between Appl. Math. Ind., Monterey, CA, Feb 1978.

3. W. S. Edelstein, "A Spatial Decay Estimate for the Heat Equation," ZAMP (Z. Angew. Math. Phys.), Vol. 20, 1969, pp. 900-906.

4. V. G. Sigillito, "On the Spatial Decay of Solutions of Parabolic Equations," ZAMP (Z. Angew. Math. Phys.) Vol. 21, 1970, pp. 1078-1081.

5. L. E. Payne, "Uniqueness Criteria for Steady State Solutions of the Navier-Stokes Equations," Atti del Simp. Inter sulle Appl. dell Anal. alla Fis. Mat., Vol. 28, 1964, pp. 130-153, Cagliari-Sassari.

6. C. R. Crawford, "A Stable Generalized Eigenvalue Problem," SIAM J. Math. Anal., Vol. 13, 1976, pp. 860-864.

7. G. W. Stewart, "Perturbation Theory for the Definite Generalized Eigenvalue Problem," University of Maryland Computer Science Technical Report TR-479, 1976.

MATHEMATICAL HYDRODYNAMICS

A well-known study of the linear theory of wake collapse in a stratified fluid is reexamined here for a special case for which the solution can be given in an integral form of sufficient simplicity that the behavior can be analyzed.

Problem

The question under study is the behavior of two-dimensional models of "wake collapse" in the linear theory of buoyant flow. These models abstract the situation existing after the rapid passage of a body causes local mixing in a stratified fluid such as the ocean. The importance of such models lies in their usefulness in studying the detection of submarine wakes.

Objective

The purpose of this study is to obtain and examine in detail a number of simple solutions to wake collapse problems. In particular, some conclusions reached by Hartman and Lewis (Ref. 1) are reexamined.

Approach

In their studies, Hartman and Lewis found a series solution for a wake collapse of a density disturbance with a circular cross section. By using certain limiting arguments, they found an oscillating jump discontinuity in their solution that persisted indefinitely and caused them some dissatisfaction with their model. In our studies (Ref. 2), we have examined the collapse of a wake with a rectangular cross section for which a solution can be given in an integral form of sufficient simplicity to permit a complete analysis of its behavior.

Progress

In the case of the rectangular wake cross section, the solution has been obtained in a tractable integral form. Suppose the density disturbance is uniform over a rectangle with sides a and b about the origin as shown below:

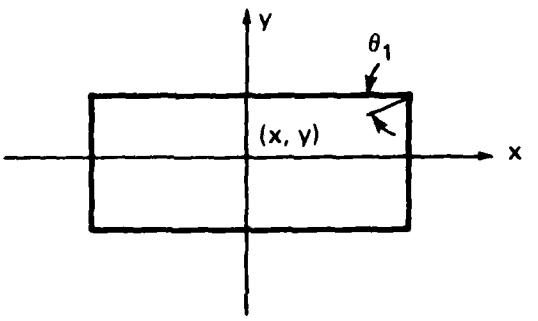

The horizontal and vertical components of the fluid velocity, u and v, are given at the point (x,y) by

$$u = (2\pi\beta)^{-1}N^2 \; J_0(Nt) * \left(\int_{\theta_2}^{\theta_1} \; \int_{\theta_3}^{\theta_4} \right)$$

$$\cot\theta \cos(Nt \sin\theta)\, d\theta \,,$$

$$v = -(2\pi\beta^{-1})N \; J_0(Nt) * \left(\int_{\theta_2}^{\theta_1} \; \int_{\theta_3}^{\theta_4} \right) \cos(Nt \sin\theta)\, d\theta \quad ,$$

where the θ_i are the angles from the point (x,y) to the vertices of the rectangle, * denotes convolution, J_o is the zero-order Bessel function of the first kind, the constant β is the negative of the rate of change of density with depth, and N is the buoyancy frequency.

From these and similar expressions, it is possible to obtain a complete analysis of the asymptotic behavior and discontinuities of the solution by establishing a number of estimates such as

$$J_o(Nt)* \cos(Nt \sin\theta) = \cos(Nt \sin\theta)/(N|\cos\theta|)$$

$$+ \sqrt{\frac{2}{\pi N}}\, t^{-1/2} \sin(Nt - \pi/4)/(N\cos^2\theta)$$

$$+ C_2(Nt, \theta)t^{-3/2}/\cos^4\theta ,$$

where $C_2(Nt, \theta)$ is bounded.

Our conclusions from this analysis are that, as time t becomes large, the velocity field due to an initially constant perturbation density over a rectangle tends to a purely vertical flow that is "plug-like" above and below the rectangle and that decays with time like $t^{-1/2}$ at every point in the flowfield. Although the flow decays at each point, this decay is not uniform with respect to position. The nonuniformity results in a persistent oscillating discontinuity in vertical velocity along the vertical sides of the rectangle on which the initial perturbation density is given. This discontinuity is like the other discontinuities that are accepted as part of the linear approximations (see, for example, Ref. 3), and thus should not cause any dissatisfaction with the linear model.

Principal Investigators: Dr. D. W. Fox, Supervisor, and Dr. J. R. Kuttler, senior mathematician, the Applied Mathematics Group of the Research Center.

References

1. R. J. Hartman and H. W. Lewis, "Wake collapse in a stratified fluid: linear treatment," J. Fluid Mech., Vol. 51, 1972, pp. 613-618.

2. D. W. Fox and J. R. Kuttler, "Wake collapse in a stratified fluid: linear treatment revisited" (to be published).

3. C. Yih, Dynamics of Non-Homogeneous Fluids, MacMillan, 1965.

THE JOHNS HOPKINS UNIVERSITY
APPLIED PHYSICS LABORATORY
LAUREL, MARYLAND

ELECTRONIC PHYSICS

Research in electronic physics is conducted at APL on the interactions of atoms, molecules, electrons, and radiation in three areas: (a) mass spectrometric studies of chemical reactions in crossed molecular beams, (b) theoretical investigations of molecular and solid-state systems, and (c) investigation of localized corrosion mechanisms. In mass spectrometry, the production of vibrationally excited DF molecules in F atom reactions is studied in a crossed molecular beam reactor. Experiments are also undertaken to determine the heat of formation of the NH radical. In theoretical investigations of molecular and solid-state systems, calculations made on the electron spin resonance (ESR) of hydrogen atoms in krypton and xenon matrices are found to be in agreement with recent experimental results. The valence bond theory developed earlier is extended to investigate the hyperfine constants for several interesting molecules. In studies of localized corrosion of aluminum, extensive measurements are made on the formation and growth of blisters under the oxide layer that precede the onset of pitting corrosion in anodized aluminum.

Problem

Improved understanding of the interactions of atoms, molecules, electrons, and radiation is essential to advance further technology in a wide variety of areas important to DoD, including lasers, energy generation, storage and conversion, and the performance of materials.

The determination of energy storage and energy transfer mechanisms is of considerable importance in the study of chemical reactions. Although this has been an area of active research, information on detailed mechanisms has been limited by experimental difficulties in observing the very short-lived reaction intermediates, such as free radicals. Identification of intermediates and their energy states remains a critical problem. The project addresses this issue.

Deterioration of materials due to corrosion is a serious problem resulting in large economic loss. In particular, it is militarily expensive because it shortens the life span of equipment and often results in catastrophic failure. The mechanisms of corrosion are complex, with a frequent coupling between chemical reaction and various physical and mechanical factors. To provide information on one phase of the corrosion problem, research is directed toward understanding the basic mechanisms involved in the initiation phase of localized corrosion in metals.

The theory of the structure of solid-state and molecular systems is important in understanding the results of experiments and for predicting the directions for future research. Because most of the problems of interest cannot be solved exactly, other methods such as the valence bond theory are being applied to these systems.

Objective

The overall objective of the project is to conduct fundamental and applied research on the interaction of atoms, molecules, and radiation with matter and to obtain definitive information on the energetics and mechanisms involved in systems of potential DoD interest. In the past year, the research objectives were

1. Mass spectrometric studies of fluorine/deuterium chemical reactions in crossed molecular beams and the thermochemistry of selected compounds, viz., the heat of formation of NH,

2. Theoretical investigations of molecular and solid-state systems, and

3. Investigation of localized corrosion of aluminum.

Approach

A multidisciplinary approach is undertaken, using mass spectrometry for probing the mechanisms of chemical reactions, optical microscopy and scanning electron microscopy for studying surface properties, and theoretical investigations for elucidating the properties of molecules and molecular ions.

In understanding chemical reactions, it is of critical importance to know the identity of the reaction intermediates and their states of excitation. A free radical mass spectrometer incorporating a collision-free modulated molecular beam sampling system has been used for a number of years at the Laboratory for studying transient chemical species. With the introduction of a high-intensity crossed molecular beam reactor, this system allows the study of atom-molecule reactions under carefully defined conditions and with an unambiguous definition of the products formed. Fluorine atom reactions were selected because of their high exothermicity and the likelihood of finding reaction products in excited states. The mass spectrometer is also very useful in carrying out thermochemical studies, especially on unstable chemical compounds that are difficult to handle otherwise. This capability was used, for example, in studying the highly endothermic compound diimide.

The mechanisms of localized corrosion are complex and not well understood. To gain information on the mechanisms involved in the initiation phase of localized corrosion in metals, a series of experiments are directed toward understanding pitting corrosion in high purity aluminum. In this work, electrochemical

methods coupled with optical microscopic and scanning electron microscopy techniques are used to obtain information on sample morphology and chemical analysis.

Theoretical investigations of molecular and solid-state systems are carried out using a valence bond theory that has been found to successfully account for the hyperfine structure interactions in halogen-molecule ions and noble gas monohalide molecules.

Progress

Significant progress has been made in the past year on research in the three areas of interest.

Mass Spectrometry of Transient Chemical Species. Research continued on the energetics and mechanisms of reaction by mass spectrometric techniques. The results of the studies on the heat of formation of diimide, the proton affinity of N_2, and the production of highly vibrationally excited molecules produced in crossed molecular beam reactions, discussed in last year's report, were published (Refs. 1, 2, and 3).

One of the goals of the research on crossed molecular beams was to use the structure in the ionization curves to give information on both the states of excitation and their relative populations. In experiments with vibrationally excited HF produced by F atom reactions with various compounds, we had encountered a disturbing interference arising from residual water vapor in the mass spectrometer. At the very low ion counting rates involved in these experiments, the small isotropic water peak, H_2O^{18}, at mass 20, although only 0.20% of the principal water peak at mass 18, falls on top of the mass 20 HF ion peak and produces noise in the measurement system. To reduce interference from this source, we decided to carry out some experiments on vibrationally excited DF (mass 21) where the isotopic ion peak from water is smaller than that at mass 20 by a factor of about 3000 and, therefore, negligible.

The experiment involved reacting F atoms from an electrical discharge with deuterium in the reaction:

$$F + D_2 \rightarrow DF^* + D. \qquad (1)$$

The exothermicity of the reaction is sufficient to populate the $v' = 4$ vibrational level of DF (1.3724 eV above the ground state). As expected, the ionization data were of substantially better quality than had been obtained for HF experiments. The observed energy

shift in ionization onset energy distinctly identified production of DF in the $v' = 4$ level. If one assumes that the ionization efficiency curves for DF in the various vibrational levels have essentially the same shape, one can use the ionization data to obtain apparent relative populations in the levels. When treated in this way, the data do not agree with previously published results obtained elsewhere. The disagreement is probably caused by kinematic factors in the mass spectrometry experiments that tend to enhance the detectability of molecules in the higher vibrational states. Additional work is needed on this problem.

In the area of thermochemistry, a study has been undertaken to determine the heat of formation of the NH radical. There has been considerable controversy and uncertainty as to the value of this parameter. The experiment essentially consists in obtaining the NH^+ ion from NH_3 by the dissociative ionization process

$$NH_3 + e \rightarrow NH^+ + H_2 + 2e, \qquad (2)$$

and generating NH radicals by some chemical reaction and then ionizing them by the process

$$NH + e \rightarrow NH^+ + 2e. \qquad (3)$$

Combining the results of reactions 2 and 3 with the known heat of formation of ammonia would give the heat of formation of NH. The NH radicals were produced by successive reactions of F atoms with NH_3 in a mixed reactor to initially generate NH_2, which was then stripped by another F atom reaction to NH. A complicating feature in this work is that a substantial fraction of the NH radicals are not in the ground state but in the $a^1\Delta$ electronically excited state. The data need to be analyzed carefully, and some additional experiments may be required to establish a precise value for the heat of formation of NH.

Theoretical Investigations of Molecular and Solid-State Systems. To provide a theoretical interpretation of some recent experimental measurements of ESR magnetic hyperfine interactions of hydrogen atoms in krypton and xenon matrices at low temperatures (~4 K), calculations were made for the transferred isotropic and anistropic hyperfine constants (hfc) for krypton and xenon nuclei (Ref. 4). These computations included relativistic effects. It was found that the experimental hfc for krypton could be accounted for by

considering only the overlap between hydrogen and its matrix environment, but in order to explain the experimental xenon data, charge transfer between the hydrogen atom and the xenon matrix had to be included.

The valence bond theory developed earlier to calculate the hfc of the rare gas monohalides (Ref. 5) has been extended to investigate the hfc and molecular structure of the molecule Kr_2F recently discovered elsewhere. Excellent agreement with experiment was obtained for a Kr-F separation of 4.5 atomic units (Ref. 6). The theory was also used to investigate the molecule F_3^{2-} created in LiF by X-ray irradiation at 77 K. It had been concluded by others, largely on the basis of positive unpaired spin density on the central F nucleus, that F_3^{2-} had a $^2\Pi$ ground state and that the molecular structure was triangular. We have been able to show that the experimental data can be accounted for very well by a linear molecule in a $^2\Sigma_u$ ground state by including van der Waals electron correlation to explain the unpaired electron density at the central F nucleus (Ref. 7).

The transferred hfc's at the nearest neighbor halogens of the U_2 center in the alkali halides have been calculated. The model for this center is a hydrogen atom at an interstitial position in the crystal. There has been considerable disagreement between theory and experiment on the magnitude of these particular transferred hfc's. We were able to obtain quantitative agreement between theory and experiment by including electron correlation in the wave function of the U_2 center. Finally, we have investigated the transferred hfc's of hydrogen atoms in the alkaline earth fluorides at both substitutional and interstitial trapping sites. Our results indicate considerable lattice distortion in the substitutional site. For the interstitial site, we have obtained quantitative agreement with experiment.

Localized Corrosion of Aluminum. As reported and published previously (Ref. 8), about two years ago we discovered that under some circumstances blistering was the mode of oxide breakdown that led to pitting corrosion in anodized aluminum. Since that time, our observations have indicated that precursive blistering is a (perhaps the) general breakdown mode in the pitting corrosion of aluminum. Others, studying hydrogen embrittlement in Al-Si-Mg alloys, have reported that at 70°C in water vapor the first observable breakdown event is blistering. Blisters have also been observed at high potentials during anodization with chloride in the solution.

Briefly, some of our observations on 99.999% aluminum made during the past year are

1. The potential at which blisters form and grow varies as a function of Cl^- concentration. This curve is very nearly coincident with that of the pitting potential as reported by others.

2. Monochromatic light was used to obtain the number of Newton's rings in growing blisters. This number was used in formulas and with strengths based on work available in current literature for thin films of Al_2O_3 to determine the pressure in a blister which is about 5 to 6 atm. For 80 nm thick oxides, blisters get about 100 μ in diameter with the central oxide about 7 μ above the metal substrate.

3. In unbroken blisters, we find a ring of chloride-bearing material around the perimeter. Using microanalysis in a scanning electron microscope and an Auger spectrometer with a sputtering gun, the ring of chloride material has been localized at the oxide metal interface. This ring also contains oxygen and Al^{3+} (a 51 eV Auger line as opposed to the 68 eV Al metal line). (It is not possible to detect hydrogen in the Auger system.) The chloride component of the material seems to be quite volatile and disappears quickly from the Auger spectrum under the conditions in the Auger spectrometer.

4. The kinetics of blister initiation seem to be field controlled. Our own measurements indicate this as do those of at least one other investigator.

Our research has led to a hypothesis of the breakdown mechanism in which the first step is the field-assisted transport of Cl^-, and perhaps H_2O, across the oxide. Since water is quite limited at the oxide-metal interface, the first reaction probably involves Al (metal) and Cl^- to produce $AlCl_3$. Next H_2O reacts either with $AlCl_3$ by

$$AlCl_3 + H_2O \rightarrow AlCl_2OH + HCl(g) \qquad (4)$$

or with Al by the $AlCl_3$ catalyzed reaction

$$2Al + 6H_2O \rightarrow 2Al(OH)_3 + 3H_2(g)\ , \qquad (5)$$

both of which are known to occur under various conditions. The gas pressurizes but cannot escape because of surface tension. A blister nucleates and begins to grow. The pressurized gas in the blister stresses the oxide and the oxide strains plastically, allowing more reactants to reach the metal substrate. The blister ultimately breaks and pitting corrosion begins on a large scale. To clarify the reaction mechanism, it would be desirable to determine the composition of the blister gas. Both mass spectrometry and Raman spectroscopy are possibilities.

Principal Investigators: Dr. S. N. Foner, Supervisor, R. L. Hudson, senior engineer, Drs. C. B. Bargeron and A. N. Jette, senior physicists, and R. B. Givens, engineering assistant, the Electronic Physics Group of the Research Center; Dr. F. J. Adrian, Supervisor, the Microwave Physics Group.

References

1. S. N. Foner and R. L. Hudson, "On the Heat of Formation of Diimide," J. Chem. Phys., Vol. 68, 1978, p. 3162.

2. S. N. Foner and R. L. Hudson, "Determination of the Proton Affinity of N_2 from Ionization Data on Trans-Diimide," J. Chem. Phys., Vol. 68, 1978, p. 3169.

3. S. N. Foner and R. L. Hudson, "Mass Spectrometry of Excited State Molecules: Observation of Highly Vibrationally Excited HF by Ionization Potential Measurement," J. Chem. Phys., Vol. 68, 1978, p. 2987.

4. J. R. Morton, K. F. Preston, S. J. Strach, F. J. Adrian, and A. N. Jette, "Anisotropic Hyperfine Interactions of Rare-Gas Nuclei Near Trapped Hydrogen Atoms," J. Chem. Phys. (in press, scheduled for 15 Mar 1979).

5. F. J. Adrian and A. N. Jette, "Valence Bond Study of Hyperfine Interactions and Structure of the Noble Gas Monohalides," J. Chem. Phys., Vol. 68, 1978, p. 4696.

6. F. J. Adrian and A. N. Jette (to be submitted to Chem. Phys. Lett.).

7. F. J. Adrian and A. N. Jette (to be submitted to J. Chem. Phys. Solids).

8. C. B. Bargeron and R. B. Givens, "Localized Corrosion of Aluminum: Blister Formation as a Precursor of Pitting," J. Electrochem. Soc., Vol. 124, 1977, p. 1845, and C. B. Bargeron and R. B. Givens, Electrochem. Soc. 153rd Meeting Proc., Vol. 78-1, 1978, p. 168.

THE JOHNS HOPKINS UNIVERSITY
APPLIED PHYSICS LABORATORY
LAUREL MARYLAND

CHEMICAL PHYSICS

MOLECULAR STRUCTURE AND CHEMICAL REACTIVITY

Work has proceeded in several interrelated areas including applications of perturbation theory to the electronic structure of atoms and molecules, calculations of reactive molecular collisions, development of a theory of chemically induced electron polarization, measurement of rates of gas phase atom-molecule reactions, and construction of a hydrogen-oxygen flame apparatus. This work has led to the publication of a dozen articles in scientific journals during fiscal year 1978.

Problem

The electronic structure of atoms and molecules plays a dominant role in chemical reactivities. Since chemical reactions pervade the fields of combustion, propulsion, air pollution, chemical synthesis, fuel production, and other energy-related phenomena, a detailed understanding of these processes is important for future DoD and civilian applications. Pollution from plant and animal respiration gases and the possible depletion of ozone in the stratosphere are problems involving the reactions of atoms, molecules, and the highly labile molecular fragments known as free radicals. Certain aspects of combustion also involve elementary gas phase chemistry, such as the inhibition of flames by the addition of chemicals, and the reverse situation of optimizing combustion for both energy efficiency and minimum pollutant production. When pollutants cannot be avoided as a product in combustion, such as the burning of sulfur-containing coal, knowledge of elementary gas reactions is necessary for possible elimination of the pollutants.

Objective

The goal of this program is to develop insight into chemical reactivities on the basis of their underlying molecular structures and mechanisms. In particular, these insights are to be exploited in the design and operation of flame reactions. A further objective is to measure the rates of various elementary chemical reactions that are relevant to combustion and atmospheric chemistry.

Approach

A quantitative description of the electronic structure of atomic and molecular species is obtained through quantum mechanical calculations using the techniques of many-body perturbation theory. Application of these methods to chemical reactions entails the calculation of the interspecies interaction potential from which information regarding the reaction mechanism can be extracted. The measurement of elementary gas phase atom-molecular reactions is accomplished using a flash-photolytic resonance-fluorescence apparatus. The interaction of low-pressure hydrogen-rich flames with gaseous droplets and particles is examined using flame and particle sampling techniques, analyzed mass spectrometry, resonance fluorescence spectrometry, scanning electron microscopy, and elemental analysis.

The direct study of atom and radical reactions in simple well-known flame environments allows derivation of chemical kinetic information under thermal conditions that are difficult to obtain by other techniques and also allows the deduction of mechanisms of combustion in more complex systems. Thus, this research is concerned with the in situ study of the kinetics of elementary atom-molecule reactions, flame reactions, and the chemistry of flame interactions with particles and other injected materials.

The molecular mechanisms responsible for observed reaction rates and properties are dependent on the electronic structures of the reactant, the intermediate, and the product chemical species. Thus, the experimental chemical kinetics measurements on elementary reactions and flames are complemented by theoretical studies directed toward the elucidation of the structures and reactivities of atoms, molecules, and free radicals. Eventually, the synthesis of experiment and theory is expected to lead to a broad understanding of the relationship betweeen molecular structures and chemical reactivities.

Progress

Work has proceeded in several interrelated areas including application of perturbation theory to the electronic structure of atoms and molecules, calculation of reactive molecular collisions, development of a theory of chemically induced electron polarization, measurement of rates of gas phase atom-molecule reactions, and construction of a hydrogen-oxygen flame apparatus. This work has led to the publication of a dozen articles in scientific journals during fiscal year 1978.

The application of diagrammatic many-body perturbation theory to the electronic structure of atoms and molecules has been advanced through the development of general computer algorithms (Refs. 1 and 2). This work makes it possible to achieve very high accuracy in the calculation of correlation energies of importance in many chemical problems. For instance, the use of polynomial basis functions has led to a new radial limit for the helium atom energy (Ref. 3). The perturbative approach has been further extended to include the evaluation of fourth-order energy contributions (Refs. 4 and 5).

Another topic involves the development of a new concept for generating a universal atomic orbital basis set (Refs. 6 and 7). The advantage of this concept is that it permits an enormous saving of computer resources by allowing the transfer of electron-repulsion integrals from one chemical system to another (Refs. 8 and 9). In related theoretical work, reactions between hydrogen molecules have been examined using quasi-classical dynamical scattering techniques (Ref. 10). In addition, formulas were developed for electron spin polarization developed by radicals in solution for simple diffusion and exponentially decreasing exchange interactions (Ref. 11).

Rate constants were determined for the reaction of hydrogen atoms with bromotrifluoromethane using the flash-photolysis resonance-fluorescence technique. The existing apparatus was modified to permit heating the reactor to 500 K and cooling to 200 K. The first application has been to measure the previously unknown temperature dependence of the rate constant for the reaction H + CF_3Br because of its value in flame inhibition (Ref. 12).

An apparatus has been designed and is currently being assembled for the study of hydrogen-oxygen flames (Ref. 13). At the present time, a low-pressure burner has been assembled for test, and a particle injection system has been devised to allow periodic introduction of particles along the flame axis. Analysis will be by mass spectrometry and a C-H-X combustion train. A proximate elemental analysis system has been devised that will allow characterization of the gas samples without requiring complete identification of the complex products. The mass spectrometer has been tested and is operational. The analytical train for analysis of complex organic mixtures is being assembled. A particle sampling probe is being constructed. The data accumulator (digital signal averager) has been found compatible with the mass spectrometer. The program required to interpret the spectra is being outlined. A bench model of the atomic resonance fluorescence has been set up to test optical properties of the proposed geometry.

Principal Investigators: Dr. D. M. Silver, Supervisor, Dr. L. Monchick, senior chemist, N. deHaas, senior physicist, and Dr. R. M. Fristrom, senior chemist, the Chemical Physics Group of the Research Center; Dr. H. J. Silverstone, Professor of Chemistry, and D. P. Carroll, graduate student, The Johns Hopkins University, Baltimore; Dr. S. Wilson, Science Research Council, Daresbury Laboratory, England; Prof. W. C. Niewpoort, Professor of Chemistry, University of Gronigen, Netherlands; Dr. N. J. Brown, University of California, Berkeley; Dr. K. H. Eberius, DFVLR Institut fur Reaktonskinetik, Stuttgart, West Germany; and Dr. K. H. Hoyermann and Dr. H. Gg. Wagner, the Institut fur Physikalische Chemie der Universitat Guttingen, West Germany. The non-APL colleagues were not funded by the IR&D Program.

References

1. D. M. Silver, "Diagrammatic Many-Body Perturbation Expansion for Atoms and Molecules: I. General Organization," Comp. Phys. Commun., Vol. 14, 1978, pp. 71-79.

2. D. M. Silver, "Diagrammatic Many-Body Perturbation Expansion for Atoms and Molecules: II. Second-Order and Third-Order Ladder Energies," Comp. Phys. Commun., Vol. 14, 1978, pp. 81-89.

3. H. J. Silverstone, D. P. Carroll, and D. M. Silver, "Piecewise Polynomial Basis Functions for Configuration Interaction and Many-Body Perturbation Theory Calculations. The Radial Limit of Helium," J. Chem. Phys., Vol. 68, 1978, pp. 616-618.

4. S. Wilson and D. M. Silver, "Diagrammatic Perturbation Theory: Evaluation of Fourth-Order Energy Terms Involving Quadruply-Excited States for Closed-Shell Systems," Molec. Phys., Vol. 36, 1978, pp. 1539-1548.

5. S. Wilson and D. M. Silver, "Diagrammatic Many-Body Perturbation Expansion for Atoms and Molecules, Fourth-Order Linked Diagrams Involving Quadruply-Excited States," Comp. Phys. Commun., Vol. 17, 1979, pp. 47-50.

6. D. M. Silver and W. C. Nieuwpoort, "Universal Atomic Basis Sets," Chem. Phys. Lett., Vol. 57, 1978, pp. 421-422.

7. D. M. Silver and S. Wilson, "Universal Basis Sets for Electronic Structure Calculations," J. Chem. Phys., Vol. 69, 1978, pp. 3787-3789.

8. D. M. Silver, "Universal Basis Sets and Transferability of Integrals," presented at the American Conference on Theoretical Chemistry, University of Colorado, Boulder, CO, 29 Jun 1978.

9. D. M. Silver, S. Wilson, and W. C. Nieuwpoort, "Universal Basis Sets and Transferability of Integrals," Int. J. Quantum Chem., Vol. 14, 1978, pp. 635-639.

10. N. J. Brown and D. M. Silver, "Reactive and Inelastic Scattering of H_2 + D_2 Using a Repulsive Model Potential Energy Surface," J. Chem. Phys., Vol. 68, 1978, pp. 3607-3617.

11. L. Monchick and F. J. Adrian, "On the Theory of Chemically Induced Electron Polarization (CIDEP): Vector Model and an Asymptotic Solution," J. Chem. Phys., Vol. 68, 1978, pp. 4376-4383.

12. D. M. Silver and N. deHaas, "Temperature Dependence of the Reaction Rate for H+CF_3Br" (to be published).

13. N. J. Brown, K. H. Eberius, R. Fristrom, K. H. Hoyermann, and H. Gg. Wagner, "Low Pressure Hydrogen/Oxygen Flame Studies," Combust. Flame, Vol. 33, 1978, pp. 151-160.

COLLISION PROCESSES

Calculations of atom-diatomic molecular collisions are found to correlate well with models hypothesizing fixed orientation of the diatomic molecule in a frame of reference rotating with the molecule. In a study of electron-molecule collisions during aurora, Born approximation calculations are found to be completely inadequate, but compound-state theory is useful.

Problem

Collision cross sections are a fundamental component of the physics of fluids and radiation transfer. For instance, the equations of fluid flow require transport cross sections as basic inputs, and, similarly, theories of laser operation require line broadening cross sections. To advance understanding of these processes, it is necessary to develop a means of estimating the required cross sections corresponding to various physical situations. Although this can be done fairly accurately for gases composed of noble gas atoms, the situation is much less satisfactory in the case of polyatomic gases. Collisions of polyatomic molecules are several orders of magnitude more difficult to calculate and describe than collisions of systems with no internal degrees of freedom. The main difficulties encountered with polyatomic systems are their rotational motion and intermolecular forces that generally depend on the relative orientations of the molecules. As a result, the motion must be followed in four or five dimensions rather than the one-dimensional motion describing collisions in noble gases. Hence, our research is aimed at developing the theoretical expertise for handling complicated molecular collision problems. Ultimately the solutions to these problems bear on the design and evaluation of the effectiveness of naval systems that depend on fluid flows, plasma, and laser phenomena.

Objective

The goal of this program is to assess the predictive ability and practicability of various methods for the calculation of molecular collision cross sections and to generalize and solve key problems in gas transport theory.

Approach

The strategy adopted is to perform highly accurate quantum mechanical calculations on several simple systems in order to (a) correlate the final cross sections with molecular forces and properties, thus assessing predictive ability, and (b) compare the results with more approximate calculation methods and theories, thus assessing their practicability.

Progress

Quantum mechanical calculations have been performed on the dynamics and corresponding cross sections of several atom-diatom (He-CO) collisions. Integral and differential scattering cross

sections of molecules in a given rotational state of principal quantum number j but with random orientation are the most common molecular beam experimental measurements used to investigate molecular forces. However, it is now becoming possible to measure rotational state depolarization cross sections — cross sections measuring the probability of reorienting the plane in which the molecule is rotating — and it is thus of interest to know something of the relative probability of such processes. Such processes are important in laser operation and spectroscopy because any alteration in the rotational vector orientation changes the subsequent polarization of the light emitted or absorbed. The "coupled states" approximation, in which it is assumed that relative orientiation of the rotating molecules stays fixed throughout a collision, was quite successful in describing He + HCl collisions (Ref. 1), particularly the approximate conservation of rotational angular momentum that seems to hold for He + HCl collisions. Accurate calculations carried out during 1978 on He + CO resulted in scattering patterns and cross sections (Ref. 2) that could be interpreted easily by the coupled states model. According to the model, the characteristic frequency of the interference pattern, observed in the scattering as a function of scattering angle, can be related to the aspect ratio of the rotor, CO, as seen by the atom, He, colliding with it, which in turn is a function of the orientation of the rotor. This correlates qualitatively with the rigorous calculations and thus supports the use of the coupled states model as an interpretive as well as at least a qualitative predictive tool in evaluating the rather detailed information that is becoming available and important in molecular and laser physics.

The type of scattering pattern calculated is shown in Fig. 1, where scattering cross sections are displayed for the processes, initial angular momentum quantum number, and final angular momentum quantum number. The short and long dashed lines correspond to orientations of the plane in which rotation takes place, either perpendicularly or parallel to the initial direction of motion. The solid line is the average of the two. In a related study completed in 1978 (Ref. 3), a model related to the coupled states model successfully correlated and predicted total differential scattering cross sections.

Other scattering calculations (Ref. 4) are being carried out in collaboration with the Max-Planck Institut fur Physik und Astrophysik in Munich. An extension of work previously carried out at APL (Ref. 5), they are concerned with the prediction of the transport properties at low temperatures of H_2 using an ab initio potential energy surface that incorporates polarization, electron correlation, and centrifugal stretching. Programs that were written during 1977 were debugged, and preliminary results

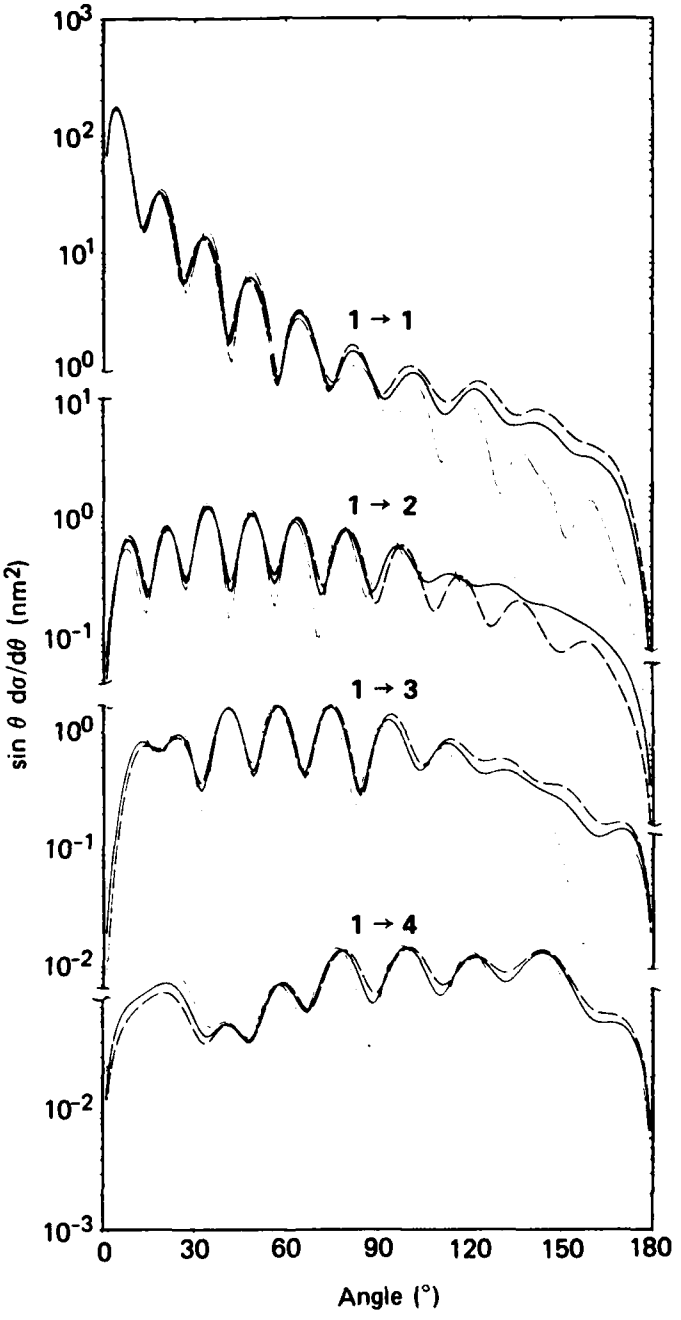

Fig. 1 Type of scattering pattern calculated.

have been obtained by the Munich computing center. The results are not quite as good as those obtained from an empirical potential energy surface (Ref. 4), but they are encouraging enough to induce the institute to finance a more expensive ab initio calculation.

Another study (Ref. 6) considered the excess radiation from the $^1\Delta_g$ state of O_2 during a nocturnal aurora; in particular, one explanation hypothesized that the excess energy was due to vibrationally excited oxygen in the ground electronic state. With the aid of compound-state electron-molecule collision theory, a relation was obtained whereby the cross section for the transition $^3\Sigma_g^-(v = 3) \longrightarrow a^1\Delta_g(v = 0)$ could be inferred from other experimental data. Although the observed cross section could not explain the observed excess radiation, the cross section was unexpectedly large, indicating that the usual methods, based on Born approximations, are inadequate for the treatment of auroral phenomena.

Principal Investigators: Dr. L. Monchick, senior chemist, and Dr. J. G. Parker, senior physicist, the Chemical Physics Group of the Research Center; Dr. T. A. Potemra, senior engineer, the Space Physics and Instrumentation Group of the Space Department; Dr. R. Goldflam and Prof. D. J. Kouri, the University of Houston; Dr. S. Green, research associate for NASA/GSFC and the Department of Chemistry, Columbia University, New York; and Dr. J. Schaefer, physicist, the Max Planck Institut fur Physik und Astrophysik, Munich. The non-APL colleagues were not funded by the IR&D Program.

References

1. L. Monchick and D. J. Kouri, "Magnetic Transitions in the Initial-ℓ Labelled Interpretation of the CS Approximation. Computations for He + HCl," J. Chem. Phys., Vol. 69, 1978, pp. 3262-3267.

2. L. Monchick, "Differential Scattering of Polarized Molecules: Computations for He + CO" (manuscript).

3. R. Goldflam, S. Green, D. J. Kouri, and L. Monchick, "Effect of Molecular Anisotropy on Beam Scattering Measurements," J. Chem. Phys., Vol. 69, 1978, pp. 598-605.

4. J. Schaefer and L. Monchick (unpublished work).

5. L. Monchick, "Multipole Interactions and Macroscopic Differences in Ortho and Para Hydrogen," Chem. Phys. Lett., Vol. 24, 1974, p. 91.

6. L. Monchick, J. G. Parker, and T. A. Potemra, "The Role of Vibrationally Excited Oxygen in the Auroral Excitation of $O_2(^1\Delta_g)$," presented at the American Geophysical Union, San Francisco, CA, 4 December 1978.

SINGLET EXCITED OXYGEN

Collisional deactivation times of laser-excited singlet molecular oxygen $O_2(^1\Delta_g)$ have been determined by monitoring the weak near-infrared fluorescence at 1.27μ accompanying radiative transition to the ground electronic state. The effect of the addition of various molecular species has also been investigated. Results during fiscal year 1978 are described in detail in two articles submitted for publication in scientific journals (Refs. 1 and 2).

Problem

The existence of singlet molecular oxygen as a long-lived metastable species was confirmed by measurements of atmospheric absorption and emission in the 1930's. It was also during this period that its importance in biochemical processes was discovered. During the past ten years, particularly the past five years, a substantial literature has been developed, calling attention to the importance of this molecule in such wide-ranging areas as atmospheric chemistry (ozone), high-altitude spectroscopy (night glow and, more recently, auroral occurrences), biochemistry (oxidation of amino acids and proteins), physical chemistry (various oxidation processes and physical quenching), biological research (damage to microorganisms), and a number of others. However, relatively little work has been undertaken in the area of physics or chemical physics directed toward the elucidation of the fundamental deactivation mechanism.

Optical radiation of oxygen at 1.064μ generated by a Nd:YAG laser produces direct excitation to the singlet excited state. Since this radiation corresponds almost exactly to one of the absorption wavelengths of atmospheric oxygen, the properties of singlet excited oxygen become important for understanding the factors limiting atmospheric laser transmission. The Nd:YAG laser is currently used by the military for optical tracking, ranging, and communication purposes through the atmosphere. Since earth satellite laser communication involves transmission through the ozone layer as well as the uv irradiated region directly above, where relatively large amounts of photoexcited singlet oxygen

are known to exist, a topic of significance is a determination of the interaction of this species with ozone. Laboratory measurements using singlet oxygen generated by microwave discharge have shown ozone to be an anomalously efficient quencher. Since the excitation energy of the singlet oxygen is close to the energy required to dissociate O from O_3, it is thought that such reaction might possibly lead to O generation, an event of importance in atmospheric chemical processes. Also important are phenomena associated with deactivation of singlet oxygen in an aqueous environment.

Objective

The goal of the program is to elucidate the mechanisms of interaction of laser-excited singlet molecular oxygen with differing environments, particularly those most likely to be involved in military laser systems.

Approach

A system for making experimental measurements of deactivation times involves as the main component a commercially available Korad Q-switched Nd:YAG laser that typically radiates a pulse of 20 ns duration, with total pulse energy being 0.1 to 1 J. The laser pulse excites dissolved oxygen in approximately one-hundredth the time for collisional deactiviation in distilled water. The laser irradiation wavelength is 1.064μ, exciting the oxygen to the first vibrational level of the $^1\Delta_g$ state. After the rapid deactivation of this vibrational energy, the most probable following transition is a collisional deactivation to the ground electronic area. In addition, a weak radiative deactivation also occurs at a wavelength of 1.27μ. This fluorescence is spectrally separated from the exciting wavelength, permitting isolation by means of appropriate optical filtering. Enhancement of this fluorescence signal against detector and electronic noise may be accomplished by means of signal averaging. Since the radiative transitions are quite weak, the controlling deactivation process is collisional; thus, the magnitude of the fluorescence signal at any time subsequent to the pulsed laser excitation is used to monitor the instantaneous density of excited oxygen molecules. Determining the decay constants for the deactivation process from the rate of fluorescence decay is accomplished automatically using available electronic instrumentation. A Biomation 8100 transient recorder outputting into a Nicolet 1070 signal averager is used to process the singlet oxygen output generated by a germanium photodiode, with the output of the 1070 interfaced to the central computer. Recently, we acquired a Quanta-Ray DCR 100 Q-switched Nd:YAG laser that provides pulse energies

ten times larger than that of the Korad unit and permits operation at higher pulse repetition rates. Calculations based on data obtained to date indicate that, with this increase in average input power, it should be possible to detect fluorescence in a fully oxygenated distilled water sample.

Progress

To provide an understanding of the fundamental processes involved in the process of collisional deactivation of $O_2(^1\Delta_g)$, experimental measurements of the fluorescent decay in high-pressure gaseous oxygen have been carried out at pressures up to 96 atm (Ref. 1). The fluorescence was observable down to pressures of the order of 35 atm. These measurements indicate the onset of the fluorescence to be immediate, appearing 10 μs after initiation of the laser pulse. Explanation of this result requires either that the probability of the radiative transition

$$O_2(^1\Delta_g)\ (v' = 1) \rightarrow O_2(^3\Sigma_g^-)\ (v = 1) + h\nu_1\ (1.28\mu)$$

takes place with the same probability as

$$O_2(^1\Delta_g)\ (v' = 0) \rightarrow O_2(^3\Sigma_g^-)\ (v = 0\ ) + h\nu_o\ (1.27\mu),$$

which is reasonable since the Franck-Condon factors for the two processes are essentially equal, or that the vibrational deactivation

$$O_2(^1\Delta_g)\ (v' = 1) \rightarrow O_2(^1\Delta_g)\ (v' = 0)$$

is much more rapid than would be expected for the vibration → translation (V-T) process. Alternative paths for vibrational deactivation are presented by the nearly resonant exchange processes,

$$O_2(^1\Delta_g)\ (v' = 1) + O_2(^3\Sigma_g^-)\ (v = 0) \rightarrow O_2(^1\Delta_g)\ (v' = 0)$$

$$+ O_2(^3\Sigma_g^-)\ (v = 1),$$

i.e., vibrational, or

$$O_2(^1\Delta_g)\ (v' = 1) + O_2(^3\Sigma_g^-)\ (v = 0) \rightarrow O_2(^3\Sigma_g^-)\ (v = 1) + O_2(^1\Delta_g)\ (v' = 0),$$

an electronic exchange.

Experimental measurements of other investigators indicate that, for molecules in the v' = 0 level, resonant electronic exchange is an extremely rapid process requiring on the order of 10 collisions. Whether or not this is true for vibrationally excited species is not clear.

Values of the time constant obtained from analysis of the time rate of fluorescence decay agree well with those obtained by other means, indicating that the deactivation process is controlled by binary collisions. A further point of interest is the fact that the magnitude of the level to which the fluorescent signal rises initially has been found to depend on the cube of the pressure. The implication of this is that the rate of spontaneous emission varies linearly with pressure.

$O_2(^1\Delta_g)$ is immune to collisional deactivation in a large number of cases. However, one notable exception is the case of aliphatic amines, which have been demonstrated as efficient quenchers with little tendency toward chemical reaction (Ref. 2). It has been suggested that the mechanism responsible for this enhanced deactivation rate involves charge transfer; however, no real proof of the validity of this hypothesis exists.

In an attempt to elucidate details of the process of collisional deactivation in this particular case, a series of measurements was devoted to determination of the rate of energy transfer from laser-generated $O_2(^1\Delta_g)$ (v' = 1) to NH_3, $NH_2(CH_3)$, and $N(CH_3)_3$. The resultant experimental observations are consistent with a deactivation model in which energy transfer from laser-excited $O_2(^1\Delta_g)$ is, in the case of NH_3 and $NH_2(CH_3)$, primarily from the v' = 1 vibrational state, while for the fully substituted $N(CH_3)_3$ molecule, transfer occurs from the v' = 0 level. Implied in this is that, in the former case, the N-H stretch must be involved, while in the latter, the C-H stretch must be dominant. If

this view is valid, it means that energy transfer from $O_2(^1\Delta_g)$ to NH_3 and $NH_2(CH_3)$ must be regarded as a characteristically different process than in the case of the fully substituted molecule. Possibly supporting this hypothesis is the fact that rather large changes were previously observed by others for $NH_2(CH_3)$ with and without NO addition (presumably to act as a scavenger for O atoms) to the discharged oxygen flow while for $N(CH_3)_3$ the difference was small.

An advantage inherent in the experimental technique used here is that generation of $O_2(^1\Delta_g)$ is "clean" compared to that obtained by means of a microwave discharge, i.e., no O or O_3. Use of high O_2 pressure is also important since it assures rapid deactivation of energy transferred to the added impurities, thus minimizing the possibility of reverse energy transfer.

Principal Investigator: Dr. J. G. Parker, senior physicist, the Chemical Physics Group of the Research Center.

References

1. J. G. Parker, "Observation of Transient $O_2(^1\Delta_g)$ Fluorescence at 1.27μ Following Pulsed Laser Irradiation of High Pressure Oxygen at 1.064μ" (to be published).

2. J. G. Parker, "Collisional Deactivation of $O_2(^1\Delta_g)$ by NH_3, $NH_2(CH_3)$ and $N(CH_3)_3$" (to be published).

THE JOHNS HOPKINS UNIVERSITY
APPLIED PHYSICS LABORATORY
LAUREL MARYLAND

FLUID MECHANICS

Validation of our finite-difference viscous flow solution technique was achieved by comparisons to exact analytic solutions for linear problems and to alternate approximate simulations for a nonlinear situation. Hydromagnetic theory was used to calculate the magnetic transient signal generated by underwater explosions and also to analyze the magnetic field induced by movement of a body through the ocean.

Problem

This research is directed toward developing advanced methods and calculations in fluid mechanics theory. The results are used to predict fluid mechanical motions and transport phenomena from the basic flow equations and to analyze hydromagnetic (HM) phenomena in ocean-like environments.

The work is concerned with two aspects of fluid mechanics, viscous and magnetic effects. Although the basic continuum governing equations for fluid flow and energy transport are known, either the nonlinearity of the equations or the complexity of their boundary conditions frequently precludes closed analytic predictions of flow properties in terms of the pertinent physical parameters. Flow separation and reattachment or modification of forced heat convection are examples of hydrodynamical phenomena that originate in the viscous tangential stresses induced by fluid-boundary interfaces. Specialized theoretical modeling techniques have to be developed to predict the viscous stress field, particularly for rheological fluids. In an environment like the ocean, the natural and body-related seawater motions interact with ambient magnetic fields of the earth and a magnetized vehicle to produce various HM phenomena. These HM effects are generally small and so have received little attention, but many have now become detectable via modern (SQUID) magnetometry and are relevant to naval research requirements in oceanography.

Objective

One goal is the development of reliable analytical and/or numerical techniques to predict the tangential stresses and their effects for steady and unsteady viscous flow in arbitrary geometries. A second goal is to analyze in detail two specific HM effects. One is sonomagnetic pulse radiation, i.e., the transient HM field induced by an underwater sound pulse (such as is generated by an underwater explosion). The other is the HM field induced by a body of arbitrary shape and magnetization moving through the ocean.

Approach

Although we realize that in general the viscous stress fields are dependent on non-Newtonian fluid characteristics, the present theoretical efforts concentrate on the simpler Newtonian fluids. Closed algebraic solutions to the linearized governing equations are obtained under certain simplified boundary conditions or dynamic assumptions. Approximate numerical simulations are used when the boundary conditions or nonlinearities do not admit the above simplification.

The HM analysis technique is also theoretical calculation, proceeding from basic physical principles in order to secure the desired reliable evaluation of effects. For the sonomagnetic pulse, the basic equations of sonomagnetism derived in the previous reporting period are analyzed for a typical model of an underwater sound pulse by a Laplace transform technique. For the body-induced HM field, we introduce an Oseen-like approximation into the basic HM equations and assume a potential flowfield around the body and a given magnetostatic potential for its magnetization field.

Progress

The viscous flow theory assumes homogenous incompressible fluid and geometries that allow reduction of the vector equations to manageable scalar ones. A driven polar section problem provided mutual support between a biorthogonal series solution and our usual finite-difference technique (Ref. 1 and Fig. 1). The conformal mapping technique, applied previously to an isolated occlusion in a straight tube, followed by an explicit marching solution of the transformed finite-difference equation, was verified by solving the identical nonlinear flow problem by a different (nonconformal) numerical mapping and solution by direct and implicit marching techniques (Ref. 2). Analytic solution of steady Newtonian viscous flow in straight rectangular ducts was basic to providing analytic fully developed forced heat convection results under a variety of thermal boundary conditions (Ref. 3). Rigorous bounds were established for uniform perimeter temperature. Finite-difference simulations essentially duplicated the results. The numerical simulations also allow "conjugate" thermal boundary conditions (heat diffusion in the solids bounding the flow is considered as part of the problem) and thus more realistic predictions for many wall materials.

The sonomagnetic theory applied earlier to continuous-wave underwater sources has now been applied to transient sources (underwater explosions/implosions) to obtain an exact expression

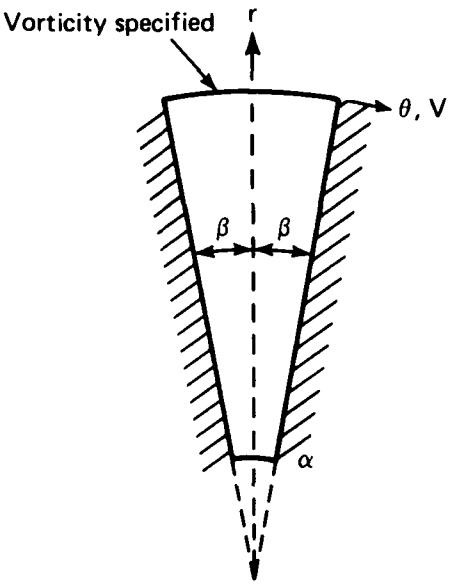

(a) Polar geometry of two-dimensional driven sector problem (viscous non-slip at the solid boundaries)

(b) Detailed comparison of the centerline velocity profile V(r) in the top vortex in driven sector flow for $\alpha = 0.05$, $\beta = 5°$

Fig. 1 Driven sector flow.

for the sonomagnetic pulse (Ref. 4) in terms of tabulated functions of distance from and time after the explosion/implosion pulse. Numerical calculations were made of the sonomagnetic field due to arbitrary sonic pulse strength, showing the evolution of the sonomagnetic pulse at fixed stations from 200 m to > 1 km from the source, as well as its spatial configuration at various epochs (Fig. 2). In analyzing the HM field of a body moving through the ocean, we obtained (Ref. 5) an explicit solution valid at distances

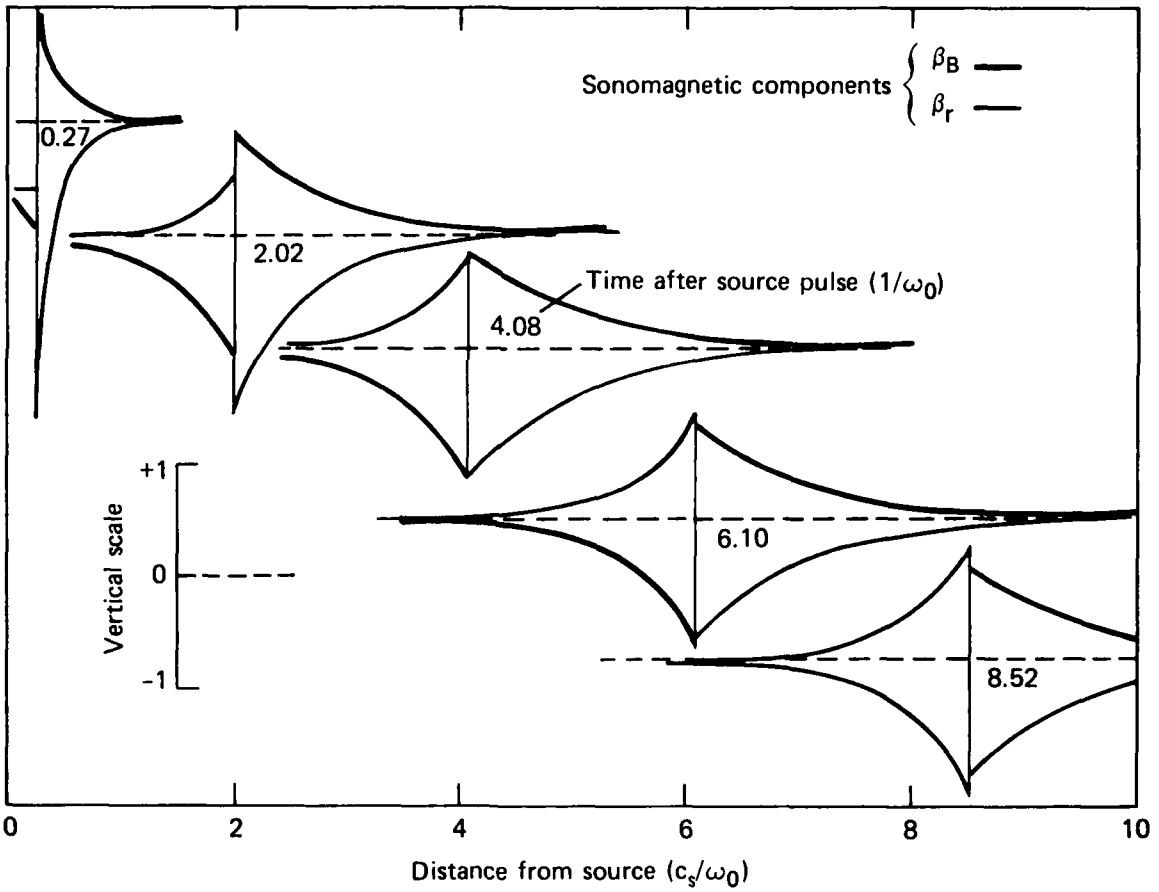

Fig. 2 Successive "snapshots" of the sonomagnetic pulse relative to acoustic impulse produced by underwater explosion or implosion. β_B and β_r are waveform components along ambient magnetic field vector and radius vector from source, respectively. For typical ocean environment, ordinate scale unit is ~ 1.3×10^{-4} γ/Pa-s, distance unit ~ 130 m, and time unit ~ 90 ms.

much greater than body-size for arbitrary body-shape and body-magnetization, delineating an HM wake-field falling relatively slowly with downstream distance. For axisymmetric flow, the solution was shown to be equivalent to that for a disembodied "effective HM dipole" and the effect of external (e.g., sea surface) boundaries was illustrated. In addition, the HM effect of eddies such as can exist in the wake of a moving body was described by a theorem expressing the HM field explicitly in terms of the eddy spin vector (Ref. 6).

Principal Investigators: Drs. J. Bird and V. O'Brien, principal physicists, the Theoretical Problems Group of the Research Center.

References

1. J. Sanders, V. O'Brien, and D. D. Joseph, "Stokes flow in a driven sector by two different methods" (manuscript for publication).

2. L. Ehrlich and V. O'Brien, "Simulating pulsatile flow in stenosed arteries," Proc. 1st Mid-Atlantic Conference on Bio-fluid Mechanics, 1978, pp. 141-150.

3. V. O'Brien, "Fully developed forced convection in rectangular ducts and illustrations of some general inequalities," ZAMP (Z. Angew. Math. Phys.) (to be published).

4. J. Bird, "Sonomagnetic Pulse from an Underwater Explosion," J. Acoust. Soc. Amer. (to be submitted for publication).

5. J. Bird, "Hydromagnetic Field of an Arbitrary Body moving through Bounded Fluid" (in preparation).

6. J. Bird, "Hydromagnetic Perturbations due to Localized Flows: An Eddy Theorem" (to be published, Phys. Fluids, Mar 1979).

OPTICAL PHYSICS AND CHEMISTRY

QUANTUM ELECTRONICS

Significant results have been obtained in understanding the plasma physics and chemistry of high-pressure gas lasers and the effects on high-power laser performance. The results are summarized in this research report and described in detail in two manuscripts being prepared for publication (Refs. 1 and 2).

Problem

DoD and civilian applications of radiation, optics, and lasers require research on the production, transmission, and detection of visible, ultraviolet, and infrared radiation. Gas lasers now available provide radiation extending over a wide spectrum and are used in a wide range of diverse applications such as short wavelength radars and radar simulation, isotope separation, the study of high-temperature gases, and communications. The performance of gas lasers, however, depends critically on and is limited by the effect of the excitation mechanism, whether electrical or chemical, on the lasing gas.

One limitation of all electrically excited gas lasers is the electrical breakdown (arcing) of the lasing gas that results when the excitation energy exceeds a critical value. In the case of pulsed lasers, breakdown can result if either the peak excitation or the average excitation is too large. Breakdown, or even a near-breakdown condition in which intense streamers are present in the gas, is serious because it limits the volume of gas that can be excited to a lasing condition and because it distorts the optical properties of the laser cavity. Both of these effects reduce the attainable laser output power and the repetition rate at which the laser can be operated. The reasons for the arc formation have not been clearly established; several suggested possibilities are the build-up of impurities produced by decomposition of the gas, thermal loading of the gas, localized thermal instabilities, inhomogeneous preionization of the gas, negative ion formation, or acoustic effects. An understanding of the details of the CO_2 laser plasma chemistry both with and without additives is therefore important, and several diagnostic approaches are needed.

Objective

The uniform glow discharge desired in a gas laser can be affected by a variety of instabilities with varying time scales and growth rates. The worst instability leads to complete gas breakdown (arcing) before laser emission. The objective of this work has

been to identify the fast growing instabilities and their dependence on repetition rate.

Approach

This work is fundamentally an experimental investigation of plasma, chemical, and kinetic processes in high-temperature laser devices combined with computer modeling of the time evolution of the laser species. A small transverse-discharge high-pressure (300 Torr) CO_2 laser is excited by two fast current pulses (less than 40 ns wide) that can be separated by 0 to 100 ms. This permits a simple simulation of high-repetition-rate operation while at the same time avoiding the problems associated with removing contaminants.

Progress

A wide variety of measurements has been made as a function of simulated repetition rate using aluminum and stainless steel cathodes, homogeneous and nonhomogeneous preionization, and added contaminants. These measurements include the time histories of visible spectra, electron density, gas current and voltage, laser gain, wavelength and output power, current filament and cathode hot spot development, and refractive effects in the laser plasma.

In order to provide a fast current excitation pulse, ten 500 pF capacitors are mounted inside the vacuum chamber directly to a pair of aluminum Rogovsky-shaped electrodes. The electrodes are 40 cm long, 2.2 cm wide, and separated by 1.3 cm. The capacitors are resonantly charged by two independently controlled external capacitor sources. The excitation current obtained with this arrangement is typically 50 ns wide and, depending on the effective gas resistance, reaches a maximum of about 600 A in 10 to 20 ns. Figure 1 shows the voltage between the electrodes and the current through the gas for a 50 ms pulse separation in which there is no arc and for a 1 ms separation in which there is a single arc.

A typical set of measurements of the laser output, laser gain on axis, gas resistance, and electron density, as a function of the spacing in ms between the two excitation pulses is shown in Fig. 2. These results have been obtained from different runs. In general, when the laser is first turned on, its output will decrease when the separation of the two current pulses is reduced below about 10 ms as indicated in curve (a). At a separation of about 2 ms the laser output drops to zero.

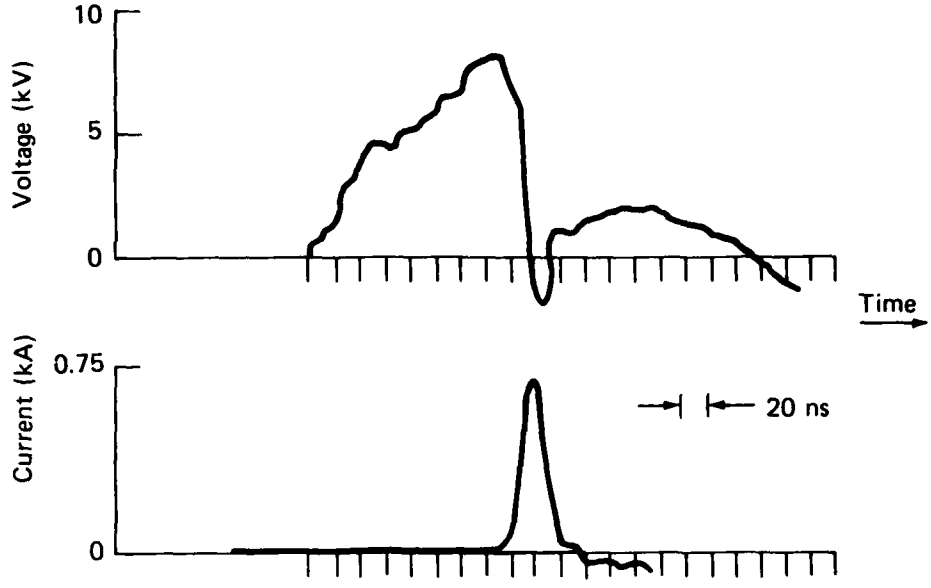

(a) 50 ms pulse separation

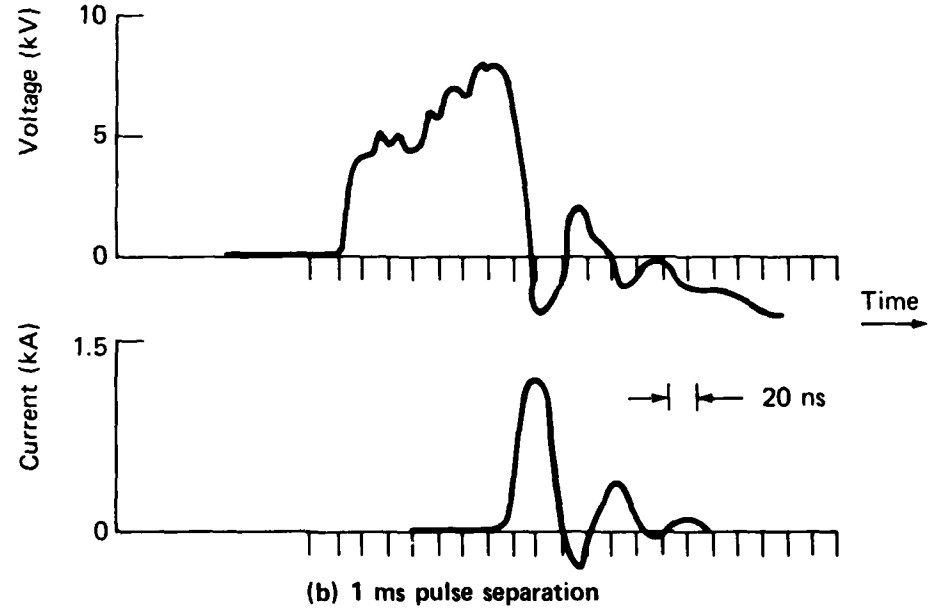

(b) 1 ms pulse separation

Fig. 1 TEA laser voltage and current as a function of excitation pulse separation.

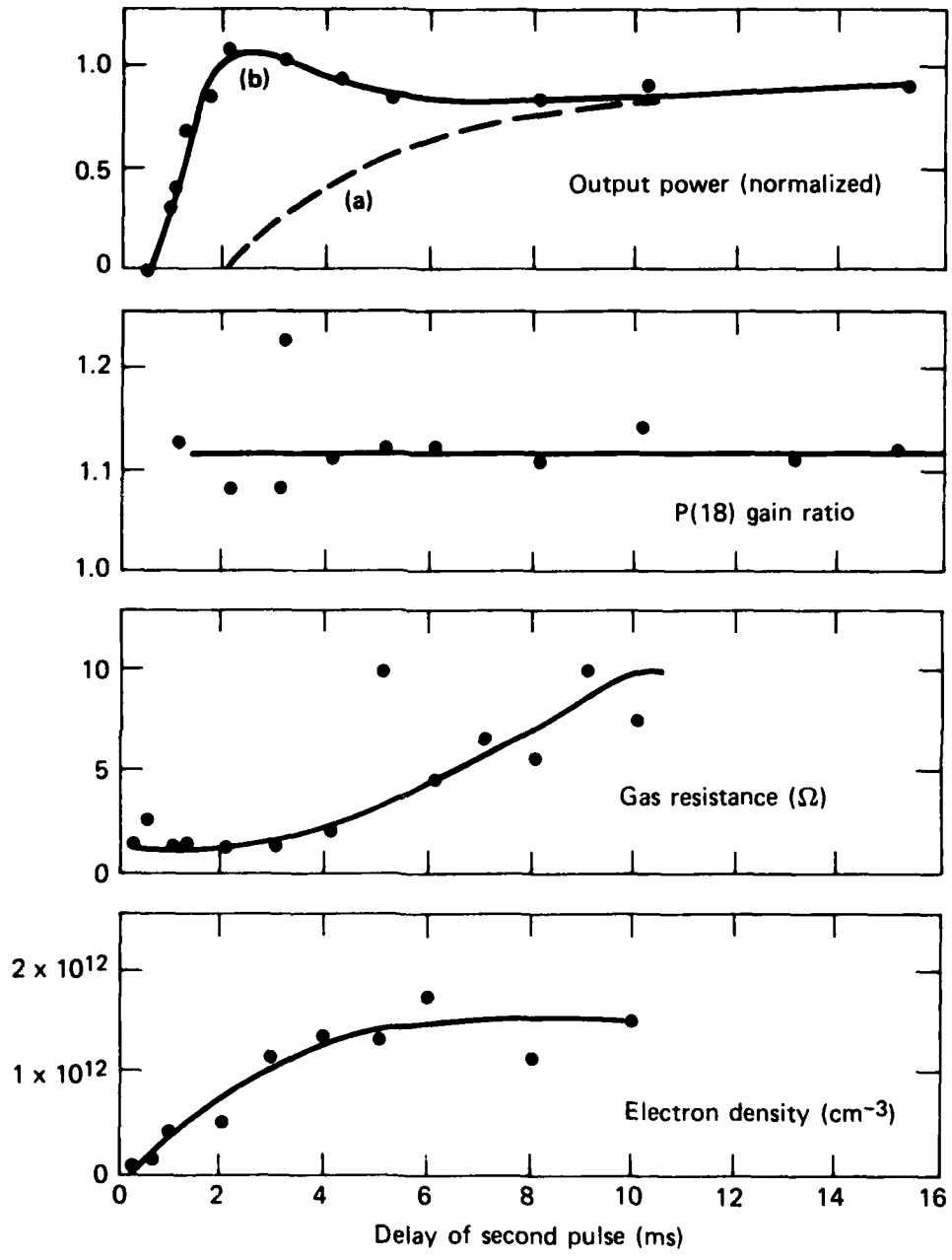

Fig. 2 TEA laser, wire trigger preionization, helium-300 Torr, CO_2 30 Torr.

After the laser has been operating for some time, however, the discharge becomes decidely more uniform and the laser output curve shown in (b) is obtained, where the change (a) to (b) can be attributed to the buildup of CO. This is verified by both the spectroscopic results and through direct addition of CO to the discharge. In both cases, pulsed emission at P(18) is observed, indicating that vibrationally excited CO is transferring energy to the CO_2.

Framing pictures indicate that, for the first 10 ns after the start of the gas current, a uniform glow discharge is present between the electrodes. But by the time of maximum current, hot spots about 5 mm apart are already forming on the cathode, and a filamentary structure (streamers) coming from the hot spots is readily apparent. The luminosity propagating back from the anode consists of much brighter filaments that are spaced ~25 mm apart. The spacing of the filaments depends on the preionization and the separation between the two excitation pulses. As the separation is decreased, the filaments become brighter, contract to occupy less gas volume, and finally constrict into an arc.

With 50 ms pulse separation, there are weak streamers, about 0.5 to 0.6 cm apart, in a fairly uniform local glow discharge. The distribution of streamers is periodic, both along and across the cathode. The periodicity is a function of the amount of CO_2 present; with helium only, the streamer spacing is 1.3 cm. The streamers actually start from hot spots on the cathode, which are well developed 10 ns after the breakdown. For this case excitation current is overdamped, the gas resistance is high ($\approx 5\Omega$), and the gas inductance is low. At the start of breakdown, an ionization wave moves from the cathode to the anode with a velocity of 3.5×10^8 cm/s and returns to the cathode with a velocity of 2.5×10^8 cm/s.

As the spacing between the excitation pulses is decreased, the number of streamers decreases; they become brighter and move away from the region opposite the trigger. At a separation of 1 ms, there is a single arc opposite the preionizer discharge. Here the excitation current is underdamped, the gas resistance has decreased ($\approx 0.1\Omega$), and the inductance of the gas has increased. The decreased resistance is attributed to increased electron density and the increased inductance to concentration of the discharge into a smaller region between the electrodes. The cathode-to-anode ionization wave starts with a velocity of 5.8×10^7 cm/s and increases to 1.6×10^8 cm/s after it is about one-third of the way across the gas. The return wave has a velocity of 3×10^7 cm/s. The periodicity of cathode hot spots (a function of gas mass and composition) and excitation pulse separation are indicative of a cathode sheath instability that leads to local increased electric fields.

This work demonstrates that the cause of breakdown can be traced directly to the interaction of the cathode sheath and a cathode heated locally by previous excitation pulses. It appears that an instability in the cathode sheath produces local concentrations of current on the cathode that in turn lead to the formation of multiple streamers in the gas. As the discharge repetition rate is increased, the cathode temperature increases, the electron density increases, and the streamers become fewer but more intense, resulting in an even higher cathode temperature until a single arc results. This problem can be reduced by proper choice of cathode material and more uniform preionization.

Principal Investigators: Dr. T. O. Poehler, Supervisor, and R. Turner, engineer, the Quantum Electronics Group of the Research Center.

References

1. R. Turner and R. A. Murphy, "Performance of CO_2 Laser at High Repetition Rates" (to be published).

2. R. Turner and R. A. Murphy, "TEA CO_2 Laser Performance using Two Current Excitation Pulses," Bull. Amer. Phys. Soc. (to be published 1979).

LASER-INDUCED GAS-SOLID CHEMISTRY

Experiments are conducted on the irradiation of selected solid-gas systems to initiate chemical reactions, particularly in NF_3-H_2 mixtures, of special interest for potential high-energy laser applications. Decomposition and reaction thresholds are determined, labile species are identified, and spontaneous emission is characterized. Solids examined include NaN_3, AgF_2, Al_2O_3, TiO_2, SiO_2, $NaBF_4$, NH_4BF_4, and NF_4BF_4.

Problem

In the area of homogeneous gas phase reactions, considerable progress has been made recently in the selective promotion of reactions and in the determination of the detailed mechanism by which gas molecules react. This progress has been largely a result of laser-induced chemistry research in which internal energy states of reactant molecules are selectively excited. These same techniques may be applied advantageously to heterogeneous chemical processes such as gas/solid systems. The ambient gas can be selectively excited, changes in the solid can be induced, or the gas and solid can be simultaneously irradiated. We have been conducting experiments in which the solid is irradiated to induce various

effects. For example, the solid may thermally decompose, thereby forming labile species, or surface sites may be activated, or absorbed molecules may be excited. Our work has initially been in the first area in which certain solid materials, although relatively stable at room temperature, can undergo thermal decomposition at slightly elevated temperatures with the possible generation of labile chemical species. Depending on the gaseous environment, a unique solid/gas chemical reaction can result. In this manner, infrared laser heating could be used to volumetrically ignite a normally stable particulate/gas mixture.

Objective

The research goals are the identification of physical and chemical processes that occur during rapid thermal decomposition via laser irradiation of selected materials and the enhancement of chemical reactions in the ambient gaseous medium. Specific information to be obtained includes: (a) the threshold for solid composition and the threshold for reaction initiation, (b) the identification of labile species and their concentration, and (c) the measurement of spontaneous emission.

Approach

In laser-induced heterogeneous systems, the solid is irradiated to achieve volumetric ignition of combustible mixtures by dispersing a powder in a reactable gas mixture, thus permitting the particulates to form reaction sites. This is particularly attractive when the solid can be externally activated, as by radiant heating. Many solids readily absorb infrared radiation, and initiation of a normally stable fuel-oxidizer mixture could be efficiently achieved at wavelengths much longer than those used in conventional ultraviolet flash-photolysis. The apparatus used in the experiments is shown in Fig. 1. A conventional CO_2 laser was used as the radiant heat source for the decomposition. The laser was electronically shuttered using an intracavity device that could vary the pulse width from a few milliseconds to cw. The laser beam was focused on the sample with a spot size of 0.1 cm. Measurements of pressure, gas composition (using a mass spectrometer, gas chromatography, or absorption spectroscopy), and emission spectra (using an optical multichannel analyzer or an infrared detector) provide information on the efficiency of the process, the identification of products, energy distribution, and the extent of reaction.

In addition to providing a new method of initiating reactions, the particle decomposition experiments are expected to

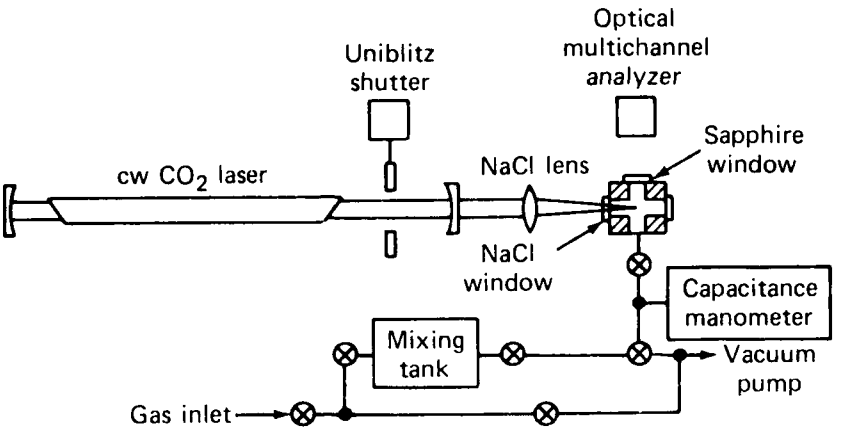

Fig. 1 Apparatus used to investigate the radiative decomposition of solids, subsequent initiation of chemical reactions, and spontaneous emission of excited products.

yield fundamental information on the transient formation of labile chemical species accompanying rapid thermal decomposition of selected materials.

Progress

Our previous work on the radiative decomposition of solids has concerned sodium azide (NaN_3) and silver difluoride (AgF_2). The decomposition of NaN_3 and AgF_2 in vacuum was measured, and NF_3-H_2 mixtures were successfully initiated by irradiating AgF_2. Infrared spontaneous emission was observed from vibrationally excited HF molecules formed during the reaction. A paper describing the decomposition of NaN_3 in vacuum has been accepted for publication (Ref. 1). Preliminary results of the AgF_2 experiments, presented at the JANNAF Combustion Meeting in September 1978, will be published in the meeting proceedings (Ref. 2), and other manuscripts describing more recent experiments are in preparation.

In the current year, additional materials were studied, thresholds for decomposition and reaction initiation were measured, and visible and infrared emissions of the excited reaction products were observed from initiated NF_3-H_2 mixtures, which are of particular interest because of potential laser applications.

The observed emission bands (see Fig. 2) in the visible spectral region result from NF ($b^1\Sigma^+ \rightarrow X^3\Sigma^-$) at 528 nm, the CN violet system at 386 and 418 nm, and the N_2 first positive system and the CN red system in the 550 to 700 nm region. The excited N_2 and NF are produced in homogeneous reactions involving H_2 and NF_3 and are evidently independent of the solid initiation. CN is produced from impurities (CO and CF_4) in the NF_3 and collisionally excited via energy transfer from excited N_2. With an AgF_2 pellet in the field of view of the detector, a broad (500-680 nm) weak emission was observed at the pellet surface even when the pellet was irradiated in vacuum. Presumably, this emission is caused by thermal excitation by the laser beam.

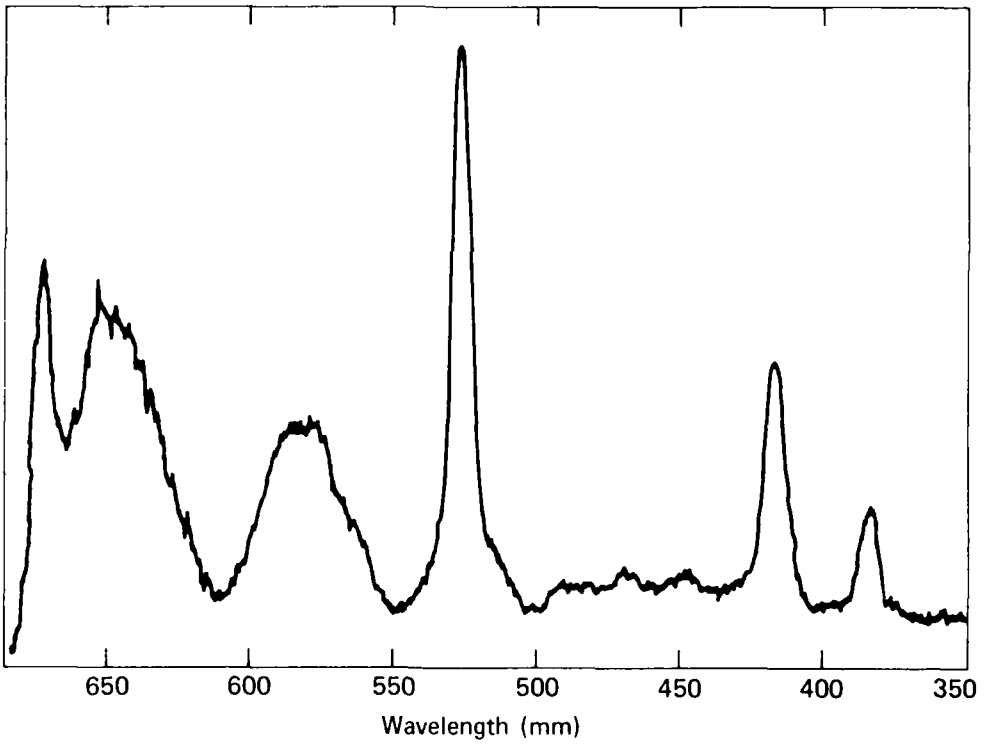

Fig. 2 Emission spectrum of initiated NF_3-H_2 mixture via irradiation of NF_4BF_4; P_{NF_3} = 72 Torr and P_{H_2} = 14 Torr.

Following the successful initiation of the NF_3-H_2 mixture via irradiation of AgF_2, NaN_3 was reexamined. It was determined that NaN_3, despite a small absorption coefficient at 10.6 μm and an unfavorable enthalpy of decomposition, is a successful initiator. Presumably, sufficient Na atoms are produced during the NaN_3 decomposition to initiate the chemical reaction between NF_3 and H_2. Tetrafluoroborates such as $NaBF_4$, NH_4BF_4, and NF_4BF_4 have been studied as sources of F atoms, but only NF_4BF_4 has initiated reactions upon irradiation. The radiative decomposition of NF_4BF_4* in vacuum has been extensively measured, and thresholds for decomposition and reaction initiation have been determined. The material is a very attractive initiator because it thermally decomposes at a relatively low temperature (230°C) to only gaseous products, which is a distinct advantage in systems where particulates can be a problem. Preliminary experiments indicate that irradiation of Al_2O_3, TiO_2, and SiO_2 also initiate NF_3-H_2 mixtures. In all cases where the NF_3-H_2 mixture has been initiated, infrared emission from vibrationally excited HF and visible emission from electronically excited NF, N_2, and CN have been observed. In certain cases, other excited species were also observed. For example, electronically excited Na atoms were produced when NaN_3 was irradiated in NF_3-H_2 mixtures.

Principal Investigators: Dr. R. C. Benson, chemist, the Excitation Mechanisms Group of the Research Center, and O. H. Dengel and R. E. Bowen, NOS/NSWC, who are not funded by the IR&D Program.

References

1. H. Y. Chiu, R. M. Somers, and R. C. Benson, "Decomposition of Solid NaN_3 by CO_2 Laser Radiation" (accepted for publication, Chem. Phys. Lett.).

2. R. C. Benson and R. M. Somers, "Initiation of H_2-F_2 and H_2-NF_3 Reactions via CO_2 Laser Irradiation of AgF_2 Particles," presented at the Fifteenth JANNAF Combustion Meeting, Newport, RI, 11-15 Sep. 1978.

*The NF_4BF_4 pellets were prepared in collaboration with O. H. Dengel and R. E. Bowen at the Naval Ordnance Station, Naval Surface Weapons Center (NOS/NSWC), Indian Head, Maryland.

MOLECULAR PHOTOPHYSICS

A semiempirical valence bond model shows that XeF has a very large dipole moment in its ground state, which may be of importance for the XeF laser and which also enables determination of the structure of the highly unusual molecule Kr_2F from its electron spin resonance (ESR) spectrum. Electron-spin-dependent interactions between a pair of ion radicals are shown to differ considerably from corresponding interactions between neutral radicals, a result important for understanding chemically induced electron polarization in, for example, chlorophyll.

Problem

The mechanism of absorption of electromagnetic radiation in matter and the resulting effects provide many challenging problems in a number of areas of importance in military and civilian technology. Significant advances in the generation, detection, and utilization of electromagnetic radiation, such as masers, lasers, and semiconducting detectors, will continue to result from skillful utilization of the electromagnetic properties of various material systems. Photochemical and photophysical processes have other important applications, including the synthesis and fabrication of unique materials and system elements. There are also adverse effects, such as photochemical degradation of materials and harmful effects on people, whose control requires an understanding of the basic photochemical and photophysical processes involved.

Objective

The project is directed toward improved understanding of selected photochemical and photophysical systems that are important in one or more of the aforementioned problem areas. A corollary objective is the development of expertise in various spectroscopic methods and the related molecular structure theory.

Current work is principally concerned with three topics:

1. Exploring the capabilities of photoacoustic spectroscopy (PAS), primarily by developing an improved instrument and using it to measure the optical absorption bands of transition metal titanates, a class of photoactivated semiconductors having potential applications in photoelectrolysis,

2. Elucidating the molecular structure and electronic energy levels of noble gas monohalides and similar molecular species that have immediate or potential applications (as, for example, for high-power ultraviolet lasers) by using matrix isolation and ESR techniques, and

3. Elucidating the mechanisms of chemically induced magnetic polarization through new applications and theory.

Approach

Photoelectrodes. Photoinduced and photoassisted reactions at electrodes are of considerable potential importance, but the controlling mechanisms are not well understood. Transition metal titanates ($MTiO_{3-x}$), where M is a transition metal and x denotes oxygen vacancy concentration, are of particular interest as electrodes for the photochemical decomposition of water, and it would be advantageous to be able to determine their optical absorption spectra prior to the fabrication of electrodes from the powdered material. Conventional spectroscopy encounters difficulties with powdered samples that neither transmit nor reflect light well. As a result, we are led to use the newly developing PAS technique. PAS is a method of indirectly detecting absorption of electromagnetic radiation by detecting the resulting heating of the sample (Ref. 1). Typically, the radiation source is modulated, producing a similarly modulated heating of the sample. This, in turn, heats a gas in contact with the sample, producing a fluctuating pressure wave that is acoustically detected by a microphone. The nature of the PAS detection process makes it applicable to samples with poor optical quality such as thin films, amorphous materials, or corroded surfaces. Furthermore, because PAS detects only that part of the absorbed radiation that is converted to heat, it can directly study nonradiative or internal conversion processes, and comparison of PAS and conventional optical spectra can reveal processes whereby the absorbed radiation is either reemitted or stored in metastable states or as photochemical reaction products.

Free Radical Structure. The experimental free radical program uses ESR spectroscopy of matrix-isolated radicals. Matrix isolation preserves highly reactive or unstable molecules long enough for detailed spectroscopic study by trapping them in an inert gas at 4 K either by depositing the species from a gas phase reaction onto a cold finger or by in situ formation from the photochemical or radiolytic decomposition of suitable precursors. ESR spectroscopy is applicable to paramagnetic molecules, which free radicals are by virtue of the magnetic moment of the unpaired electron in the broken bond. ESR observes transitions of the electron magnetic moment between its parallel and perpendicular orientations with respect to an external magnetic field, the transition frequency for a typical 3000 g field being in the microwave region around 9000 MHz. Secondary magnetic interactions between the unpaired electron and the molecular framework, particularly the magnetic nuclei, give each radical a characteristic ESR spectrum that

can be used to identify the radical and obtain information about its molecular structure. Various quantum mechanical theories of molecular structure and chemical bonding are used to extract from the ESR spectra information about the molecular structure of the radicals, their electronic energy levels, and possible interactions with surrounding atoms and molecules.

Chemically Induced Spin Polarization. Free radical reactions occurring in liquids often lead to nuclear spin polarizations of the diamagnetic products and reactants, and electron spin polarization of the free radical intermediates. These phenomena, known respectively as chemically induced nuclear/electron spin polarization (CIDNP/CIDEP), are important because much valuable information about the free radical intermediates and mechanistic details is contained in the polarization data (Ref. 2). The theories needed to extract this information require solution of time-dependent quantum-mechanical equations (Schrodinger equation) for mixing of electron spin states either in a pair of radicals (radical pair mechanism) or a triplet molecule (triplet mechanism), where the mixing interactions are being modulated by translational and/or rotational diffusion of the molecular species. Quantum theory is also involved in determining certain intermolecular interactions involved in the mixing process.

Progress

Photoelectrodes. PAS is a relatively new technique with capabilities and limitations that are as yet not thoroughly understood (Ref. 1). Accordingly, much of the present effort is concerned with optimizing spectrometer performance for various types of samples (e.g., thick versus thin or strongly versus weakly absorbing) (Ref. 3), and finding cell designs capable of operation at cryogenic temperatures (77 and hopefully 4 K) as well as room temperature. The processes of light absorption, its conversion to heat, and various thermal conductivity effects involved in the photoacoustic effect have been analyzed to determine the parameters and spectrometer design that will achieve optimal spectrometer sensitivity and stability for various samples in the cw and pulsed modes of operation. The theoretical predictions have been incorporated in the design and operating tradeoffs of the PAS spectrometer system and successfully tested with samples whose optical spectra and nonradiative processes are known from conventional optical spectroscopy (Refs. 3, 4, and 5). A number of improvements to the PAS cell and microphone preamplifier have been made for operation at the temperature of liquid nitrogen (77 K) with the ability to vary temperature between 77 K and room temperature (Ref. 4), a rather rare capability.

PAS spectra have now been measured for a number of transition metal titanates composed of $MTiO_{3-x}$. The PAS spectra were generally consistent with single crystal spectra for the few cases where single crystal spectra were available, and transitions specific to the titanate complex were separable from those associated with transitions of the transition metal atom. Comparison of these results with the activation spectrum of these materials used as electrodes in photoelectrolysis cells is expected to help in understanding the mechanisms of the photoelectrolysis process. Results are to be submitted for publication.

Free Radical Structure. Work of the previous year (on the application of a valence bond function to interpret electron-nuclear hyperfine interactions in the noble gas monohalides and thereby obtain bond lengths and charge distributions in the molecules (Ref. 6)) has been extended in several directions. Dipole moments of the noble gas monohalides were calculated and found to be surprisingly large, e.g., $\mu_{XeF} = 4$ D in the ground state. The magnitude of the dipole moment is important for calculating intermolecular interactions that can affect laser emissions from these molecules, and results were communicated to scientists at Bell Laboratories and Harvard University who expect to do molecular beam studies of XeF. Also, considerable progress has been made in using this method to determine the structures of the highly unusual molecules Kr_2F and F_3^{2-}.

Another application of this theory was to interpret ESR results on hydrogen atoms trapped in the inert gases Xe and Kr, obtained by scientists at the National Research Council of Canada. The theory confirmed their experimental finding that the H atoms were trapped at the octahedrally-symmetric interstitial sites of the Kr and Xe matrices. Some worrisome aspects of the experimental results were explained by a weak charge transfer interaction between H and Xe atoms, as described by admixture of a small ionic valence bond (VB) component, $Xe^+...H^-$, with the covalent VB component, Xe...H, in XeH "molecules" formed by the trapped H atom and the nearest neighbor Xe atoms. The demonstration that the H atoms are trapped interstitially, rather than substitutionally as found in most previous work, may be important for the storage of H atoms and their utilization in a solid-state maser device. There are many more interstitial sites in a crystal than there are vacant substitutional sites, and the ability to trap H atoms interstitially may lead to methods for trapping relatively large numbers of H atoms.

Modifications are nearly complete on a new system for ESR spectroscopy on matrix isolated species at variable temperatures between 8 K and room temperature. The system, which will

minimize the leak problems experienced with conventional cryostats, is based on an Air Products Helitran device consisting of a liquid helium transfer line, for cooling by a regulated flow of helium gas, and a vacuum shroud with a quartz tip, which is joined to the helium refrigeration system by a helical thread. This thread enables the cooled deposition rod with deposited sample to be lowered into a microwave cavity for ESR study. Several problems arose with this system, which is a new and highly experimental Air Products design; particularly, it was found here and by groups at Bell Laboratories that manual raising and lowering of the rod by rotating about the helical thread was very difficult and tended to shake the deposited sample off the rod. Accordingly, a motor-driver gear system has been designed and built to raise and lower the sample. Also, several support bearings had to be designed and fabricated to eliminate friction between moving metal surfaces.

Chemically Induced Magnetic Polarization. F. J. Adrian was co-chairman, along with Professor J. K. S. Wan of Queen's University, Kingston, Canada, of an international workshop in chemically induced magnetic polarization held 7-10 June 1978 at Queen's University. The object of the workshop was to bring together persons in various fields where chemically induced magnetic polarization has current or potential applications, with emphasis on introducing the subject to prospective new users. In connection with this conference, a paper was prepared for *Reviews of Reactive Intermediates* (Ref. 8). This paper is largely a review of how the combination of electron-spin-selective reaction with magnetic mixing of the reactive and unreactive electron spin states leads to polarization (radical pair mechanism). It also contained an important new result: the demonstration that in ionic radical pairs, the singlet electron spin state is not necessarily lower in energy than the triplet state, in contrast with neutral radical pairs where the covalent-bond-forming singlet is invariably lower in energy than the antibonding triplet. An immediate application of this theory supported results of scientists at the University of California at Berkeley on electron spin polarization arising out of light-induced radical-ion pair formation in a photosynthetic system, work also reported at the Kingston conference.

Further work has been done in applying integral equation methods to the solution of the stochastic Liouville equation (Ref. 7) for chemically induced electron polarization by separation-dependent singlet-triplet mixing in a freely diffusing radical pair. The initial study considered polarization by mixing the singlet and nonmagnetic ($M_S = 0$) triplet sublevel of the radical pair. Current work is on nuclear and electron polarization from mixing the singlet and the $M_S = -1$ triplet component. In this

case, the polarization arises from state mixing as the radicals diffuse through the region where these two levels cross. Since this level crossing region is where the magnetic Zeeman splitting of the electron triplet level is equal to the valence bonding interaction, which splits the singlet and triplet levels, it is likely this theory will enable information about the chemical bonding interaction to be deduced from the polarization data. Preliminary results support experimental findings elsewhere that $S\text{-}T_{-1}$ polarization can occur if one component of the radical pair has a large electron-nuclear hyperfine interaction that permits rapid singlet-triplet mixing, or if the reaction occurs in a viscous solvent so the slowly diffusing radicals remain a long time in the level crossing region.

Principal Investigators: Dr. F. J. Adrian, Supervisor, and Drs. L. C. Aamodt and J. C. Murphy, senior physicists, the Microwave Physics Group; Dr. A. N. Jette, senior physicist, the Electronic Physics Group; and Dr. L. Monchick, senior chemist, the Chemical Physics Group; all in the Research Center.

References

1. Optoacoustic Spectroscopy, Yoh-han Pai (ed.), Academic Press, New York, 1977.

2. Chemically Induced Magnetic Polarization, L. T. Muus et al. (eds.), D. Reidel, Dordrecht, Holland, 1977.

3. L. C. Aamodt and J. C. Murphy, "Size Considerations in Design of Cells for Photoacoustic Spectroscopy," J. Appl. Phys., Vol. 48, Mar 1977, p. 927.

4. J. C. Murphy and L. C. Aamodt, "Photoacoustic Spectroscopy of Luminescent Solids: Ruby," J. Appl. Phys., Vol. 48, Aug 1977, p. 3502.

5. L. C. Aamodt and J. C. Murphy, "Size Considerations in the Design of Cells for Photoacoustic Spectroscopy. II. Pulsed Excitation Response," J. Appl. Phys., Vol. 49, Jun 1978, p. 3036.

6. F. J. Adrian and A. N. Jette, "Valence Bond Study of Hyperfine Interactions and Structure of the Noble Gas Monohalides," J. Chem. Phys., Vol. 68, 15 May 1978, p. 4696.

7. L. Monchick and F. J. Adrian, "On the Theory of Chemically Induced Electron Polarization (CIDEP): Vector Model and an Asymptotic Solution," J. Chem. Phys., Vol. 68, 15 May 1978, p. 4376.

8. F. J. Adrian, "Principles of the Radical Pair Mechanism of Chemically Induced Nuclear and Electron Spin Polarization," Rev. Chem. Intermed., Vol. 3(1-2), 1979, p. 3-43.

SPECTROSCOPY OF DONOR-ACCEPTOR MOLECULES

A study of the spectra of zinc porphin in anthracene is completed. Conventional polarized optical absorption spectra and fluorescence spectra obtained at 4.2 K show multiplet inequivalent zinc porphin sites in anthracene. Techniques for the selective excitation of fluorescence using a scanning dye laser provide single-site fluorescence and excitation spectra. The two lowest excited electronic states are identified and the excited and ground state vibronic energy levels are measured. Most of the stronger vibronic lines are in agreement with calculated vibrational frequencies of the molecule.

Problem

Porphyrin compounds are of interest because they exhibit a variety of physical and chemical properties that generally depend on the particular metal ion that is bonded to the center of the planar molecules. Various forms exhibit fluorescence, phosphorescence, paramagnetism, organic semiconduction, photoconduction, and other solid-state characteristics relevant to DoD research requirements. Some are active catalysts or photosensitizers. Porphyrins occur as important constituents in natural chemical and physical systems. Furthermore, their diversity of structure and of chemical and physical properties makes them attractive as model compounds for studies that correlate quantum mechanical descriptions with chemical and physical functions.

Delocalized electrons of highly conjugated organic molecules are easily excited to higher energy states by optical, electrical, or chemical stimuli and are primarily responsible for the properties of these types of molecules. Changes in the electronic and vibrational structure of these molecules resulting from such external stimuli are of primary concern in this work. These changes are relevant to a basic understanding of the molecular, physical, and chemical properties of interest.

Optical molecular spectroscopy is used as the primary experimental technique in these studies because the excited states of these types of molecules are in the visible and near-ultraviolet region of the spectrum and the optical spectra are a direct result of the interaction of light with the delocalized π electrons. Elec-

tromagnetic radiation can either be absorbed, resulting in molecular excitation, or emitted upon molecular deexcitation. Experimental spectroscopic results are used in an effort to describe the system and its properties in terms of a theoretical model based on quantum mechanical principles.

Objective

The objective of this project is to advance the understanding of chemical, physical, and molecular functions by studying perturbations in molecular structure that occur as a result of interaction with other chemical species or physical forces. The immediate goal is to test and improve current theoretical models of free porphyrin compounds by experimental spectroscopic studies of porphins, the parent compounds of the general class of porphyrins. These studies are conducted with "isolated" porphins in a suitable host matrix. A longer term goal is to study these same porphin species complexed with chemical ligands that are believed to be involved in biologically active forms of porphyrins. The changes in the observed spectra for the complexed species will be related to the interactions between the attacking chemical ligands and the porphin molecules.

Approach

Optical spectroscopy and electron spin resonance (ESR) are the experimental methods used in this project. Because they are not easily vaporized, the molecules studied require a liquid solvent or a solid host matrix. The host, however, can cause loss of spectral information in the guest molecule of interest because of excessive spectral line broadening. This effect is largely eliminated in these studies by using crystalline host materials and making spectral observations at a low sample temperature (4.2 K). This allows transitions between the ground and the excited electronic and vibrational states to be resolved. The absorption spectra provide the excited electronic and vibrational energy levels, while the luminescence spectra yield the electronic ground state vibrational levels. Problems in interpretation of the spectra can arise because the guest molecules often reside in different types of sites in the host lattice. Since molecules in different sites yield slightly different spectra, multiplets occur in spectral regions where only one line would normally be observed. To eliminate this ambiguity, high resolution selective excitation of fluorescence techniques are used to obtain the spectrum of a single site. The method consists of first recording the fluorescence spectrum that results from excitation of a single sharp absorption line. Then the excitation source is scanned through the region of the absorption spectrum while the detector is tuned

to one of the fluorescence lines of a particular site. This gives an unambiguous correlation between the absorption and fluorescence spectra of a given site.

ESR is used to obtain information on the electronic ground state magnetic parameters for those molecules that exhibit paramagnetism. These parameters are typically the magnetic g factor, hyperfine structure constants, and superhyperfine structure constants. The superhyperfine structure constants are due to interactions between the paramagnetic metal ion in the center of the porphyrin and the neighboring nitrogen atoms. Often these magnetic parameters are anisotropic. In these cases, information about the orientation of the guest molecules in the host crystals can be obtained.

Progress

A study of zinc porphin in anthracene (ZnP/A) using conventional and single-site optical techniques was undertaken and completed in the past year (Ref. 1). Conventional polarized optical absorption spectra and fluorescence spectra of ZnP/A were taken at 4.2 K. The spectra of ZnP/A were of interest because a comparison of these spectra with those of zinc porphin in another host, triphenylene (Ref. 2), provided a measure of the effect of the host lattice on the vibronic structure of free zinc porphin. The general pattern of sharp spectral lines observed for ZnP/A was consistent with that found in triphenylene. Thus, it appeared that these host materials did not significantly perturb the structure of the host zinc porphin species. Vibrational frequencies were assigned from the experimental data and compared to published theoretical vibrational frequencies for metallo-porphin.

A vibrational analysis of free base porphin was done using a potential field similar to a published calculation for metallo-porphin. Detailed comparison of the experimental and theoretical vibronic levels was difficult in many cases, however, because of the large number of vibrational energy levels. Theoretical transition intensities would greatly facilitate the correlation between theoretical and experimental energy levels. A calculation of the intensities was done with the assumption that vibronic borrowing is the principal mechanism that provides intensity to the forbidden Q band vibronic levels. The results were not in agreement with experimental data. The electronic wave functions used in this calculation, however, did not use self-consistent molecular orbitals and did not include configuration interaction. Steps to obtain improved electronic wave functions will be made in the near future.

Principal Investigators: Drs. J. Bohandy and B. F. Kim, senior physicists, the Microwave Physics Group of the Research Center.

References

1. J. Bohandy and B. F. Kim, "Conventional and Dye Laser Optical Spectra of Zinc Porphin in Anthracene," Spectrochim. Acta (in press).

2. B. F. Kim and J. Bohandy, "Single Site Spectra of Zn Porphin in Triphenylene," J. Mol. Spectrosc., Vol. 65, No. 90, 1977.

THE JOHNS HOPKINS UNIVERSITY
APPLIED PHYSICS LABORATORY
LAUREL MARYLAND

PHYSIOLOGY

A general theory of visual sensation as a space-time field was developed and applied to the analysis of a variety of spatio-temporal visual phenomena. Data analysis methods for intensity correlation spectroscopy of polydisperse samples have been improved by finding exact solutions in the Rayleigh-Gans limit for cumulant expansion parameters in terms of continuous size distribution parameters. Validation of our previous numerical scheme for nonlinear unsteady flow simulation in a stenosed artery was achieved by an alternate mapping technique followed by one of several different solution methods.

Problem

Visual sensation is the output of an impressively complex but efficient data processing system and as such, as well as in its own right, has attracted intensive study. But separate aspects have been pursued almost independently; for example, systems analyses have focused on achromatic brightness space-time variations, while color models have concentrated on uniform-static chromatism. A unified and quantitative framework is needed to comprehend the total system output — brightness and color varying in time and space.

The mean size and polydispersity of complex biological macromolecules (such as serum lipoproteins) are important properties that are related to the functioning of the macromolecules. Convenient experimental and analytic methods are needed to characterize these properties.

The blood flow problem is to determine how the pulsatile hemodynamics influence the development of atherosclerosis. In the absence of reliable experimental data, the effects of hemodynamic properties that might affect growth of atherosclerotic occlusions can be estimated from time-dependent flow calculations, provided an accurate convergence scheme is developed.

Objective

The objective of this work is the formulation of accepted principles into a comprehensive mathematical theory of visual sensation as a vector function and the development of its space-time functional properties as a formal field theory.

Regarding work on characterizing the mean size and polydispersity of biomacromolecules, our overall objective is to develop the light scattering method of intensity correlation spectroscopy (ICS) as a rapid and accurate method of investigating

these properties. The objective of our current limited program (approximately 0.1 man-year) was to extend and verify our previous approximate solutions for cumulant expansion parameters in terms of model size distribution parameters by finding exact solutions in the Rayleigh-Gans (R-G) limit.

An immediate objective of the arterial flow simulation is to develop a systematic approach to predicting flow within an axisymmetric atherosclerotic occlusion with stationary walls (arterial walls unresponsive to pulsing flow).

Approach

The vision theory is based on the fundamental Helmholtz and Hering principles. The former is expressed as: any retinal illumination is transformed upon quantum absorptions into a four vector (three cone-type receptors plus the rod receptors) distributed over retinal space-time. The latter is expressed as follows: visual sensation is a three vector in a Cartesian half-space ("red-green" and "blue-yellow" axes and a "white" semiaxis with "black" at origin) distributed over sensory space-time. We express the transmutation from quantum absorptions to visual sensations as a vector physiological operator. This formulation makes it clear that most psychophysical experiments produce linearization, and consequently the space-time sensory field is developable in terms of a Green's function matrix for the visual system.

Macromolecular solutions are often examined using ICS, which can determine molecular diffusion coefficients, and therefore particle size, from the autocorrelation function of the time-dependent intensity fluctuations in the light scattered from the particles as they diffuse in solution. An expansion technique is used to analyze the autocorrelation function, and the coefficients, called cumulants, are related to the sample polydispersity. Our approach to characterizing polydispersity is to relate cumulants to the parameters of specific model size distributions.

Viscous incompressible blood flow within an axisymmetric geometry can be characterized by coupled equations for stream function and vorticity. The approach is to simulate the solution by numerical methods. An isolated stenosis is mapped to a more convenient computation plane and the transformed nonlinear equations solved by finite-difference approximation. Arbitrary pulse waves are allowed. Multiple stenoses can be handled by the same technique.

Progress

The basic formulation of the general vision theory (Ref. 1) was sufficient to demonstrate the reason (heretofore lacking) for the success of linear models of color vision, despite patent nonlinearities of the visual system. We also demonstrate (Ref. 2) how nonlinear static intensity-level effects (viz., hue shifts and unique-hue invariance) can be modeled from the theory. The space-time field theory (Ref. 2) was then developed and applied to the analysis of intensity and/or chromaticity variations, including color-flicker and wavelength-pulse experiments. Further, the field theory was shown to predict several chromatic generalizations of brightness space-time reciprocity laws and to yield Abney's law of luminance additivity for heterochromatic flicker and minimally distinct border techniques (see Fig. 1).

We previously showed that good descriptions of very-low-density lipoprotein (VLDL) sizes are provided by three bell-shaped distributions of radii. During the present period we found exact solutions for the cumulants in the R-G limit for one of these distributions. This exact solution confirms our earlier conclusion, which was based on an approximate solution, that VLDL (with diameters of 30 to > 90 nm) can be treated as Rayleigh scatterers for scattering angles of $\leq 90°$.

Validation of our earlier blood flow calculations (which consisted of a conformal mapping of the median plane stenosis geometry to a rectangular domain, followed by explicit marching to a nonlinear Newtonian solution in the transformation domain) was sought by alternate approximation schemes. A test case of a moderate occlusion (75% open) with a Reynolds number of about 100 was selected and solved independently by other finite-difference methods. The flow domain was mapped numerically (unconformally) to a rectangular working domain. The solution was obtained directly (via a novel method) and by implicit time marching. The attempts to secure the solution by explicit time marching failed to converge, probably due to errors incurred by the numerical mapping. The implicit marching technique revealed some difficulty in imposing the correct vorticity boundary condition; the difficulty was ultimately remedied. The final agreement of the various numerical schemes is shown in Fig. 2 by the distributions of vorticity along the (arterial) wall and across the occlusion throat (i.e., at $Z/R_0 = 0$). The region of negative vorticity just downstream of the throat marks the separated recirculation region. Other pulsatile flow calculations revealed how the recirculation region grew and shrank with the amount of oscillatory flux relative to the mean amount at the same (test) mean Reynolds number and fixed reduced frequency (Ref. 3).

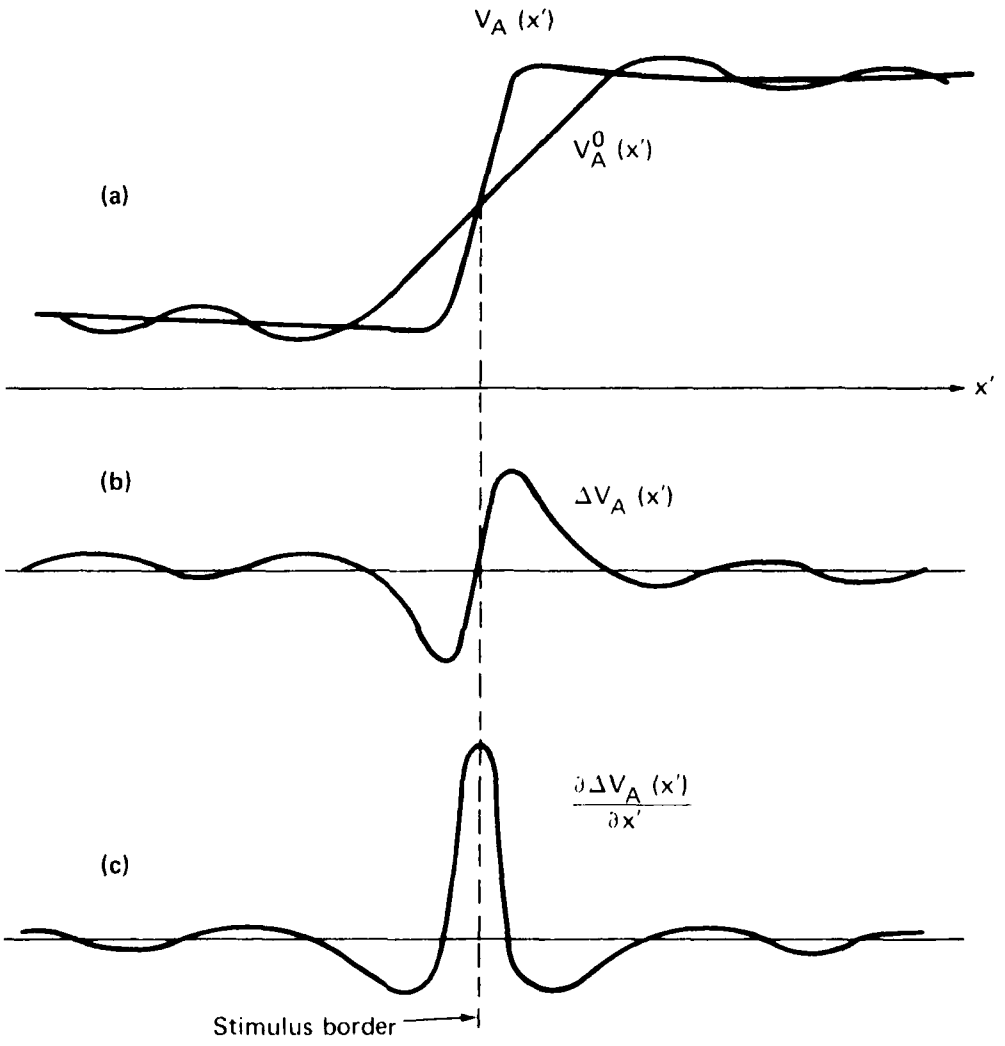

Fig. 1 Schematic of achromatic sensation component as a function of the sensory coordinate (x') for minimally distinct border observations. V_A represents actual spatial-step sensation and V_A^0 its low frequency portion (a), ΔV_A is the high frequency residue (b), whose rate of change across the border $\partial \Delta V_A / \partial x'$ is a measure of border distinctness (c). The theory given in Ref. 2 shows that the border distinctness is an additive luminance measure and suggests analogous additive measures.

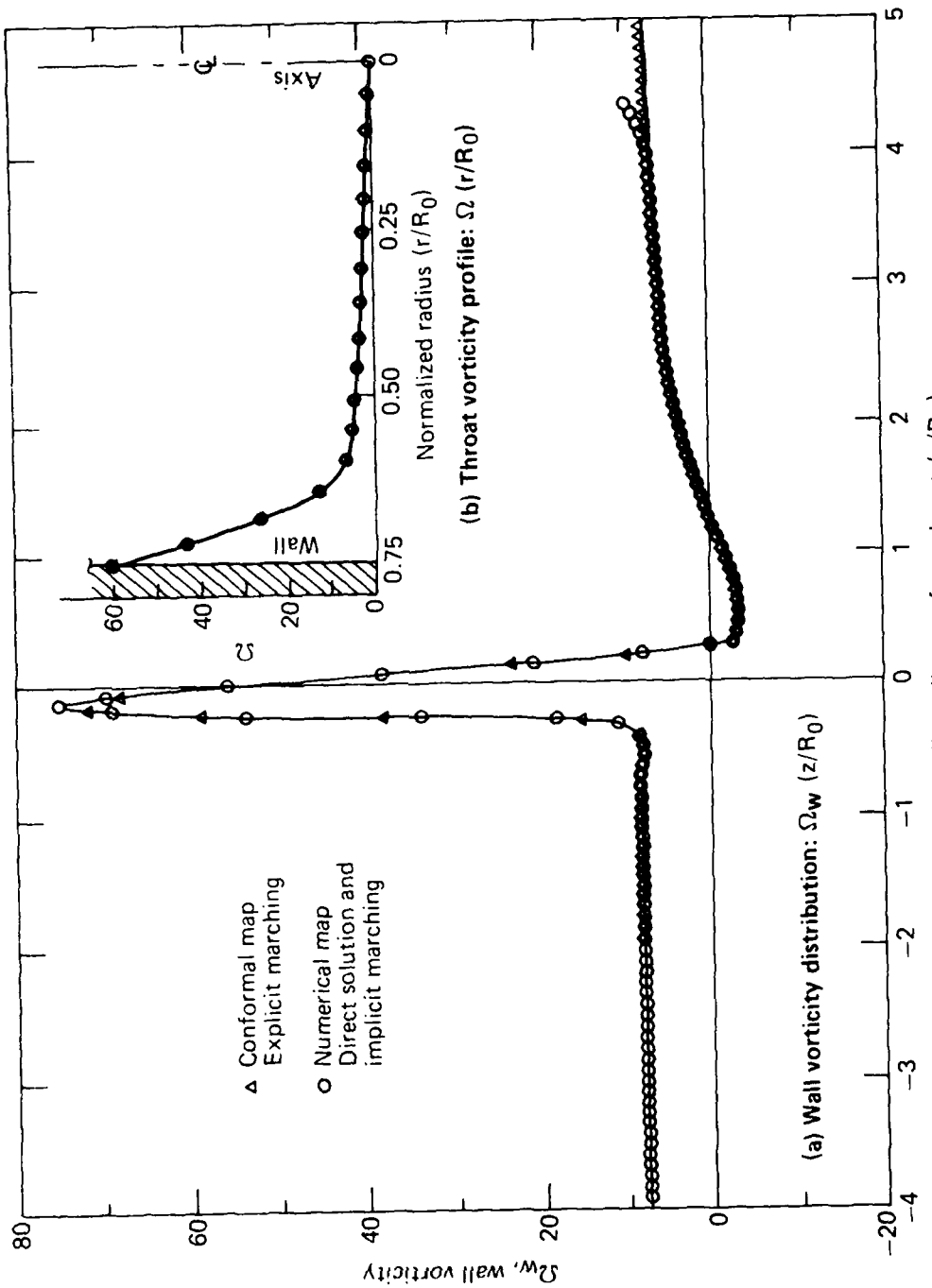

Fig. 2 Comparison of steady stenosis flow solutions.

Principal Investigators: Drs. J. F. Bird and V. O'Brien, principal physicists, R. McCally, senior physicist, in the Theoretical Problems Group of the Research Center; Dr. R. W. Massof, instructor of ophthalmology, the Wilmer Institute of JHU. Dr. Massof is not funded by the IR&D Program.

References

1. R. W. Massof and J. F. Bird, "A General Zone Theory of Color and Brightness Vision. I. Basic Formulation," J. Opt. Soc. Am., Vol. 68, Nov 1978, pp. 1465-1471.

2. J. F. Bird and R. W. Massof, "A General Zone Theory of Color and Brightness Vision. II. The Space-Time Field," J. Opt. Soc. Am., Vol. 68, Nov 1978, pp. 1471-1481.

3. L. W. Ehrlich and V. O'Brien, "Simulating Pulsatile Flow in Stenosed Arteries," First Mid-Atlantic Conference on Bio-Fluid Mechanics, VPI&SU, Blacksburg, VA, 9-11 Aug 1978.

THE JOHNS HOPKINS UNIVERSITY
APPLIED PHYSICS LABORATORY
LAUREL MARYLAND

SOLID-STATE PHYSICS

ORGANIC AND ELECTROLYTE SEMICONDUCTOR PHYSICS

Significant results are obtained in developing new materials for solar energy conversion and in synthesizing organic solids with useful electronic properties. In the latter work, a particularly interesting high-speed switching and memory behavior has been discovered in certain organic semiconductors. The results are summarized here and described in detail in several publications referenced in the article.

Problem

Developing an understanding of the relationship of the composition and structure of materials to their useful functional properties provides a basis for creating advanced materials for electronic, optical, and magnetic applications. The range of materials currently available for such applications is limited to a relatively few elements and simple compounds discovered by empirical methods. It has therefore been impossible to provide materials that exactly meet specific requirements for physical properties and match a particular application.

It is essential that we discover the general relationships among material synthesis procedures, the composition and structure of the materials produced, and the required useful physical properties. Using these relationships to design and produce a material of a desirable composition and structure is another general problem to be addressed. Finally, it is important to continue to develop new analytical methods to improve the basic material characterization procedures as unique materials are attained.

Objective

The program this year included several mutually supportive projects. The specific goals of these projects were

1. The development and evaluation of candidate materials having band gaps matched to the solar spectrum, with emphasis on $Ti_xV_{1-x}O_2$ alloys and titanates of the form $MTiO_3$;

2. The synthesis and study of organic conductors with increased two-dimensional character (compounds related to HMTSF-TCNQ), tellurium analogues of TTF-TCNQ, and organic conducting polymers; and

3. The preparation of transition metal-metalloid alloys (initially Fe_xB_{1-x}) together with preliminary examination of infrared and magnetic properties. The theoretical model already formulated for amorphous magnetism will be further developed.

Approach

The general approach in this program is to develop new materials of potential technological importance and to utilize quantitative measurement techniques to understand their physics and chemistry. Understanding the basic relationship can produce materials of the composition and structure expected to be useful in particular applications.

Candidate materials for solar energy conversion and the investigation of the basic mechanisms of interfacial electron transfer and anodic stability include hitherto unavailable mixed transition metal oxides. Thus, by proper choice of composition, one can fabricate materials with suitable band gaps for absorbing higher fractions of the solar spectrum.

The program also included development of both single-crystal and polycrystalline specimens of substituted perovskites ($A_xB_{1-x}O_3$) produced by rf sputtering or vapor transport methods as a function of x and the degree of reduction. The substitution is selectively on the A or B site with a range of alloy compositions and includes aliovalent substitution for oxygen vacancy control. Physical measurements specific to semiconductor-electrolyte systems, including standard measurements relating electrode potential to the electrolysis current density, are made as well as impedance measurements.

The spectral response of the photovoltage is central to evaluating band gap and the impurity contribution to the photoelectrode (PE) behavior. This response and the quantum efficiency of the PE must be determined as new compounds or alloys are introduced. Further, the transient photoresponse can be used to evaluate both the flat-band potential and the individual electron and hole exchange currents.

In the areas of organic materials, emphasis is on synthesis of compounds related to HMTSF-TCNQ. When new charge-transfer compounds are prepared, they are subjected to a series of physical experiments that include optical and infrared spectral measurements, dc and microwave complex conductivity, and electron spin resonance (ESR) studies.

Theoretical work integrates with the experiments, including both analysis of particular experiments and the development of general models by which the wide range of results can be understood and from which chemical principles for modification of the materials can be deduced.

Progress

In the current investigations of semiconducting oxides for energy conversion and electrochemical applications, mixed phase alloys of several transition metal oxides have shown promising results, particularly $Ti_xV_{1-x}O_2$ using both single-crystal and ceramic specimens. In experiments on these materials, the optical absorption spectrum and the peak in the photoelectrolysis spectrum shift continuously as a function of x, the fractional T concentration. For $Ti_{0.75}V_{0.25}O_2$, the edge of the PE spectrum is shifted approximately 1 eV from that found in TiO_2 to 2.25 eV, close to the value needed for efficient solar energy utilization (Ref. 1). Large area Ti_x-$V_{1-x}O_2$ films with good electrical and optical properties have now been prepared by rf sputtering techniques. VO_2 films prepared by this process are observed to exhibit high temperature switching characteristics identified with high quality VO_2 crystals. Several perovskite compounds, including $NiTO_3$ and $FeTiO_3$, have been obtained as 0.5 cm diameter single crystals by flux melt techniques. Further work is now carried out with support from the Office of Naval Research and the U.S. Army.

A new organic charge transfer salt HMTSF-TCNQ-F_4, which is isostructural with the conductor HMTSF-TCNQ, has been obtained (Ref. 2). The new compound is an electrical semiconductor with a resistivity of $\rho(300K) \sim 10^3$ Ω-cm and an E_{act} of ~0.3 eV. ESR measurements indicate a phase transition near T = 100 K and a small, isotropic spin susceptibility that is weakly temperature dependent. A series of alloys of $HMTSF(TCNQ)_x(TCNQ\text{-}F_4)_{1-x}$ is in preparation.

TTF-TCNQ crystals of sufficient magnetic purity had previously been prepared so that only one EPR signal is visible, and no Curie susceptibility is detectable down to 4.2 K. Below the 38 K phase transition, the magnetic susceptibility obtained by integrating the EPR signal is the sum of two activated components, one with E_{act} ~100 K and the other with E_{act} ~10 K, which are precisely the activation energies for the low-field dc conductivity, and the apparent differences between the activation energies for conduction

and magnetism result from the difference in preexponential factors. These results together with results of non-ohmic voltage-current measurements now imply that the important excitations in both experiments are simple single particles rather than phase solitons or spin waves (Refs. 3 and 4).

Stable and reproducible current-controlled bistable electrical switching has been observed in polycrystalline organic semiconducting films (Ref. 5). The effect has been observed in a lamellar structure with a film of microcrystalline Cu-TCNQ between Cu and Al electrodes where the Cu-TCNQ is grown on a Cu substrate by a spontaneous electrolysis technique. The switching effect is insensitive to moisture and is observed over a large temperature range. The current-voltage characteristics reveal an abrupt decrease in impedance from 2 MΩ to less than 200 Ω at a field strength of 4×10^3 V/cm. The transition from a high- to a low-impedance state occurs with delay and switching times of approximately 15 and 10 ns, respectively. Switching with high-power dissipation yields a low-impedance memory state that can be erased by application of a short current pulse. An interpretation of this behavior is based on the bulk properties of the mixed valence semiconductor Cu-TCNQ.

Figure 1 shows a typical dc current voltage curve of one such unit with a Cu-TCNQ layer approximately 10 μm thick. No initial forming was necessary to observe switching, and the electrical characteristics are essentially independent of the direction of the current flow. The cell initially was an ohmic, high-resistance state provided the field strength across the sample did not exceed 3×10^3 V/cm corresponding to V_L; the impedance of this OFF state was 2 MΩ. Above V_L, but below the threshold voltage, V_{th}, the I-V curve shows superlinear or non-ohmic preswitching behavior. At the threshold voltage (5.5 V in this case), an abrupt switching occurs from a high-impedance to a low-impedance state. The low resistance or ON state is non-ohmic with a decrease in the impedance to less than 200 Ω. When the applied voltage is removed, the device acts either as a threshold switch returning to the OFF state or, under conditions of higher power dissipation, as a memory switch remaining in the ON state. When operating as a memory state switch, it is possible to drive the unit back to the high-impedance state by the application of a short pulse of current of either polarity. In addition, the high-resistance state can also be reestablished by allowing the cell to remain for extended periods of time without an external electric field.

Finally, a theoretical model has been constructed to discuss the magnetic phenomena in structurally and chemically disordered solids. The structural disorder is stimulated by incorporating fluctuations in the exchange interactions, and the model is

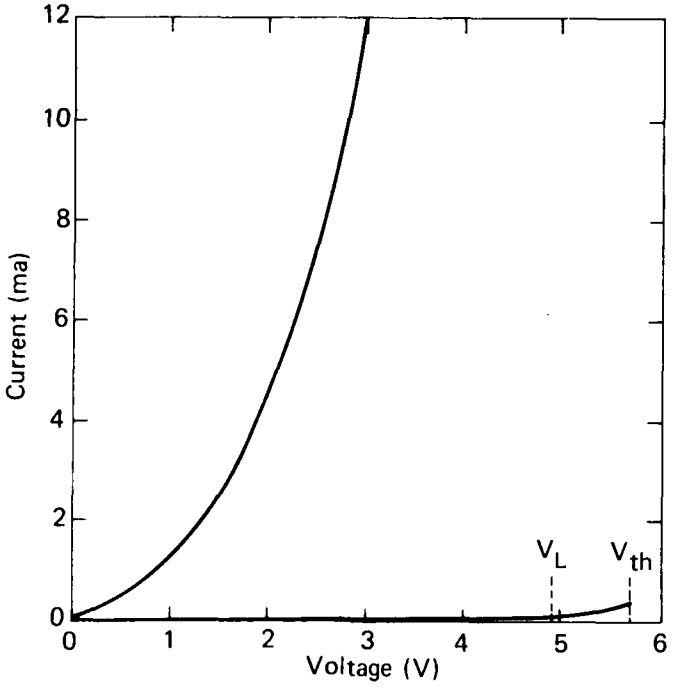

Fig. 1 Typical current/voltage curve, Cu-TCNQ layer ≈ 10 μm thick.

self-consistently solved with the Bethe-Peierls-Weiss approximation. Under appropriate modifications, the model can accommodate site-diluted, bond-diluted, or bond-disordered magnetic systems. The model has been applied mainly to a solid in which positive and negative exchange interactions, in varying concentration, are distributed at random on a lattice (Ref. 6). Depending on the relative abundance of positive bonds, conventional magnetically ordered structures, as well as the spin glass phase, are obtained.

Principal Investigators: Dr. T. O. Poehler, Supervisor, and Dr. K. Moorjani, physicist, in the Quantum Electronics Group, and Dr. J. C. Murphy, senior physicist, in the Microwave Physics Group; all of the Research Center; Professors A. N. Bloch and D. B. Cowan, the Chemistry Department of The Johns Hopkins University, and S. K. Ghatak, a faculty member of the Free University of Berlin. The non-APL colleagues are not funded by the IR&D Program.

References

1. T. O. Poehler, J. C. Murphy, K. Moorjani, and J. W. Leight, "Photocurrent Spectroscopy of Mixed Oxide Semiconductor-Electrolyte Interface Devices" (to be published).

2. M. E. Hawley, T. O. Poehler, T. F. Carruthers, A. N. Bloch, and D. O. Cowan, "Magnetic and Electrical Behavior of a New Organic Charge Transfer Salt", Bull. Am. Phys. Soc., Vol. 23, 1978, p. 424 (in press).

3. A. N. Bloch, T. O. Poehler, and D. O. Cowan, "Chemical Trends in Organic Conductors: Stabilization of the Nearly One-Dimensional Metallic State," Organic Conductors and Semiconductors, T. Pal, G. Bruner, A. Janossy, and J. Solzom (eds.), Springer-Verlag, Berlin, 1977.

4. T. E. Carruthers, A. N. Bloch, T. O. Poehler, and M. E. Hawley, "The Nature of Semiconducting TTF-TCNQ at Low Temperatures," Bull. Am. Phys. Soc., Vol. 23, 1978, p. 381.

5. R. S. Potember, T. O. Poehler, and D. O. Cowan, "Electrical Switching and Memory Phenomena in Cu-TCNQ Thin Films," Appl. Phys. Lett. (in press).

6. K. Moorjani and S. K. Ghatak, "Random Exchange Interactions and the Frustration Effect," Solid State Comm., Vol. 26, 1978, p. 357.

SEMICONDUCTOR PHYSICS

Research was conducted on polycrystalline silicon films, transition metal boride layers, amorphous boron layers, and sputter-ion-source mass spectrometry. Boride and silicon layers are being used to form the bottom electrode and semiconducting layer, respectively, in experimental solar cell structures. Studies of amorphous boron have led to a model for the behavior of hydrogen and carbon impurities in the amorphous matrix. Sputter-ion-source mass spectrometry has led to a better understanding of the positive-ion yields from the ion bombardment of solids.

Problem

The goal of the solid-state research project is to develop an understanding of phenomena in thin films and bulk materials in order to provide basic backgrounds and innovative ideas leading to

the development of new and improved electronic devices and circuitry. The project is both theoretical and experimental and ranges from fundamental concepts to practical device development. Both the crystalline and the noncrystalline phases are studied. This is a broad program with emphasis on those areas where, by virtue of experience and knowledge, advances in the field can be anticipated.

The present research problem is concerned with thin vacuum-deposited films. Research in the past has played an essential role in integrated circuits and microelectronics. Thin films are used as interconnections, electrodes, and dielectrics in commercial microcircuits, and for photodetectors, reflective and antireflective surfaces, and interference filters, as well as Schottky diodes, tunnel devices, superconducting junctions, etc. Exploration of thin-film transistors led to the development of field effect devices such as MOS and MIS single-crystal devices. Progress in thin-film semiconductors for active devices however has been slow and even stalled. It is now believed, through careful detailed studies using recently available analytical instruments, that significant advances can be made toward active thin-film devices.

The study is relevant to solar cells, vacuum processes in space, large area devices, electronics circuitry, and the physics of amorphous and crystalline layers. It is relevant to problem areas R011-02, Solid State Physics; R021-02, Physical Electronics; and R021-03, Electronic Components, as listed in Naval Research Requirements ONR INST 3910.2, January 1977.

Objective

The present overall objective is to develop the maximum useful electronic properties in vacuum-deposited crystalline and noncrystalline semiconducting layers. This objective necessitates research in interfacial interactions, grain structure, and impurity effects as well as physical phenomena in films. Extreme purity and large defect-free crystallites are absolutely essential. Work at APL in the past has concentrated on methods of producing the extreme purity required (Ref. 1). A steady improvement in the purity of the films has been achieved by extensive use of secondary-ion mass spectra analysis coupled with appropriate changes in vacuum system and procedures. Studies must now turn to techniques for improving the crystallite size.

A second objective is to develop stable conducting layers that are capable of withstanding high temperature and that do not react with materials such as silicon. Such layers may be used, for example, as conductors and resistors in microcircuits and as back electrodes in diodes and avalanche devices. The transition

metal diborides are particularly good candidates for these layers. Compounds such as TiB_2, for example, have a melting point of about 2900°C, a hardness close to diamond, and a resistivity of 9 to 15 μΩ-cm. TaB_2, ZrB_2, and CrB_2 are other candidates for this study.

A third specific objective is to gain an understanding of the role of impurities in amorphous boron layers so that the layers may be applied to useful electronic functions.

Approach

Pure samples are formed in high vacuum under very clean conditions. Deposition rates and substrate temperaures are controlled to achieve various supersaturation ratios. It has been shown previously that the supersaturation ratio influences grain size, but this phenomenon requires further detailed study (Ref. 2). The effect of impurities, particularly gaseous impurities, on grain growth must be examined. The influence of fluxes and underlying layers must also be explored.

Up until now, the p-n junctions made in silicon films were formed by a double diffusion technique (Ref. 3). Double diffusions take considerable time, are limited to surface regions only, and produce a particular type of profile. It is preferable to be able to dope during deposition so that films with controlled impurity profiles can be formed. Doping during deposition will thus be carried out from an electron beam heated boron source. Initially, the p-type silicon films will be doped with phosphorous by diffusion, forming p-n junctions. Diodes, junction transistors, and field effect transistors will be formed and evaluated. Schottky barriers to the polycrystalline sample will also be examined.

Studies are also being carried out on transition metal diborides such as TiB_2. Films are being formed from separate layers of titanium and boron, which are deposited consecutively. The TiB_2 forms by diffusion very rapidly at temperatures between 800 and 900°C. The TiB_2 layers have been used successfully as the bottom electrode for silicon films. Silicon samples using this electrode on sapphire have been processed at 1000°C without any noticeable detrimental effects. A TiB_2 layer on a ceramic substrate has been elevated to over 1200°C by self-joule heating; this raises some interesting possibilities. The temperature coefficients of resistance, the stability of the films with time, the reaction time of the films, and the grain structure must be determined before a complete use of the material is possible. The optical properties of the materials may also be examined.

The samples are examined by X ray, by secondary ion mass analysis, and by scanning electron microscope. Thus, the atomic structure, the grain structure, and the chemical composition are determined. The secondary ion mass spectrometer (SIMS) is particularly important in determining impurities, doping profiles, and interfacial reactions. Special attention must consequently be given to its calibration, which requires the knowledge of sputtering ion yields of a particular species from a particular matrix. For many years, it had been assumed that sputtering with ~10 KeV primary ions produced secondary ions having a narrow energy distribution in a low energy range (0 to 50 eV). However, this has been found to be incorrect, especially for singly ionized elemental species, X^+ (Ref. 4). Accordingly, the secondary ion energy distribution (SIED) has to be known for accurate ion yield evaluation. The mass spectrometer at APL is constructed in such a way that these SIED curves can be obtained. To contribute to the body of knowledge on ion production by sputtering, many classes of solids must be studied.

Progress

The nature of this program demands that the research efforts be carried out in parallel rather than sequentially. Thus, concurrent studies in crystalline growth, conducting layers, junction formation, and SIMS analysis are carried out.

Details of the crystallite growth process using scanning electron microscope photographs of film cross sections have aided the progress of growing large grains in silicon from small seeds on the substrate. Important information on the increase of grain size with increase in film thickness was obtained. Figure 1 illustrates the growth of lateral grain size with thickness. Curves of diffusion length, open-circuit voltage, and short-circuit current versus grain size were obtained. Figure 2 shows the effect of grain size on open-circuit voltage (V_{oc}) and short-circuit current (J_{sc}). Linear extrapolation of the data indicates that grain diameters of approximately 30 μm would yield devices with an efficiency of about 10%. (The grain lengths perpendicular to the substrate would be equal to or greater than 30 μm.) The effect of grain size on photovoltaic properties of p-n junctions has been examined using a series of samples having 0.3 μm to 5 μm grain diameters (Ref. 2). Silicon was also deposited successfully on top of metal boride (TiB_2) layers. The TiB_2 conducting layer was formed from the diffusion couple, boron/titanium.

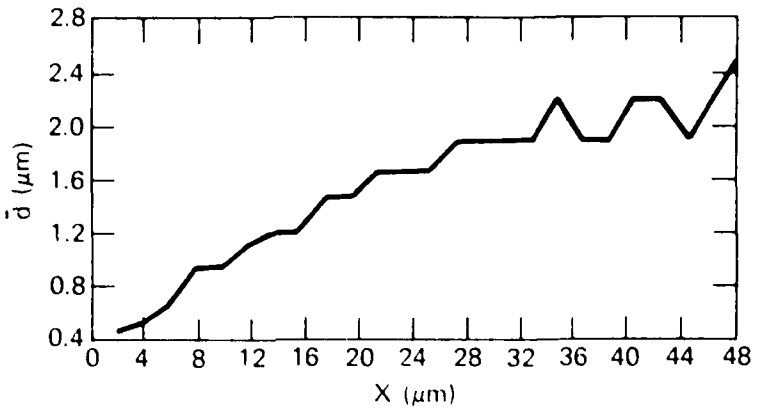

Fig. 1 Plot of average grain diameter ($\bar{d}$) versus film thickness (X).

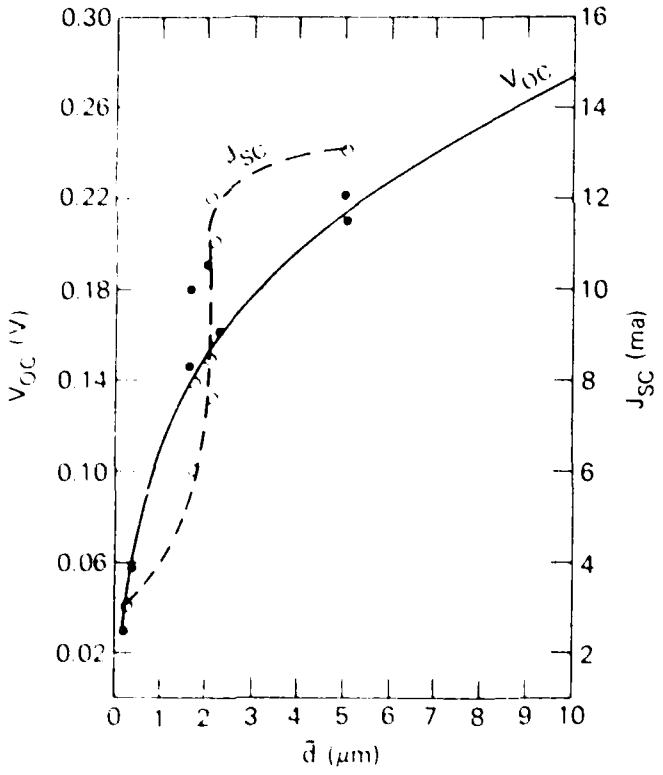

Fig. 2 Open-circuit voltage and short-circuit current as a function of grain diameter of silicon samples.

Studies in 1978 included work on amorphous boron layers. The intent was to determine the role of impurities such as hydrogen and carbon in the amorphous matrix (Ref. 5). The results indicate that films containing hydrogen show an increase in resistivity with increasing hydrogen content. The optical absorption was found to decrease with increasing hydrogen content. No nonlinearities were found in low-temperature conductivity measurements on layered samples. These results, in conjunction with the earlier electron spin resonance data (Ref. 6), which showed a decrease in spin density with increasing hydrogen (but not carbon) content, led to a model for amorphous boron with a high density of localized levels in the energy gap. The density of localized levels near the band edges seems to be reduced by the hydrogen. The carbon and hydrogen appear to bond to the icosahedral atom groups of the boron in a different manner; the carbon must replace intericosahedral bonds whereas the hydrogen must accommodate dangling bonds on the icosahedra themselves. Both of these processes tend to localize valence electrons and thus decrease the carrier mobility in the films. Proposed density of state models for crystalline amorphous boron are given in Fig. 3. Hydrogen tends to reduce the number of "intrinsic" states near the Fermi energy.

Work on ion yield from a sputtering source was carried out on glasses (Ref. 4). Glasses constitute a class of solids advantageous for studies of ion production. Many elements can be uniformly dispersed in an amorphous matrix; furthermore, work function differences for elements in a specified glass do not arise. In addition, one is not worried about sputtering rate differences or other sputtering artifacts. Several glasses obtained from the National Bureau of Standards were examined. The glasses contain known amounts of additives such Ti, Mn, Fe, Co, Cu, and Zr, as well as the more common elements O, Mg, Al, Si, Ca, and B. A strong linear correlation between the partitioning of the primary energy and the first ionization potential of the element was observed.

Principal Investigators: Dr. C. Feldman, Supervisor, Dr. F. G. Satkiewicz, senior chemist, and Dr. N. A. Blum, senior physicist, of the Solid State Physics Group in the Research Center. Dr. G. W. Turner, doctoral student at The Johns Hopkins University; Dr. G. Jones, postdoctoral fellow, the Solid State Physics Group; and Dr. H. K. Charles, Jr., senior engineer, the Microelectronics Group of the Engineering Facilities Division.

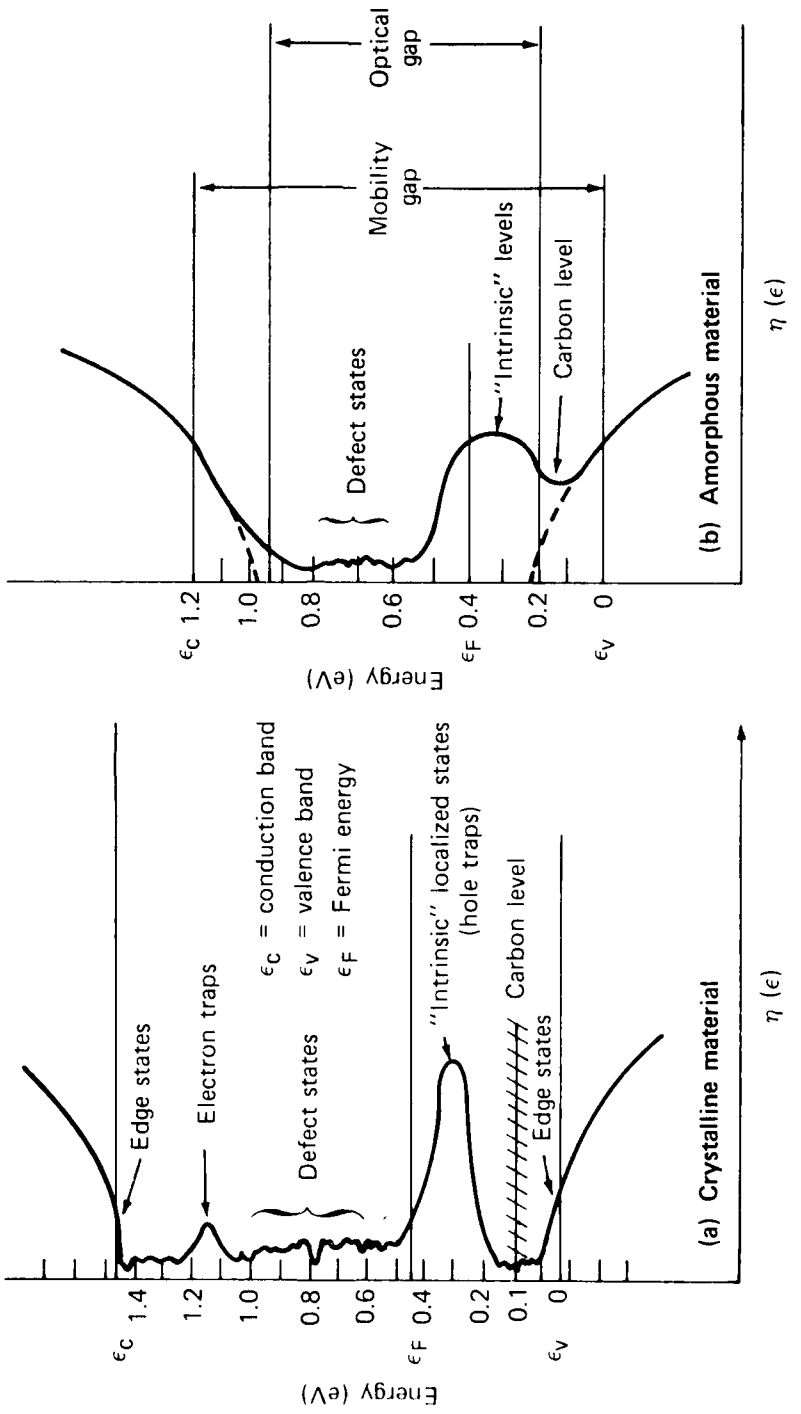

Fig. 3 Proposed density for electron states η (ϵ) as a function of energy for boron.

References

1. C. Feldman and F. G. Satkiewicz, "Mass Spectra Analyses of Impurities and Ion Clusters in Amorphous and Crystalline Silicon Films," J. Electrochem. Soc., Vol. 120, 1973, p. 1111.

2. C. Feldman, N. A. Blum, H. K. Charles, Jr., and F. G. Satkiewicz, "Evaporated Polycrystalline Silicon Film for Photovoltaic Applications - Grain Size Effects," J. Electron. Mat., Vol. 7, 1978, p. 309.

3. C. Feldman and R. Plachy, "Vacuum Deposited Silicon Devices on Fused Silica Substrates," J. Electrochem. Soc., Vol. 121, 1974, p. 685.

4. F. G. Satkiewicz, "Relative Fields of Positive Ions Sputtered from Solid Glasses," Proc. 25th Annu. Conf. Mass Spectrom., 1977, p. 312.

5. G. W. Turner, "The Effects of Carbon and Hydrogen on the Electronic and Optical Properties of Amorphous Boron Thin Films," PhD thesis, The Johns Hopkins University, Baltimore, MD, 1978.

6. C. Feldman, H. K. Charles, Jr., F. G. Satkiewicz, and J. Bohandy, "Electrical Properties of Carbon-Doped Amorphous Boron Films," J. Less-Common Metals, Vol. 47, 1976, p. 141.

THE JOHNS HOPKINS UNIVERSITY
APPLIED PHYSICS LABORATORY
LAUREL, MARYLAND

WAVE PROPAGATION AND SCATTERING

Stochastic vector variational principles are formulated in vector-dyadic form to yield the statistical moments of the components of the scattered electromagnetic field amplitude. Mathematical formulas are derived for analyzing the internal wave front induced by a submerged body moving within a stratified fluid. Fourth-neighbor Ising models are analyzed to examine the influence of the interatomic potential on phase transitions.

Problem

The investigation of wave propagation and scattering involves three subproblem areas, namely, the propagation, the scattering, and the absorption of electromagnetic waves. Understanding in these three areas provides potential tools for characterizing various media such as the ocean's surface, particulate matter in the ocean, chaff and other obscurants, aerosols, bubbles, and military targets. Except for the most idealized situations, the analytic treatment of these problems remains approximate and fails to provide built-in measures of validity. We recently achieved a breakthrough when we developed a variational principle to analyze the scattering of scalar waves by a random rough surface at which homogeneous boundary conditions were satisfied. It is important that this method be generalized to include vector waves with both absorption and scattering from random surfaces and volumes.

When a body moves through a stratified fluid, it excites disturbances of the fluid that travel outward from the body in all directions. If the speed of the body is greater than the speed of the fastest internal wave, the wave front is closely analagous to a "Mach cone." The behavior of these disturbances at positions far from the wave front is well known in the linear hydrodynamic approximation to the thin thermocline problem. However, the region in the immediate neighborhood of the wave front is not amenable to the analytic techniques that have been applied to this problem, and it is important to develop techniques to predict behavior in this transition region.

Changes of state, one of the most common characteristics of materials, include the gas-liquid, paramagnetic-ferromagnetic, and disordered alloy-ordered alloy transitions. These diverse transitions show remarkably similar characteristics, which has led to intensive investigation of the Ising model in which these transitions are equivalent. It is well known that the simple nearest-neighbor Ising model has been particularly rewarding for deducing

the fundamental nature of phase transition in the vicinity of the transition point. Certain universality theorems suggest that behavior in the critical region is insensitive to the interaction range of the potential (as long as the range is finite), and it is important to develop general theorems for deducing thermodynamic behavior of higher-neighbor models.

Objective

The objective of the work on scattering and absorption by random media is a better understanding of these phenomena that could lead to improved design and utilization of systems such as radar, sonar, altimeters, and radiowave communication links. The main objective during this past year has been to generalize the stochastic variational principle to account for absorption and for the vector nature of the electromagnetic field.

The goal of our analysis of internal wave fronts is to elucidate characteristics of the disturbances that are excited when a body moves through a stratified medium and, in particular, the detailed nature of the transition zone that occurs at the wave front when the speed of the body is greater than the speed of the fastest internal waves.

The objective of the theoretical modeling of phase transitions is to deduce the manner in which the characteristics of these transitions depend on the interatomic forces, which could aid in the prediction and correlation of material properties.

Approach

Dyadic Green's function formalisms have been used by others to obtain variationally invariant expressions for an arbitrary component of the field scattered by deterministic scatterers, and we extend these results to obtain invariant expressions in the case of stochastic scatterers.

We analyze the linear hydrodynamic equations near an internal wave front by applying the stationary phase approximation technique for the case where the stationary point coincides with the end point of integration.

Graph-theoretic techniques are used to develop six terms in virial-like high-temperature series for fourth-neighbor Ising models, which are then analyzed to obtain the coexistence curves for various sets of interaction energies.

Progress

Work carried out during the previous year in applying the scalar stochastic variational principle to improve the first-order perturbation result for scattering from classic model rough surfaces was published during this reporting period (Ref. 1). More recent research on the development and comparison of exact, variational, and first-order-perturbational solutions to the problem of scattering of a scalar wave for a simple example of a classic random rough surface model is described in detail in another publication (Ref. 2). In brief, these results demonstrate that the variational principle accounts for multiple scattering, at least for the idealized problem. In addition, we have formulated stochastic vector variational principles for treating the scattering problem depicted in Fig. 1. Here a plane wave electric field polarized in the direction $\hat{E}_i$ is incident on a stochastic assembly of scatterers contained within a volume V_0, and interest is on the amplitude of the wave scattered in the $\vec{k}_s$ direction and polarized in an arbitrary direction $\hat{x}_j$. These principles have been formulated in vector-dyadic

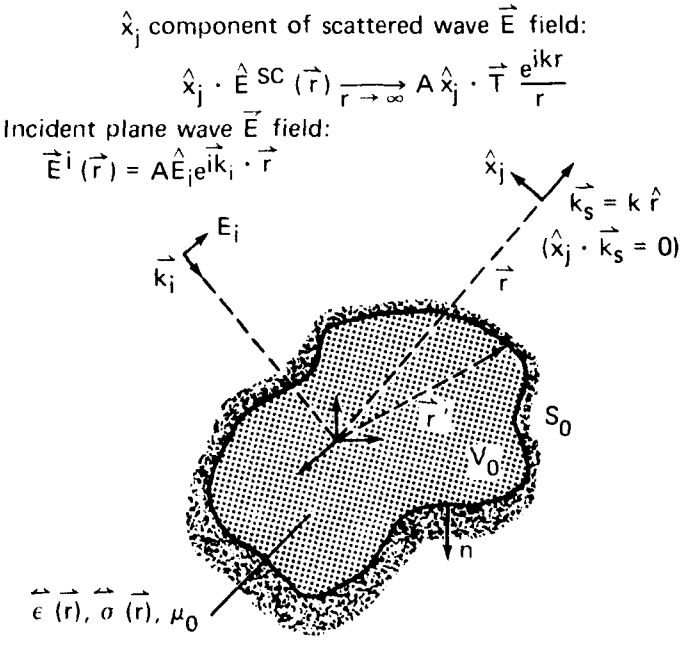

Fig. 1 Geometry for scattering by a finitely conducting, dielectric scattering volume, V_0, with self-adjoint, ϵ and σ, and with free-space permeability, μ_0.

form to yield the statistical moments of the components of the scattered field amplitude. The formulations are for conducting and dielectric scatterers with random characteristics and are based on previous formalisms developed for scattering from deterministic objects. Detailed descriptions of the results are included in Ref. 3.

We have solved the linearized hydrodynamic equations describing the internal wave field induced by a submerged body moving at constant speed in a thin thermocline and have obtained the far-field limit for the steady-state thermocline displacement and velocity in the neighborhood of the internal wave Mach front (Ref. 4). Exploration of this region required asymptotic solutions of the hydrodynamic equations to a higher degree of approximation than had been achieved previously. These improvements required the analytic evaluation of certain integrals and sums, which we were able to achieve. The method of solution is rather general, but explicit results are obtained only for the case of an arbitrarily thin and infinitely deep fluid with a rigid upper surface. The fields described by the hydrodynamic equations are resolved into two parts, one being that which propagates with the sound velocity (infinitely fast in the incompressible fluid) and the other being the internal wave field. The short internal waves travel more slowly than the long waves so that the front is expected to be a region of smooth transition from the internal wave field to the field that propagates with the sound velocity. The analysis demonstrates this to be the case and predicts the behavior of the transition region in detail.

The coefficients in a virial-like expansion for the free energy of fourth-neighbor Ising models were obtained for arbitrary interaction energies (Ref. 5). This expansion, which is valid for all densities, was shown to reproduce previous results that were valid only at the critical density or only for equal strength interactions. The reduced phase diagrams (cf. Fig. 2) for these models are not sensitive functions of the histogram shape used to mimic various potentials but depend mostly on the effective number of nearest neighbors.

Principal Investigators: Drs. R. H. Andreo, senior physicist, and R. A. Farrell, Supervisor, the Theoretical Problems Group; Dr. E. P. Gray, Research Center Office; Dr. R. W. Hart, Chairman of the Research Center; Dr. J. A. Krill, senior engineer, the Ship Radar Systems Group, Fleet Systems Department; and Dr. P. H. E. Meijer, Professor of Physics, The Catholic University of America. Dr. Meijer is not funded by the IR&D Program.

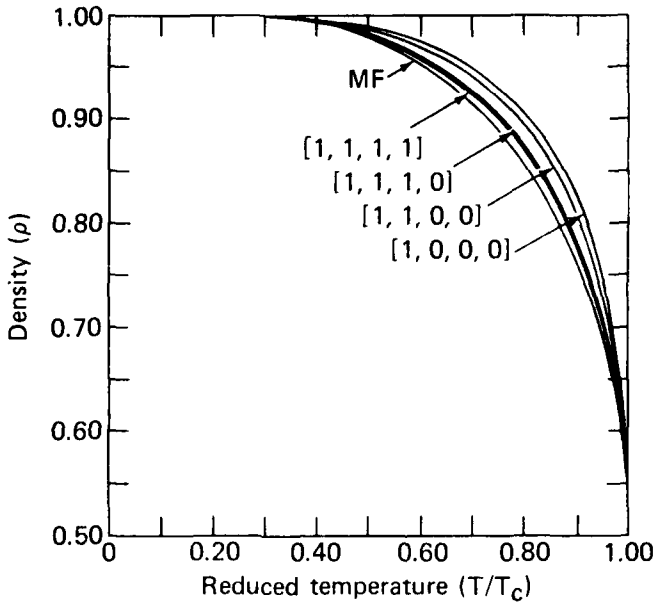

Fig. 2 Coexistence curves for n^{th} neighbor models on the face-centered-cubic lattice. Density is the fraction of sites that are occupied; T_c is the critical temperature. *The molecular field (infinite range) curve is labeled MF; the other curves are* labeled by the values of the i^{th} neighbor interaction energies, J_i $[J_1, J_2, J_3, J_4]$, with all the other J's equal to zero.

References

1. E. P. Gray, R. W. Hart, and R. A. Farrell, "An Application of a Variational Principle for Scattering by Random Rough Surfaces," Radio Sci., Vol. 13, No. 2, 1978, pp. 333-348.

2. J. A. Krill and R. A. Farrell, "Comparisons between Variational, Perturbational, and Exact Solutions from a Random Rough Surface Model," J. Opt. Soc. Am., Vol. 68, No. 6, 1978, pp. 768-774.

3. J. A. Krill, "The Variational Treatment of Stochastic Scattering Problems," Ph.D. dissertation, 1978.

4. R. W. Hart, E. P. Gray, and R. A. Farrell, "Internal Wave Fronts in the Theory of Incompressible Flow around Bodies Moving in a Stratified Medium" (in preparation).

5. R. A. Farrell, S. Favin, J. T. Sullivan, S. Vilmol-vanich, and P. H. E. Meijer, "Coexistence Curves for Fourth-Neighbor Ising Models on the Face Centered Cubic Lattice" (to appear in Phys. Rev., 1979).

THE JOHNS HOPKINS UNIVERSITY
APPLIED PHYSICS LABORATORY
LAUREL MARYLAND

LABORATORY-WIDE RESEARCH AND EXPLORATORY DEVELOPMENT

INTRODUCTION

This component of the IR&D Program fosters initial investigation of new concepts and techniques in the task-oriented units of the Laboratory. Emphasis is placed on short-term projects to provide the basis for soliciting sponsors for future work.

A prime objective is the development of expertise in frontier areas of technology within the engineering-task-oriented administrative units of the Laboratory, through exploring the feasibility of new concepts preliminary to the preparation of proposals to prospective funding agencies. Individual projects are generally small, fractional man-year efforts exploring the validity and/or utility of innovative approaches to known problems. Sixteen projects were carried out during this reporting period, the total level of effort amounting to about 10 man-years. Results are described in more detail in the more than 30 publications and reports referenced in the following articles.

ATMOSPHERIC SCIENCE

NEW SATELLITE INSTRUMENTATION

Analyses of data obtained from spacecraft and the development of new spacecraft instrumentation provide significant new understanding of the earth's atmosphere, ionosphere, magnetosphere, and solar and interplanetary phenomena. Results are discussed below and described in several publications published during fiscal year 1978 or currently in press.

Problem

Understanding the complicated physical and chemical processes involved in solar-terrestrial relationships is fundamental to a wide variety of important civilian and military applications such as radio and optical transmissions, weather prediction, and the modeling of the nuclear burst environment.

The sun dominates the earth's environment in many ways. Its light supplies energy to life on earth and to weather processes. Shorter wavelength energy ionizes the atmosphere producing the ionosphere, and the constant outflow of the solar wind plasma distorts the earth's magnetic field into the comet-like configuration called the magnetosphere. Disturbances on the sun produce a variety of changes in the interplanetary environment that, in turn, produce geomagnetic storms, auroras, polar radio blackouts, and other significant effects on the earth's environment. There is also statistical evidence for changes in weather patterns on the earth associated with subtle changes in the magnetic field of the sun (referred to as the "interplanetary magnetic field"). (Besides the influence of the sun, evidence also indicates the existence of high-energy particles in the earth's environment whose origin is Jupiter.) However, these processes are difficult to study and, in spite of their importance, many aspects remain poorly understood.

Objective

The Laboratory's Space Physics and Instrumentation Group is internationally recognized for its research activities directed toward developing an understanding of the chemical and physical processes involved in the earth's atmosphere, ionosphere, and magnetosphere and in solar and interplanetary phenomena. Of particular interest are the properties and characteristics of particles and magnetic fields that comprise the interplanetary and earth environments. Objectives aimed at understanding these phenomena include

1. The investigation of the dynamic properties of the the aurora and the relationship to precipitating energetic particles, Birkeland currents, and plasma instabilities,

2. Determination of the control of coronal magnetic fields on the solar wind,

3. Determination of the propagation characteristics of solar and magnetospheric energetic particles, and

4. The investigation of particle sources in the Jovian magnetosphere.

Figure 1 indicates the regime of the heliosphere analyzed in the correlative solar-terrestrial studies completed this year. Results are described in detail in numerous publications (Refs. 1 through 13).

The objective of the present IR&D project is to support the overall program with timely complementary investigations that otherwise could not be carried out.

Approach

The approach to a solution of the problems outlined above centers on the unique and extensive data base acquired by a variety of APL experiments on board numerous NASA and DoD spacecraft. The IMP-7 and -8 spacecraft, with nearly circular orbits, are the only spacecraft that can sample the interplanetary inputs to the magnetosphere and upstream magnetospheric emissions over a wide range of longitudes in a relatively short time. Therefore, they provide a nearly ideal data base for solar-terrestrial studies. With their unique orbits, they have provided a new understanding of solar-interplanetary and magnetospheric physics during the decline and minimum periods of Solar Cycle 20. Now, with the rise of Cycle 21 and the increased solar activity and corresponding decrease in interplanetary order, new relationships must appear in the IMP data.

The Voyager Low Energy Charged Particle instruments have also been normalized to our instruments on IMP-7 and -8, and future studies can be carried out using IMP-8 throughout the Jovian encounters of Voyagers 1 and 2 (March and July 1979, respectively). For example, Jovian electrons show a "solar cycle" variation at 1 AU that will be studied with Voyager and which, through the normalization with IMP-7 and -8, may be traced accurately back to 1972.

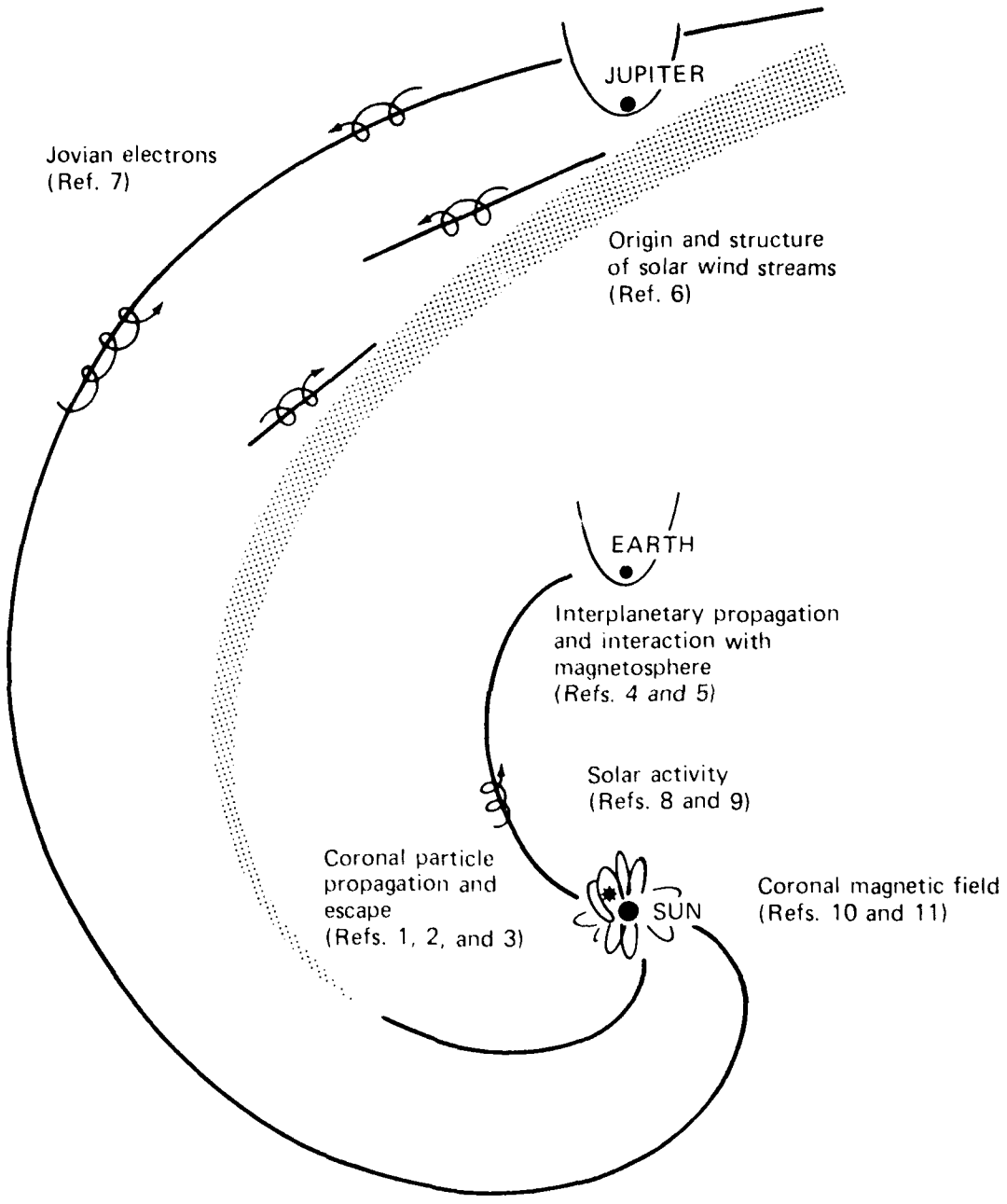

Fig. 1 Schematic representation of the heliosphere and the regime investigated in each of the referenced studies conducted during 1978.

This data base is exploited through the extensive research program of the Physics and Instrumentation Group and involves the participation of many other organizations, including the universities of Tokyo, Calgary, Kiel, New Hampshire, Kansas, and Iowa; the Max-Planck Institutes in Munich and Lindau; and the Danish Meteorological Institute, the Kiruna Geophysical Institute, the Norwegian Defence Research Establishment, NOAA, AFGL, and the Canadian Department of Energy, Mines, and Resources.

The approach adopted in the present project is to provide a postdoctoral fellow (R. D. Zwickl), guided by Dr. E. C. Roelof, to pursue timely lines of research that emerge from and complement the extensive research program. The IR&D project also utilizes extensive APL instrumentation experience to a needed new type of energetic particle detector.

Progress

The project achieved significant results during the present reporting period, as outlined below and as described more fully in the referenced publications.

Coronal Particle Propagation. Roelof, Krimigis, and Gold (Ref. 1) demonstrated (using solar wind mapping of interplanetary field lines) that coronal magnetic fields can produce astonishingly ordered energetic particle emission profiles (e.g., over equatorial coronal holes). In Ref. 2, Zwickl et al. identified the eastern boundary of a solar wind stream in the vicinity of a nearby active region as a likely escape location for small solar particle events enriched in high-Z ions during the years 1972-76 at the end of Solar Cycle 20. From the similarity of the proton and alpha spectral indices in the small Z-rich and large solar flare particle events, Zwickl et al. argued that the higher Z enrichment in the small events was not due to the final acceleration process, but rather to a preenrichment of the flare substrate plasma. Further evidence for this effect was found by Briggs, Armstrong, and Krimigis (Ref. 12). By comparing sequential large flares, they showed that the p/a ratio significantly increased from the first to the second flare, and they claimed that the increase was proportional to the time interval between the first and second flares of the pair. Similar evidence, given in Ref. 13 from spacecraft measurements taken roughly a solar cycle apart (Mariner IV, 1964-65, and IMP-7/8, 1973-74), shows that energetic solar particles are often preferentially injected into the interplanetary medium at locations remote ($\geq 60°$) from their likely acceleration sites in active regions.

AD-A086 948 JOHNS HOPKINS UNIV LAUREL MD APPLIED PHYSICS LAB F/G 5/2
INDIRECTLY FUNDED RESEARCH AND EXPLORATORY DEVELOPMENT AT THE A--ETC(U)
DEC 79 R W HART N00024-78-C-5384
UNCLASSIFIED JHU/APL/SR-79-2 NL

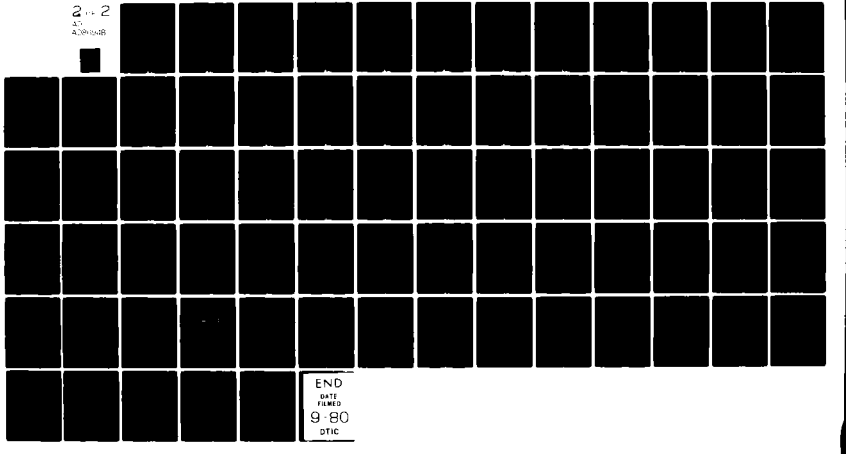

Interplanetary Propagation and Interaction with the Magnetosphere. Zwickl and Roelof (Ref. 4), using <1 MeV proton anisotrophy data from IMP-7 and -8, demonstrated that the dominant mechanism for interplanetary transport of these particles transverse to the magnetic field is simply the $\underline{E} \times \underline{B}$ drift, i.e., the particle guiding centers stay on the "same" field line without measurable transverse scattering. In order to draw these conclusions on interplanetary propagation, they identified and quantitatively compensated for several effects due to proximity to the magnetosphere (e.g., reflection of particles and magnetospheric bursts). Their results further validate the field-line mapping technique described by Roelof and Gold in Ref. 5, which is central to the prediction of the history of energetic particle events.

Origin and Structure of Solar Wind Streams. Mitchell, Roelof, and Wolfe (Ref. 6) compared solar wind velocity structure mapped from Pioneers 10 and 11 as far as ~ 5 AU with that mapped from IMP-7 and -8 to deduce strong latitude gradients. However, they showed that these structures agreed with the general shape of coronal magnetic polarity regions for series of recurrent streams from Carrington Rotations 1587 through 1640.

Jovian Electrons. Regarding Jupiter as a source of test particles (energetic electrons) to probe the outer heliosphere, Gold and Roelof (Ref. 7) have presented a new model for propagation in which the solar wind stream-stream interaction regions form "diffusive walls" to "scatter-free cavities." Evidence for their model is drawn from the relationship of Jovian electron events and solar wind stream structure observed between 1 and 6 AU. Thus, Jovian electrons have revealed to us a new propagation model that must apply to all particles in the heliosphere (Jovian, galactic, or solar) and that had not been obtained from solar or galactic particle measurements alone.

Supporting Research and Technology Activities. A vital part of the research activity concerns the development of new instrumentation that advances the state of the art in the detection and analysis of energetic particles in planetary magnetospheres and in interplanetary space. These activities date back to the mid-1960's when solid-state particle detectors with high energy thresholds were successfully flown on the IMP-4, -5, -6, -7, and -8 spacecraft. The development of low-noise solid-state particle detectors with very low energy thresholds for both electrons and protons resulted in the selection of these detectors by NASA for the Voyager Program, which has carred them to the vicinity of Jupiter. Similar instruments have been selected by NASA for the Galileo Program, in which a spacecraft will be placed in orbit around Jupiter, and the Solar Polar Program, in which APL instruments will fly by Jupiter

and then loop over the pole of the sun. Very thin solid-state detectors, presently being flight-tested on board the Voyager spacecraft, will be part of the Active Magnetospheric Particle Tracer Explorer (AMPTE). In this program, the source of the Van Allen particles will be investigated by injecting an artificial ion cloud outside of the magnetosphere and following the progress of these tracer ions with instrumentation aboard the APL-built Charge Composition Explorer Spacecraft.

Our present particle telescope development efforts use extremely thin foils (5 to 10 μ g/cm^2) as telescope front elements, with particle time-of-flight measurement though the detection of secondary electrons emitted when incident particles penetrate the front and back telescope elements. This concept has now been proven in laboratory trials using microchannel array plates for secondary electron detection and a solid-state detector for the rear element. Present effort is focused on the fabrication of flight electronics, including a microprocessor-based data system, and a flight-worthy detector head with improved secondary electron optics. This ion composition telescope, covering an energy range (approximately 5 to 100 keV/nucleon) not heretofore measured with composition instruments in the earth's magnetosphere, is being prepared for a test flight in prototype form on the German Firewheel Program.

The Firewheel is an experimental spacecraft to be launched in March 1980 into a 200 km by 10 R_e equatorial orbit on the second test flight of the Ariane rocket. The spacecraft is being provided by the West German Max-Planck Institute for Extraterrestrial Physics. It contains 300 kg of chemical releases to be injected into the earth's magnetosphere; APL has been invited to provide low-energy particle instrumentation for the mission. Because Firewheel is a low-budget, short-lived program (the spacecraft is battery powered, with a lifetime of one to two months) it affords a unique opportunity to test new technology and detector concepts (the weight and volume available allow prototype fabrication techniques to be used to reduce costs). The orbital data from the prototype ion composition telescope will not only be of great scientific interest — providing for the first time radiation belt composition measurements over the important ring current energy range around the earth — but will also serve to validate a new generation of detector instrumentation developed by the group for the upcoming AMPTE program and for future long-duration NASA spacecraft missions.

Principal Investigators: Dr. S. M. Krimigis, Supervisor, Drs. R. E. Gold, R. W. McEntire, and E. C. Roelof, senior physicists, and Dr. R. D. Zwickl, postdoctoral research fellow, Space Physics and Instrumentation Group of the Space Department.

References

1. E. C. Roelof, S. M. Krimigis, and R. E. Gold, "Coronal propagation and storage at energies ≈ 1 MeV/nuclleon," A Close-Up of the Sun, Eds., M. Neugebauer and R. W. Davies, Jet Propulsion Laboratory Publication 78-70, 1978, p. 219.

2. R. D. Zwickl, E. C. Roelof, R. E. Gold, S. M. Krimigis, and T. P. Armstrong, "Z-rich solar particle event characteristics 1972-1976," Astrophys. J., Vol. 225, 1978, p. 281.

3. E. C. Roelof, S. M. Krimigis, J. T. Nolte, and J. M. Davis, "Energetic solar particle events in 1965: Relationship to coronal magnetic structure" (submitted to J. Geophys. Res., 1979).

4. R. D. Zwickl and E. C. Roelof, "Interplanetary propagation of < 1 MeV protons in non-impulsive energetic particle events" (submited to J. Geophys. Res., 1979).

5. E. C. Roelof and R. E. Gold, "Prediction of solar energetic particle event histories using real-time particle and solar wind measurements," NATO/AGARD Symposium, Operational Modelling of the Aerospace Propagation Environment (Ottawa), AGARD-CPP-238, 1978, p. 27-1.

6. D. G. Mitchell, E. C. Roelof, and J. H. Wolfe, "Latitude dependence of solar wind velocity observed ≥ 1 AU" (submitted to J. Geophys. Res., 1979).

7. R. E. Gold and E. C. Roelof, "Jovian electron propagation via solar wind stream interaction regions" (submitted to J. Geophys. Res., 1979).

8. J. M. Hanson, R. E. Gold, and E. C. Roelof, "Solar Activity Charts for Carrington Rotations 1600-1611," JHU/APL Preprint 78-06, 1978.

9. H. W. Dodson-Prince, E. R. Hedeman, and O. C. Mohler, "Survey and Comparison of Solar Activity and Energetic Particle Emission in 1970," Air Force Geophysical Laboratory Technical Report, AFGL-TR-77-0222, 1977.

10. P. S. McIntosh, "Annotated Atlas of H_α Synoptic Charts for Solar Cycle 20 (1964-1974)," NOAA/EDIS Special Report UAG-70, WDC-A, Boulder, Colo., 1979.

11. J. M. Hanson and E. C. Roelof, "Synoptic Charts of Large-Scale Coronal X-Ray Structure During Skylab, April 1973-February 1974," JHU/APL Preprint 78-05, 1978.

12. P. R. Briggs, T. P. Armstrong, and S. M. Krimigis, "Hydrogen Over Helium Enhancement in Successive Solar Flare Particle Events from the Same Active Region," Astrophys. J., Vol. 228, 1979, p. L83.

13. E. C. Roelof, "Solar Energetic Particles: From the Corona to the Magnetotail," Geophys. Monograph, Vol. 21, 1979, p. 220.

ATMOSPHERIC DRAG EXPERIMENT

It is necessary to understand the interaction between upper atmosphere molecules and satellite surfaces to enable accurate prediction of satellite drag forces. Several theoretical models have been proposed, but whether or not any one of them is valid remains in doubt because of a lack of definitive experimental data. This project proposes and evaluates a simple experiment to obtain the required data.

Problem

Accurate prediction of atmospheric drag forces on earth satellites is important for several reasons. The computation of lifetime and reentry point for satellites such as Skylab and the Russian nuclear-powered satellite that landed in Canada requires this information. So, too, does long-term prediction of ephemerides of navigation satellites. In addition, the design of low-drag satellite configurations and the use of drag forces for attitude control require knowledge of the atmosphere-satellite surface interaction mechanism.

This mechanism has been very difficult to study experimentally because of the necessity of reproducing the required high energy molecular beams on the ground. It has been difficult to study in orbit due to the lack of knowledge of atmospheric density. Theoretically, the interaction mechanism is not yet well understood, due in large part to the lack of experimental data.

Objective

To evaluate the drag mechanism, it was important to design an in-orbit experiment that is accurate enough to distinguish between the various theoretically proposed interaction models, that does not require knowledge of atmospheric density, and that is relatively inexpensive. The objective of this study is the development, in concept, of such an experiment and an examination of its feasibility.

Approach

Consider a flat plate of area A whose surface normal makes an angle θ to the incoming atmospheric beam (see Fig. 1). The atmosphere has density ρ and speed V. The drag force on the plate will be given by

$$F_d = \frac{1}{2} \rho V^2 \, A \cos \theta \, C_D(\theta, i) \, , \qquad (1)$$

where $C_D(\theta, i)$ is the drag coefficient for a plate of material i at incident angle θ. Equation 1 is actually the definition of the drag coefficient.

To measure C_D, it is therefore necessary to know ρ and V. The latter quantity is readily available, but the atmospheric density is highly variable during even a single satellite orbit. Therefore, the following density independent experiment concept is proposed.

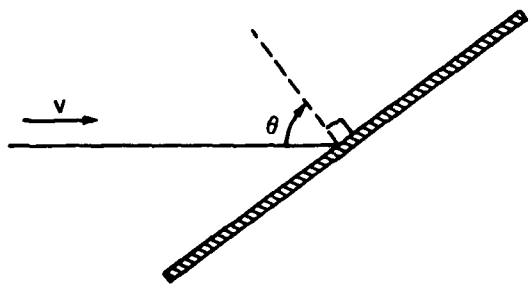

Fig. 1 Geometry of the experiment.

A torsional balance is constructed as shown in Fig. 2. Two plates, whose surfaces are coated with materials i and j, are mounted on the balance. One is fixed at normal incidence to the incoming atmosphere beam, and the other is free to rotate so as to change its incident angle. If the rotation axis is along the arm of the balance, as shown, any lift forces generated by the rotatable plate will not torque the balance in the direction it is free to move. Movable shutters are placed in front of the fixed plate so as to expose an adjustable area of it to the atmospheric beam.

To perform the experiment, an angle θ is selected and the movable plate rotated to this angle. Then, the shutters are adjusted until the balance arm comes to the initial, "zero" position. The forces on the two places must then be equal, hence

$$\frac{1}{2}\rho V^2 A \cos\theta\, C_D(\theta,i) = \frac{1}{2}\rho V^2 \quad a(\theta)\, C_D(0,j)\ , \qquad (2)$$

where $a(\theta)$ is the area exposed by the shutters when equilibrium is reached with the movable plate at angle θ. From Equation 2,

$$\frac{C_D(\theta,\ i)}{C_D(0,j)} = \frac{a(\theta)}{A\cos\theta}\ . \qquad (3)$$

The quantities on the right are known, so the ratio on the left can be determined independently of atmospheric density.

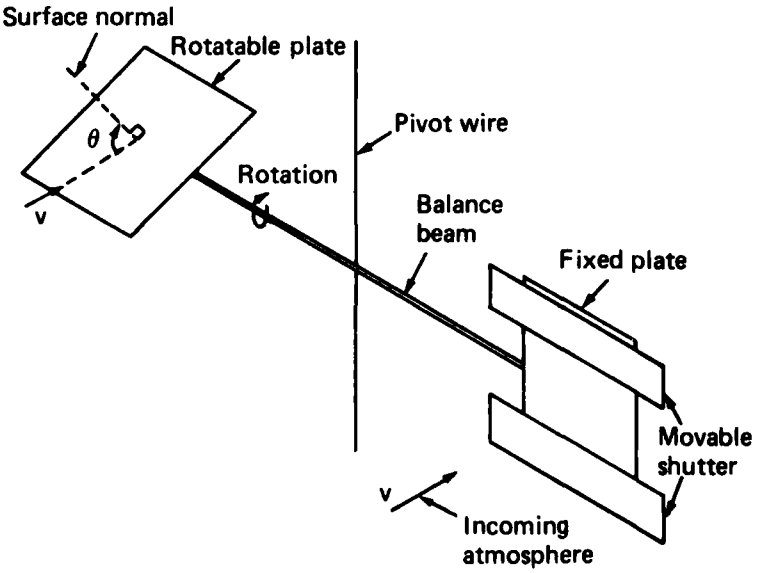

Fig. 2 Conceptual design for the experiment.

By choosing both plates of the same material, the functions $C_D(\theta,i)$ can be determined to within a multiplicative constant. By choosing the plates of different materials, the various $C_D(0,i)/C_D(0,j)$ ratios can be measured, so that a single absolute measurement of C_D for a single material will, in principle, allow all drag coefficients to be determined absolutely.

Other balance configurations can be chosen to compare the lift forces on two plates, or even the lift force on one plate with the drag force on the other.

Progress

To enable the accurate prediction of satellite drag forces, it is necessary to understand the interaction between upper atmosphere molecules and satellite surfaces. To study this interaction, the concept of the following experiment, to be launched and operated from STS and/or Spacelab, has been developed.

A pair of flat plates, possibly of different materials, with adjustable incident angles are mounted on a sensitive torsional balance. The plates are exposed to the incident atmospheric stream. One plate is rotated to a desired incident angle; shutters shielding the other plate are moved to adjust the area of it which is exposed. In this way, the balance is steered to the null position, and drag forces variation with incident angle and surface material can be measured without knowledge of atmospheric density. The accuracy of the experiment would be great enough to establish the molecule-surface interaction mechanism that is operating. The instrument could then be used in the non-null mode to measure atmospheric density.

The experiment was designed in concept and its feasibility demonstrated. It was found that relative drag force could be measured as a function of incident angle to an accuracy of 0.5% and that measurements could be taken at 4 min intervals. This precision would allow most proposed drag mechanisms to be distinguished from one another. Accordingly, this project led to the preparation of a formal proposal and its submission to a prospective funding agency.

Principal Investigator: Dr. R. R. Newton, Supervisor, Space Sciences Branch, and Dr. A. D. Goldfinger, senior physicist, Space Analysis and Instrumentation Group, of the Space Department.

THE JOHNS HOPKINS UNIVERSITY
APPLIED PHYSICS LABORATORY
LAUREL, MARYLAND

SALT DRIFT

General methods of data reduction to obtain aerosol size spectra are developed and applied to perform modeling estimates of salt impact from cooling towers.

Problem

The development of improved techniques for measurement of air polluting processes is a requirement of NASA, Navy, Air Force, and Army Environmental Protection Technology programs, as well as the Environmental Protection Agency and the Power Plant Siting Program of the State of Maryland. An important aspect of general concern is the validation of models for the prediction of aerosol distributions. This project addresses this general problem in the specific context of salt deposition from cooling towers.

The validation of models that predict the salt deposition from cooling towers requires that both the predicted drop size distribution and the total deposition at the downfield receptors agree with measured values. A complete experiment therefore requires the simultaneous collection of a complete set of source term data, plant operating data, meteorological data, and deposition data. In the previous year, and largely under separate funding, total deposition and drop size distribution data were collected from a dyed drift test. The major problem area was the development of the methods for data recovery from the deposition filter papers.

Objective

The objective was to develop a drop size counting and sorting technique (for aerosol droplets ≈50 μm to ≈1000 μm diameter) with as many as 2000 drops per filter paper. Approximately 10% statistical accuracy was desired in each particle size increment.

Approach

The basic techniques developed incorporated manual counting through a microscope. This provides a "reference library" of meticulously counted filter papers that will be used later to assess the suitability of automatic optical scanner counting. Preliminary investigations of such methods have been done, but problems of contrast, uniformity of images, and resolution have not yet been resolved.

Progress

The development and use of improved modeling for the prediction of aerosol distribution and salt deposition from cooling towers are required in the prediction of salt impact from such systems. During the previous year, a dye tracer test was conducted to obtain source term and deposition data uncontaminated by salt from other sources. This year's work developed methods of reducing data to obtain aerosol size spectra and used these data, together with previously acquired source and meteorological data, to conduct modeling estimates of salt impact. The data reduction is now complete and preliminary modeling has been done. The methods have been developed and the counting and sizing of the droplet stains have been completed. An adequate method of automatic processing has not been found, although some initial tests have been done. These data have been used in the model validation work.

The data yielded excellent results, showing the methods to be of general applicability. The methodology and results have been reported in a project report (Ref. 1), and papers have been presented at specialized technical symposia (Refs. 2, 3, and 4).

Principal Investigators: Dr. M. L. Moon, Supervisor, J. H. Meyer, meteorologist, and E. A. Davis, senior physicist, in the Power Plant Site Evaluation Group.

References

1. J. H. Meyer and W. D. Stanbro, "Cooling Tower Drift Dye Tracer Experiment, June 16 and 17, 1977," CPCTP-16, Vol. 2, APL/JHU, Aug 1977.

2. J. H. Meyer and W. D. Stanbro, "Fluorescent Dye, A Novel Technique to Trace Cooling Tower Drift," Proceedings 4th Joint Conference on Sensing of Environmental Pollutants, American Chemical Society, 1978, p. 164.

3. J. H. Meyer and W. D. Stanbro, "Separation of Chalk Point Drift Sources Using a Fluorescent Dye," CPCTP-27, A Symposium on Environmental Effects of Cooling Tower Emissions, Vol. 1, APL/JHU, 1978, p. III-83.

4. E. A. Davis and M. L. Moon, "Modeling Analysis of the Chalk Point Dye Tracer Experiment," CPCTP-22, A Symposium on the Environmental Effects of Cooling Tower Emissions, Vol. 1, APL/JHU, 1978, p. III-19.

THE JOHNS HOPKINS UNIVERSITY
APPLIED PHYSICS LABORATORY
LAUREL MARYLAND

BIOMEDICAL SCIENCE

POWERED WHEELCHAIR

A new powered wheelchair control concept proposed to overcome limitations of conventional systems has been implemented, demonstrated, and tested. Directly funded sponsorship has been obtained for further development.

Problem

Powered wheelchairs have undergone a great deal of development over the past several years, with some commercial models available only within the past few years. Many of these models, such as the Everest & Jennings Power Drive, Independence Wheelchair, Rolls Electric, California Medical Aids, Inc., Power Aid, and Motorette, are controlled with some form of two-axis joy stick. Some potential users, for example, elderly persons and persons with muscular deficiencies, lack the skill and time response needed to operate such an electric powered chair. Others who may be capable of operating nonpowered wheelchairs with hand rim control tire and cannot maintain their desired mobility.

In 1972, APL proposed a new concept to overcome some of the control limitations of available electric powered wheelchairs. A power-assist model using the outer hand rim for control was proposed. A patent (#4 050 533) was granted on this concept in September 1977, assigned to the Veterans Administration. Power assist was achieved by decoupling the hand rim on conventional manually powered wheelchairs and using a transducer that measured the velocity of the hand rim to effect control of the power drive for each wheel. This concept is similar to automotive power steering. Manual control of the hand rim with power assist from the drive motors is believed to be a practical solution to the problem of control in tight quarters as well as out of doors. It may be particularly applicable to those handicapped persons with little or no hand grip, various limb deficiencies, or slow motion response.

Objective

The objective of this project is to explore the utility of hand rim control for powered wheelchairs. Parameter values of the input sensor mounted on the hand rim and motor control parameters need to be determined. An electric wheelchair needs to be modified for hand rim control and evaluated to verify its controllability in tight quarters, smoothness of motion, and other basic operating parameters.

Approach

The technical approach is to design a hand rim controller for a powered wheelchair and implement this design on one of the Invacare powered wheelchairs presently on loan to APL from the Veterans Administration, Castle Point, New York. The design approach consists of the following steps:

1. The design and fabrication of a new hand rim spindle to decouple the hand rim from the drive wheels. This arrangement allows free wheeling of the hand rim independently of the drive wheel.

2. Mounting permanent magnet tachometers on each side of the wheelchair to sense motion independently of the powered wheel and the hand drive rim (wheel) and modification of the power motor drive electronics to allow the drive motor to operate as a closed loop velocity servo. The tachometer output from the hand rim is summed with the tachometer feedback from the driven wheel to form an error signal to drive the servo, with parameter values matched to actual chair dynamics to yield a stable operating system.

3. The conduct of limited tests using several selected handicapped persons to verify the utility of the controller.

Progress

An experimental wheelchair test model was modified for hand rim control. A tachometer sensed hand rim velocity and commanded the power servo to follow the signal. Two control versions were investigated. One model provided 100% power assist and required only 1/4 pound of force on the hand rim for control, so that it could be driven by forearm contact alone on the hand rim without any physical grip. The performance of this wheelchair has been excellent in close quarters as well as on irregular outdoor terrain. It seems to be particularly advantageous for going up or down grades. The second model featured partial power assist. It is intended for persons who could provide 3 to 5 pounds of manual force to operate the wheelchair in a conventional manner with the power drive supplying the balance of any required force in excess of the present amount. This allows minimal power drain and hence reduces battery size, yet provides power assistance for inclines, turning on rugs, and other motions requiring high force levels. This wheelchair

operates very similarly to a manually powered wheelchair until a force greater than the preset value causes the hand rim to slip relative to the main wheel, thereby activitating the power system.

The demonstration model was tested on level surfaces, irregular sidewalks, grassy areas, and grades. The results to date have been highly encouraging. One individual paralyzed from the waist down and with limited arm strength used the experimental wheelchair for two days to compare its performance to a manually propelled chair in the home and in a grocery store. This individual was able to function with much less fatigue in the home, allowing her to perform additional tasks without getting tired, and was able to shop without assistance in the grocery store, a task which she was unable to do without assistance in her manually propelled wheelchair.

Clinical tests will be continued by potential users at Baltimore City Hospital and other rehabilitation centers in the Baltimore, Maryland, area.

Principal Investigator: W. Seamone, senior engineer, Fleet Systems Department.

ARTERIAL HEMODYNAMICS

Velocity profiles in a cast of a human artery are measured for the first time. Such measurements, coupled with histologic studies on the vessels from which the casts are made, can illuminate the role of fluid mechanics in the development of arterial disease. Further work is continuing under NIH sponsorship.

Problem

The distribution of atherosclerotic lesions in the large arteries strongly suggests that blood flow patterns (hemodynamics) adjacent to the vessel wall play a role in the development of the disease. It is not yet clear which aspects of the blood flowfield are most important in this regard, in part because the distribution of these "hemodynamic stress factors" in the vasculature is not known with a resolution comparable to the scale of atherosclerotic foci. Similarly, the mechanisms by which these stresses provoke or contribute to the pathologic response are still speculative, and quantitative response data are extremely limited.

Objective

The long-term objective of this study is to understand the morphological response of the human vascular wall to hemodynamic stress. Achievement of this objective would provide important new information regarding the causes of arterial disease.

Approach

Flows of a fluid dynamically similar to in vivo arterial flows are passed through casts of human arteries, the flowfield is measured noninvasively with a laser Doppler velocimeter, and the hemodynamic environment at the wall of the cast is compared with histologic observations on the parent vessel from which the cast was made. High-resolution quantitative results correlating hemodynamic stress with arterial morphology can thereby be obtained. Conclusions regarding the mechanisms of hemodynamic insult and arterial response should follow.

Progress

During the present reporting period, measurements were made of the velocity profile along the outer walls of a cast of a human aortic bifurcation, as described below and in Ref. 1.

The aortic bifurcation of a 55-year-old female with minimal atherosclerotic involvement was obtained at autopsy and fixed with formalin under mean physiologic pressure. After fixation, the arterial segment was injected with a water-soluble contrast medium and radiographed, and a Silastic rubber mold of the vessel lumen was prepared. After the rubber had vulcanized, the artery was split longitudinally and removed. The Silastic mold is shown in Fig. 1. A polyester cast was then polymerized around the mold;

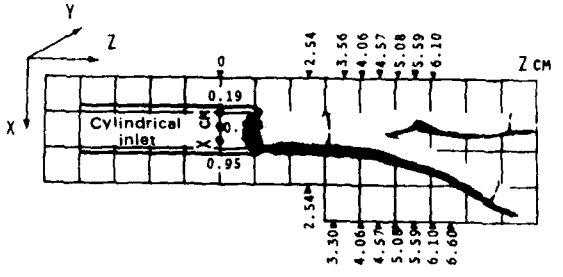

Fig. 1 Silastic mold of human aortic bifurcation. Velocities were measured at longitudinal positions (Z) indicated by small black arrows. The crease in the upper daughter at Z = 5.8 cm is an artifact.

during this procedure, the termini of the mold were held at coordinates determined from the radiographs, giving a branch angle of 27° in the plane of the daughters. After removal from the hardened polyester, the Silastic mold was sectioned 1 cm proximal and 2.5 cm distal to the bifurcation and the luminal areas were measured; the cross-sectional area of each daughter was 35% of that of the parent.

For this initial experiment, a steady flow at an inlet Reynolds number of 170 was passed through the cast using a gravity head. The refractive index of the fluid was close enough to that of the polyester to permit noninvasive velocity measurement by our laser Doppler velocimeter, which was modified so that two velocity components could be measured at each selected point in the flow. Post-test measurements showed that the flow was essentially equally partitioned between the two daughter vessels.

Two components of velocity were measured at various distances from the outer walls of the branch and at several stations along the lengths of the parent and of each daughter. The velocity components obtained at each station were used to compute the velocity component parallel to the wall as a function of distance from the wall. The longitudinal (Z) coordinates of the stations at which these velocities were obtained are marked in Fig. 1. The velocity data were interpolated to give the component parallel to, and 380 μm from, each station along the wall. These velocities, essentially proportional to wall shear, are plotted against longitidunal distance in Fig. 2. The calculated value of $v_{w,||}$ at Z = 7.25 cm is less than the highest value measured in either daughter, suggesting that relative shear maxima do exist along the outer walls of bifurcations.

Principal Invesitgators: Dr. M. H. Friedman, Deputy Director of Biomedical Engineering Programs, and Dr. G. M. Hutchins, Associate Professor of Pathology in The Johns Hopkins School of Medicine. Dr. Hutchins is not supported by the IR&D Program.

Reference

1. M. H. Friedman, C. B. Bargeron, O. J. Deters, F. F. Mark, and G. M. Hutchins, "LDV Measurements of Velocity Profiles in Arterial Casts," Proc. 31st Ann. Conf. on Engineering in Medicine and Biology, Oct 1978.

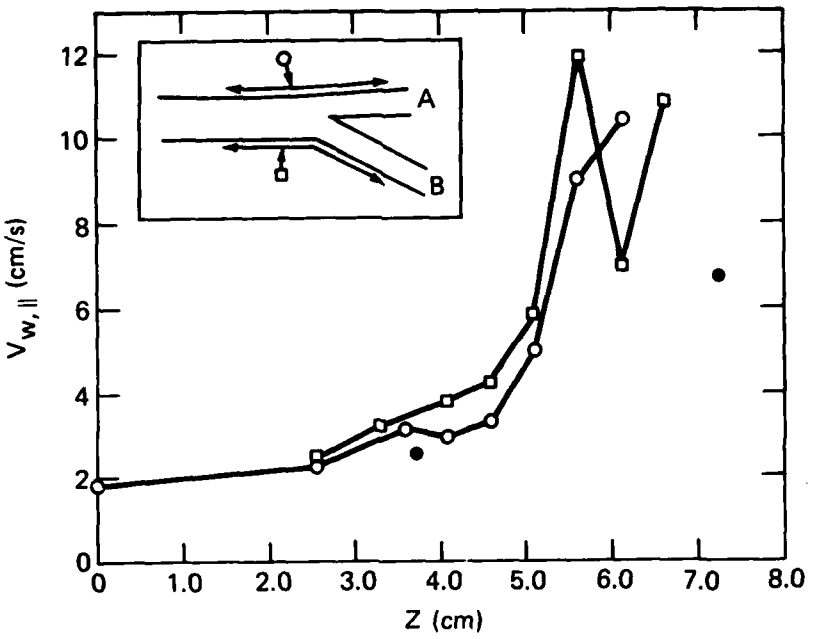

Fig. 2 Velocity profiles 380 μm from the outer walls of the branch in Fig. 1. ●: calculated $v_{w,\parallel}$ at indicated Z values, based on measured luminal areas, assuming circular cross sections and fully developed flow.

APPLIED PHYSIOLOGY

Four problem areas of applied physiology are addressed in this section.

MEMBRANE TRANSPORT

The measured flux of sucrose across a dialysis membrane (Cuprophan) in the presence of a concentration gradient is found to be significantly greater than the flux predicted from tracer permeabilities measured in the absence of a concentration gradient of the abundant species. The difference can be explained if the membrane is heteroporous.

Problem

Conventional techniques for measuring membrane transport properties are based on the implicit assumptions that the membrane is homogeneous (i.e., it contains only one kind of transport pathway) and that the solutions bounding the membrane are dilute and ideal. However, these assumptions are often not valid and can lead

to significant errors in the prediction of membrane performance. There is therefore a need to extend the understanding of the influence of structure and solution nonideality on membrane transport to permit the more rigorous interpretation of transport experiments and the more confident design of separation devices. In addition, a fundamental understanding of transport across biological membranes, where structural effects are surely present, is an important prerequisite to later investigations of the effects of various stimuli (e.g., electromagnetic radiation, hyperbaric environments, toxic chemicals, or vibration) on membrane function.

Objective

The objective of the membrane transport research is to develop and apply methods to delineate transport processes in a complex membrane system. Transport properties of a solute/membrane system are measured to demonstrate the importance of membrane structure and solution nonideality to membrane performance prediction.

Approach

The overall approach of membrane transport research couples a theoretical description of transport across membrane structure, based on the principles of irreversible thermodynamics, with experimental transport data obtained in a novel APL membrane transport chamber (developed previously) that uses laser interferometry to measure the solute concentration difference across the membrane in an unsteady experiment. The earlier theoretical studies have shown that the effects of structure and solution nonideality are manifested in an unexpectedly high flux of solute when there is a concentration difference across the membrane — when, that is, the true flux is higher than that predicted on the basis of conventionally measured tracer permeabilities. In our procedure, solute flux under a concentration gradient is computed from interferometric measurements of the temporal decay of an initial concentration difference imposed across the membrane in an essentially constant-volume cell. Besides providing a direct measure of transmembrane solute flux, this experimental technique yields values for the hydraulic conductivity (L_p) and reflection coefficient (σ) of the preparation in a single experiment; conventional membrane characterization schemes require separate experiments for L_p, σ, and tracer permeability (ω_T). By comparing the true solute flux under a concentration difference with that predicted from conventionally determined permeabilities, the influence of membrane structure and solution nonideality on flux predictability is determined.

Progress

The interferometric membrane transport chamber has been used to measure L_p, σ, ω_T, and effective permeability under a concentration gradient (ω_p) for the solute/membrane system, sucrose/Cuprophan 150 PM (Ref. 1). As shown in Fig. 1, ω_p, ω_T, and L_p decrease with increasing sucrose concentration, whereas σ increases. In addition, ω_p is significantly greater than ω_T at all solute concentrations, a result that is consistent with our previous analysis and suggests that the membrane possesses a degree of heteroporosity. However, the concentrations used in this study are high enough that

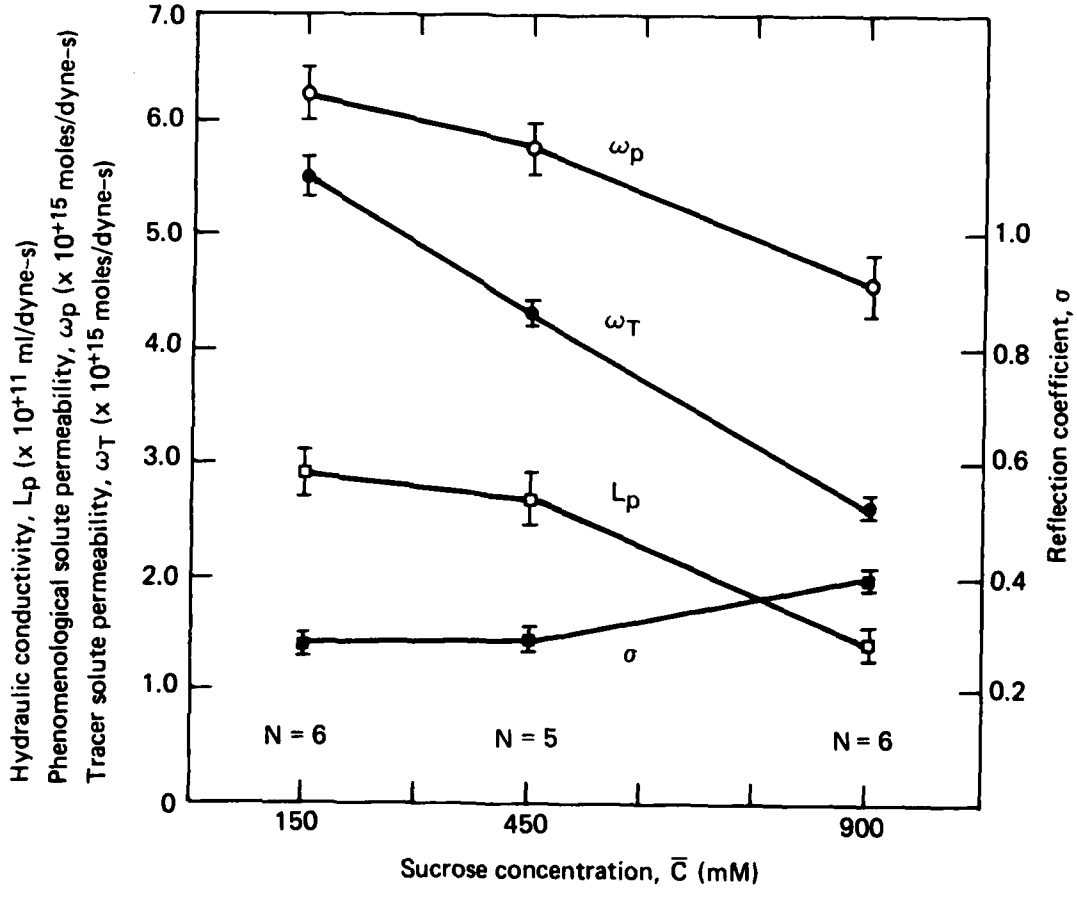

Fig. 1 Transport coefficients for Cuprophan at 37°C with sucrose as the solute.

our previous assumptions of solution ideality and diluteness fail; additionally, the presence of unstirred layers adjacent to the membrane cannot be ignored. Therefore, a more exact set of membrane transport equations has been derived, based on the Stefan-Maxwell equations, for a membrane bounded by nonideal, nondilute solutions, and finite unstirred boundary layers. For this case, ω_p differs from ω_T even for a homoporous membrane, but not enough to account for the differences shown in Fig. 1.

To demonstrate that the observed difference between ω_p and ω_T is consistent with heteroporosity, a model heteroporous membrane has been considered consisting of three parallel paths so chosen as to emphasize the effect. In Fig. 2, the permeability ratio ω_p/ω_T for Cuprophan is compared with the ratios for the homoporous membrane and the model heteroporous membrane. At all concentrations, the Cuprophan permeability ratio falls between the ratios for the model heteroporous membrane and the homoporous membrane. Thus, the differences between ω_p and ω_T can be explained if Cuprophan possesses some degree of heteroporosity with respect to sucrose (Ref. 1).

Principal Investigators: Dr. M. H. Friedman, Deputy Director, R. A. Meyer, Special Advisor, and E. C. Hills, technical aide, the Biomedical Engineering Programs Office.

Reference

1. M. H. Friedman, R. A. Meyer, and E. C. Hills, "Membrane Permeabilities Measured in the Presence and Absence of a Concentration Gradient are Different: A Membrane Structure Effect?" 23rd Annual Biophysical Society Meeting (Abstract), Atlanta, Georgia, Feb 1979.

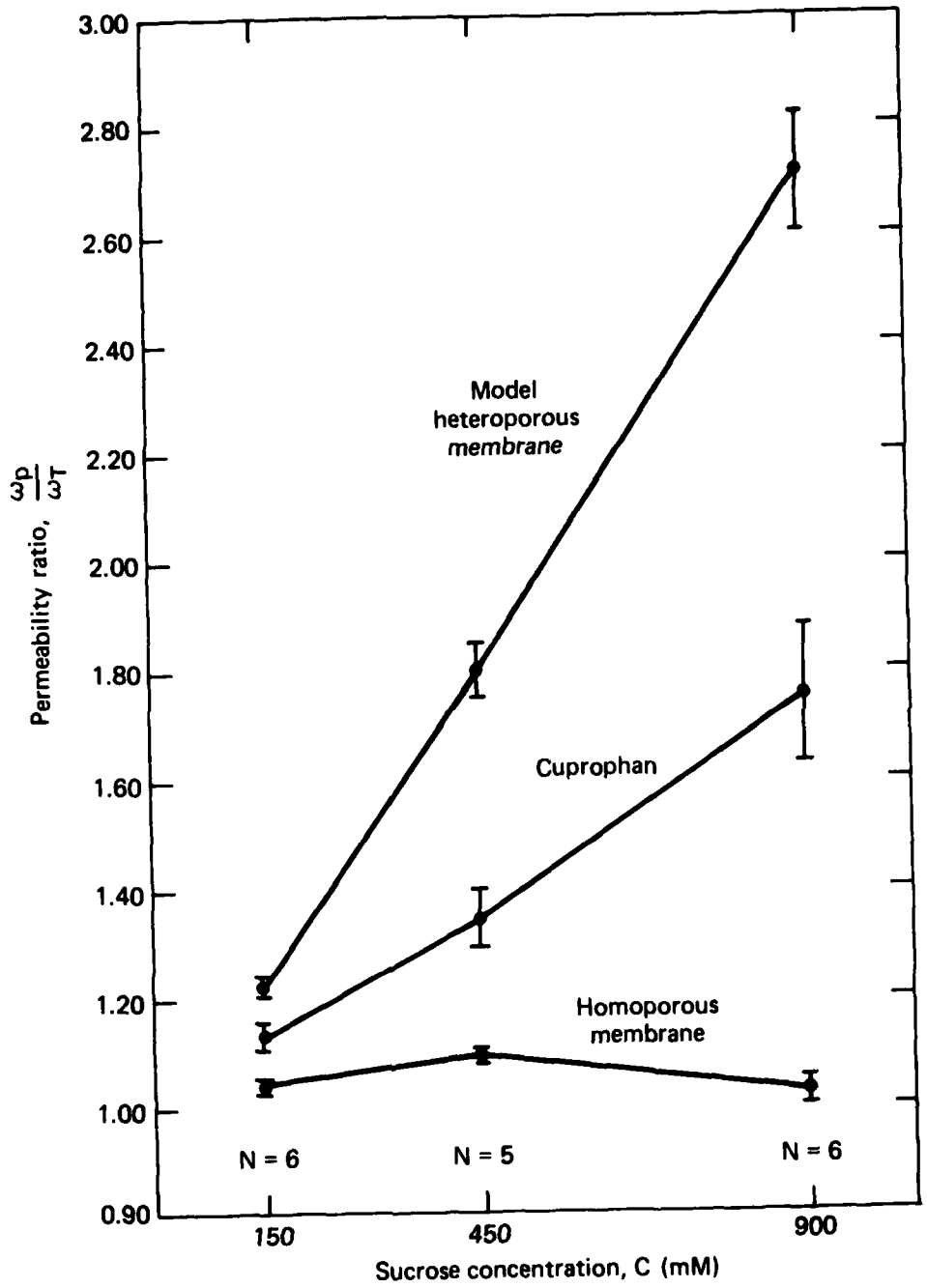

Fig. 2 Comparison of Cuprophan with homoporous and model heteroporous membranes.

THE JOHNS HOPKINS UNIVERSITY
APPLIED PHYSICS LABORATORY
LAUREL MARYLAND

PAIN PHYSIOLOGY

A distinct population of cutaneous nociceptive A-fibers has been found that develops prolonged increased sensitivity following noxious heat stimulation and could thus be responsible for the increased magnitude of pain that follows a cutaneous burn.

Problem

The neurophysiological mechanisms behind pain perception are not well known. An understanding of the neural encoding of pain stimuli along the whole neural network starting from the peripheral receptor and ending at higher order neural centers is required. Research was carried out to facilitate the development and assessment of new therapeutic modalities for the treatment of pain patients.

Objective

The objective of the pain physiology research has been to contribute to the understanding of the physiological and psychophysical aspects of pain perception. The immediate objective is to explore the peripheral neural coding mechanism for thermal and mechanical pain perception and the peripheral mechanism for hyperalgesia induced either from cutaneous injury or peripheral nerve injury.

Approach

The overall approach is to determine how controlled pain stimuli are encoded at different levels in the nervous system. A laser thermal stimulator developed at APL delivers a controlled thermal stimulus to the subject. Standard neurophysiological techniques are used on primates to isolate and record reactions from individual neural fibers. The intensity, sequence, duration, and repetition rate of the thermal stimuli are varied to fully characterize the neural coding mechanisms both before and after therapeutic interventions. Similar paradigms are used with human subjects to determine the significance of particular neural events.

Progress

During the past year, the analysis of data from the A-fiber nociceptive afferents was completed (Ref. 1). These fibers are a distinct population of mechanically sensitive cutaneous nociceptive afferents that develop prolonged increased sensitivity following

noxious heat stimulation of their receptive fields. Thus, the increased magnitude of pain (i.e., hyperalgesia) that follows a cutaneous burn may be mediated, at least in part, by activity in these fibers. Further work is now being carried on under NIH sponsorship.

Principal Investigators: J. N. Campbell, fellow in the Neurosurgery Department of the Johns Hopkins Medical Institute, and R. A. Meyer, Special Advisor, Biomedical Engineering Programs Office.

Reference

1. J. N. Campbell, R. A. Meyer, and R. H. LaMotte, "Sensitization of Myelinated Nociceptive Afferents that Innervate the Monkey Hand" (submitted for publication).

NEUROPHYSIOLOGICAL CORRELATES OF ATTENTION AND DISTRACTION

The activity of cortical neurons in the postcentral gyrus is studied in relation to the behavioral states of attention and distraction.

Problem

Cortical neurons appear to be arranged in a rectangular array. All the neurons in a column orthogonal to the cortical surface respond to the same aspect of a stimulus. Parallel to the cortical surface, the neurons are arranged in six layers. Layer IV receives stimulus information in most behavioral states. Whether or not the stimulus information propagates to other levels in the column is known to depend on the sleep state of the animal. The problem is to determine what combinations of cortical layers in the various columns are active or suppressed during the behavioral states of attention and distraction in the awake animal. A second problem involves a search for the centers that modulate the activity of these layers. Anatomically the second and third layers of the cortex are heavily innervated by the nonspecific thalamic neurons of the intralamina nucleus, and the fourth layer by the specific neurons of the ventral posterolateral nucleus. It is postulated that the influence of these two systems may govern the levels of responsiveness in the various layers of the postcentral gyrus.

Objective

The mapping of the somatosensory system on the postcentral gyrus has been known for a long time. Less well known is the mechanism that controls what stimulus receives attention. The

objective of the research is to investigate the mechanisms in this area of the brain responsible for activating specific cortical layers that behaviorally are related to ignoring or attending to an applied stimulus. This requires a study of the responsiveness of the neurons in various layers of the sensory cortex to threshold stimuli under conditions of attentiveness and under conditions in which another distracting stimulus coexists.

Approach

Cortical neurons that respond to light pressure on the glabrous skin of the hand are selected for study in a macaque monkey. By means of a vibratory stimulator, the skin surface can be moved at a controlled vibratory amplitude and frequency. This stimulus produces neural activity in the sensory neurons of the cortex that can readily be identified by electrophysiological means. The cortical neurons generate an electrical impulse train that is entrained to the stimulus. The degree of entrainment is related to the stimulus intensity. In addition, the degree of entrainment will vary in a reproducible manner in neurons of the various cortical layers depending on the behaviorial state of the animal.

In an alert animal that has become accustomed to vibratory stimuli, the degree of entrainment of a particular cortical neuron is established by using stimuli of various intensities. This establishes a control. The same intensity series is repeated when the animal is distracted by an intense strobotactic light. The control run is then repeated without the presence of the distracting stimulus. This procedure is repeated for all the neurons in a column to measure the susceptibility of the neural response to the presence of distraction as a function of the layer in which the neuron is located.

Progress

An electrophysiological laboratory was established at Baltimore City Hospital to conduct these experiments; all of the necessary laboratory apparatus has been acquired and put in working order. A digital computer (PDP 11/40) was programmed to administer the stimuli and to process the responses, which are in the form of neural impulse trains. Initial data have produced some unexpected results, e.g., in the neurons thus far studied, acoustical noise is much more distracting (as measured by neural response) than bright flashing lights. Histological studies will be required to identify in which layers the responding neurons are located.

THE JOHNS HOPKINS UNIVERSITY
APPLIED PHYSICS LABORATORY
LAUREL MARYLAND

Principal Investigators: Dr. L. Viernstein, Medical Staff, Operational Systems Development Branch Office, and Dr. G. Gucer, Chief of the Division of Neurosurgery of Baltimore City Hospital. Dr. Gucer is not funded by the IR&D Program.

OPHTHALMIC ULTRASOUND

The potential of synthetic aperture data processing techniques for improving the resolution of ophthalmic ultrasound systems is explored and found to be favorable.

Problem

Current ophthalmic ultrasound systems lack the resolution required for satisfactory diagnosis of significant eye problems. This deficiency is particularly significant for diabetics where chronic problems tend to limit the usefulness of the normal visual observations.

Objective

The objective of this study was to demonstrate the feasibility of using state-of-the-art technology to significantly improve the resolution of clinical ophthalmic ultrasound systems.

Approach

Significant resolution improvements were sought by the digital recording of the ultrasound signals for subsequent synthetic aperture processing.

Progress

In addition to analytic work, a NASA high speed digital recorder (100 mb/s) available at APL was used to record typical ultrasound echoes. These were transferred to the APL central computer for processing. Up to 3000 sequential returns were summed to demonstrate coherent integration gains, and the expected improvements in signal-to-noise ratios were obtained. The coherent integration signal-to-noise ratio improvement can be used to increase tissue penetration in B-scan ultrasonograms by applying a time-varying gain to the echo returns, as illustrated by Figs. 1 and 2.

THE JOHNS HOPKINS UNIVERSITY
APPLIED PHYSICS LABORATORY
LAUREL MARYLAND

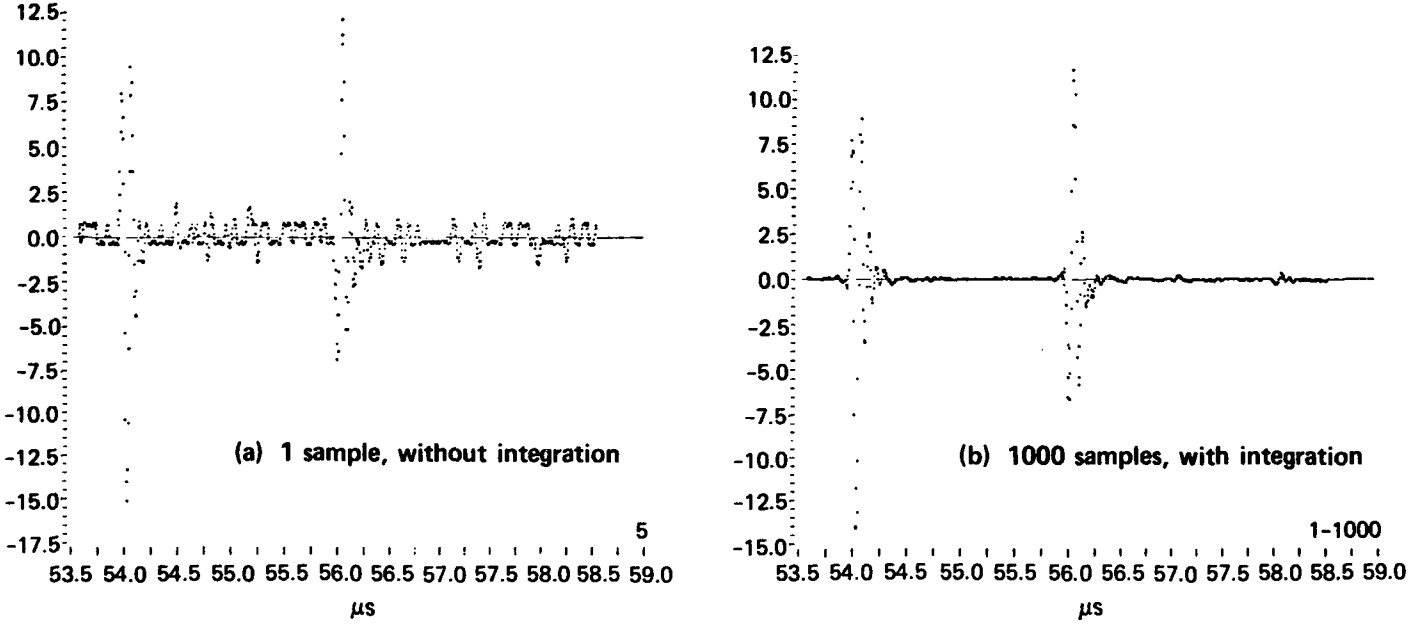

Fig. 1 Noise reduction with coherent integration. (a) is the amplitude of the return signal from a single pulse; (b) is the amplitude obtained by averaging 1000 sequential echoes. Returns that are constant (in time) are not affected by this process; random noise is reduced.

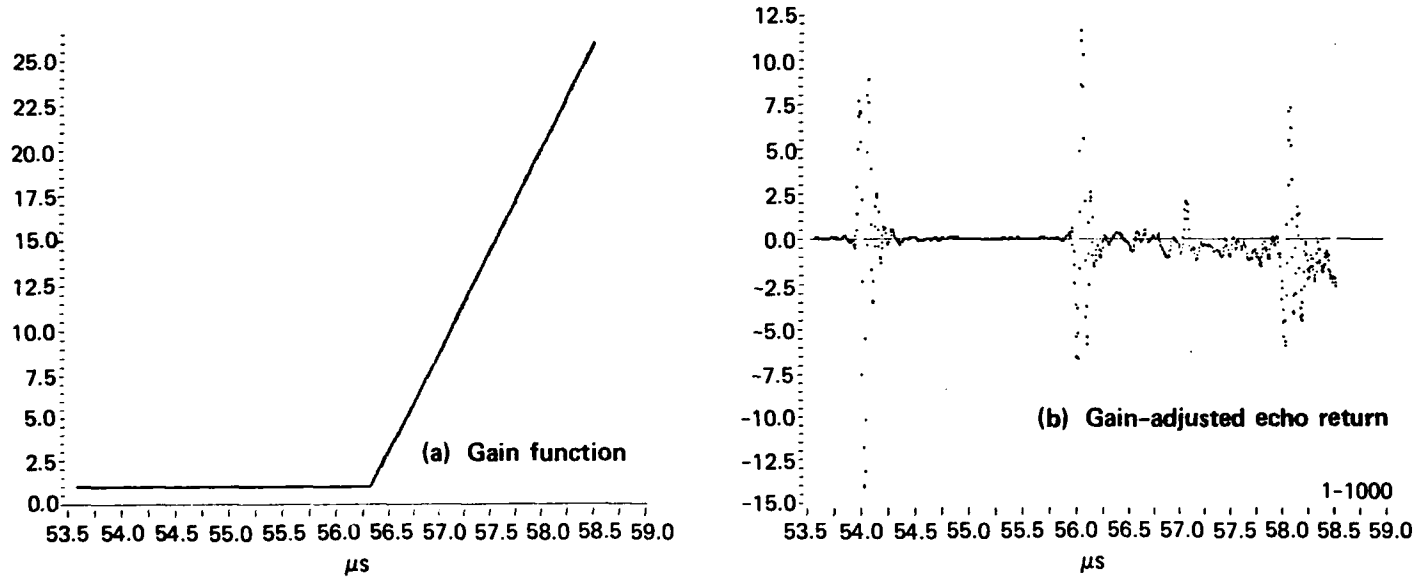

Fig. 2 Application of time-varying gain function to 1000 sample integrated echo return.

Figure 1(a) shows two strong returns at times of 54 and 56 ms. If a sequence of such pictures is observed on an oscilloscope, it would be noted that these strong echoes do not change; the low-level signals vary rapidly with time. Thus, when N such returns are averaged the signal will remain constant, but the noise average will decrease. The result of averaging 1000 such returns is shown in Fig. 1(b). In this figure there appears to be a third echo at approximately 58 ms, but its amplitude is low.

Figure 2 shows the result of applying a time varying gain to the data shown in Fig. 1(b) in order to make the weak signal at 58 ms more visible. Figure 2(a) shows the gain versus time, and Fig. 2(b) shows the resulting signal. The returns at 54, 56, and 58 ms are valid signals; the one at 57 ms is doubtful.

Principal Investigator: Dr. J. B. Garrison, senior physicist, the Director's Staff.

Reference

1. "Results of Ophthalmic Ultrasound Pilot Study," to J. B. Garrison from S. H. Jones, CSC-5-079, 2 Jan 1979.

THE JOHNS HOPKINS UNIVERSITY
APPLIED PHYSICS LABORATORY
LAUREL, MARYLAND

ELECTRONICS/ELECTRICAL ENGINEERING

SPEECH SYNTHESIS

An experimental facility is assembled that enables exploration of the utility of computer synthesized speech in the Command Information Center (CIC) context.

Problem

The performance of human decision makers is frequently limited by the rate at which they can take in and properly evaluate the required information. For example, the CIC of any modern warship includes several consoles that allow the commander and his staff to interact with each other, with the sensors, with the weapons systems, and with the supporting computer(s), including those associated with command and control functions. In all cases, the purpose of the console is to provide a mechanism for the equipment to display data and for the operator to control both the data to be presented and the way in which the data are processed. That is, it is one implementation of a man-machine interface.

The data presented by a modern console intensively engage and easily saturate the operator's visual and tactile senses. The audio channel traditionally has been little used, however, since adequate techniques to effectively synthesize speech have not been available. Now that units for computer-generated speech are readily available, they are finding increased use, e.g., in commercial airlines as emergency warning enunciators, within the telephone companies to assist dissemination of changed and disconnected numbers, and in a few complex machines to aid the operators. Accordingly, it becomes prudent to consider the extent to which computer-synthesized speech can be useful in alleviating DoD man-machine interface problems.

Objective

The objective of this project is to establish a state-of-the-art experimental facility suitable for exploring the uses of synthetic speech in areas of concern to the Communications, Command, and Control Project (PME-108) of the Naval Electronic Systems Command, the Aegis Project (PMS-400), and the Trident Technology Improvement Community. The next step would be experiments to demonstrate the utility of speech synthesis in the CIC milieu.

Approach

Advances in the state of the art of microelectronics and in physiology have recently raised promising new possibilities in man-machine communications. In particular, electronic devices are now available whose output is intelligible speech. They are controlled by a stream of digital information, usually but not necessarily from a general-purpose digital computer. The devices are generally called "speech synthesizers," and are becoming increasingly common in the nonmilitary sector of the economy.

Two general areas of applicability of speech synthesizers are particularly noteworthy — as a highly efficient demodulator and as a man-machine interface device. First, a speech synthesizer requires only about 300 bits of information per second to generate speech, while most normal voice circuits require a bandwidth of approximately 3000 Hz. Thus, computer-synthesized speech offers a 10/1 reduction in bandwidth requirements, compatible with digital data communications networks such as AUTODIN II and the ARPA net. Second, and of direct interest, the evolving speech synthesizer technology presents a completely new, unexplored information channel between Naval personnel and supporting equipment. The latter category covers the entire spectrum: sensor suites, command and control systems, and weapons systems, either in a stand-alone configuration or integrated. Two areas of immediate promise are augmentation of the usual visual communications channel to commanders in CIC's and response to operator queries about data in radar track files.

The essential first step toward exploring the potential of synthetic speech in these and other areas is to establish a basic experimental capability; this is the approach adopted here. For this, the state-of-the-art technology must be surveyed, and both software and hardware of suitable flexibility must be acquired and tested in the CIC environment.

Progress

In late 1977, a speech synthesizer was obtained, together with its supporting audio amplifier subsystem. The unit model ML-1 VOTRAX, developed and manufactured by the Vocal Interface Division of Federal Screw Works, represents the current state of the art in research-quality digital speech synthesizers. It has 122 phonemes (sounds), eight levels of inflection (pitch), and four phoneme rates (duration). It constructs words on the principle of concatenating the smallest discernible units of speech: the phonemes. The result is that it provides the ultimate flexibility of an unlimited vocabulary. Indeed, one computer service company reports a vocabulary of over 300 000 words.

The first major milestone was achieved in September 1978 when the VOTRAX unit was successfully attached to the PDP 11/45 minicomputer in the Embedded Computer Systems Engineering Laboratory (Refs. 1 and 2). This computer uses the modern and efficient UNIX operating system and supports the high-level system programming language C.

The second milestone was reached when one of the experimenters typed "1+1" on the computer terminal and a "voice" spoke the sentence, "One plus one is two." The actual program is, of course, much more general in the sense that it can vocalize any of the four elementary functions of addition, subtraction, multiplication, or division and utters the results by their names, not as digits (i.e., the number 1342 is uttered as "one thousand three hundred forty-two," not as "one three four two"). More significantly, this milestone demonstrated that the speech synthesis experimental apparatus is fully operational.

The third milestone was the completion of three computer programs that support the human factor or systems engineer as he develops speech segments for use in the various applications (Ref. 3).

The final milestone was reached when a mechanical voice said, "Watch out. Watch out. There is a shark. It is right behind you." This was the demonstration of a remarkable computer algorithm (designed and implemented by Dr. M. D. McIlroy of Bell Telephone Laboratories, see Ref. 4); it converts English words into a phoneme string. Functionally, it is identical to that of the programs of milestone three. However, it requires no dictionary, and the English words are converted to phonemes by application of a series of rules. The results are of very high quality.

This milestone is most significant since arbitary English text can be uttered by the synthesizer. Any word, however complex, can be spoken. Numbers are spoken. Significant punctuation symbols are "vocalized," so that "?", for example, becomes "query." Upper case words are spelled, thus allowing the communications of acronyms such as APL, and nonsense and misspelled "words" are uttered (see Ref. 5). The program then provides an elegant solution to the problem addressed earlier. The systems engineer now has a powerful tool for the creation of spoken messages, with virtually no constraint on his vocabulary. Another important result deriving from the "no dictionary" feature is that messages can be composed in real time, using real data, with no constraint on the vocabulary.

THE JOHNS HOPKINS UNIVERSITY
APPLIED PHYSICS LABORATORY
LAUREL, MARYLAND

Principal Investigator: M. D. Granger, associate engineer, Computer Systems Group of the Fleet Systems Department.

References

1. M. D. Granger, "VOTRAX I/O and Cable," APL/JHU F3C-1-373, 28 Dec 1978.

2. M. D. Granger, "VOTRAX Programming Using UNIX," F3C-1-302, 4 May 1978.

3. M. D. Granger, "Voice Synthesis Programming," F3C-1-374, 2 Jan 1979.

4. M. D. McIlroy, "Synthetic English Speech by Rule," Bell Telephone Laboratories, Computing Science Technical Report No. 14, 14 Sep 1977.

5. M. D. Granger, "Voice Synthesis," F3C-1-366, 12 Dec 1978.

MICROPROCESSOR NETWORK

An electrical analog of the cochlea is assembled and interfaced with a prototype microprocessor network designed to model and demonstrate the utility of a novel auditory perception concept based on comparative transient analysis.

Problem

Increased understanding of auditory recognition processes is required to facilitate the design of automated systems that interface with human input/output capabilities and to simulate and optimize training and weapon system behavior.

Objective

The objective is to develop a flexible facility that provides the basis for seeking directly funded support to evaluate the utility of comparative transient analysis (CTA) techniques in the context of information processing in general and speech perception/recognition in particular.

Approach

Speech sound characterization and recognition is selected as the application area because of the limited success of many previous investigations in this field. Thus, if the CTA concepts proved effective in such an application, their utility would be clearly established. In addition, solutions to a variety of command/control interface tasks could be envisaged. Moreover, the electrical analog of the outer middle ear and cochlea is well known so that the sensory transducing element is readily simulated. A microcomputer can be viewed as a universal active device whose transfer function may be almost arbitrarily defined, and cost and production trends permit contemplation of networks containing large numbers of such devices. Because each is potentially capable of emulating the functional behavior of neuron arrays, a powerful means of modeling biological processing methods appears feasible. A new class of computing machines might be created whose operations consist of CTA's implemented through many digital microcomputer n-port modules with analog transfer functions.

As noted in Ref. 1, a number of processing concepts appropriate to such machines have been suggested by various investigators over the years. While the proposed techniques are conceptually simple when considered in isolation, their value when applied collectively to practical tasks remains undemonstrated.

Progress

Consideration of the objective dictates that the facility to be developed should

1. Transform speech sounds into a dynamic "image" that should be derived using an electrical model of the cochlea,

2. Include multiple microcomputers that will provide experience with interfacing issues in pipeline processing networks and also permit experiments in real-time speech analysis, and

3. Provide an interface to the comprehensive analysis and software development capabilities of the APL central computer facility.

Figure 1 illustrates the major hardware elements of the facility and provides a convenient framework for discussing its capability. Each of the six microcomputers is an evolution of an

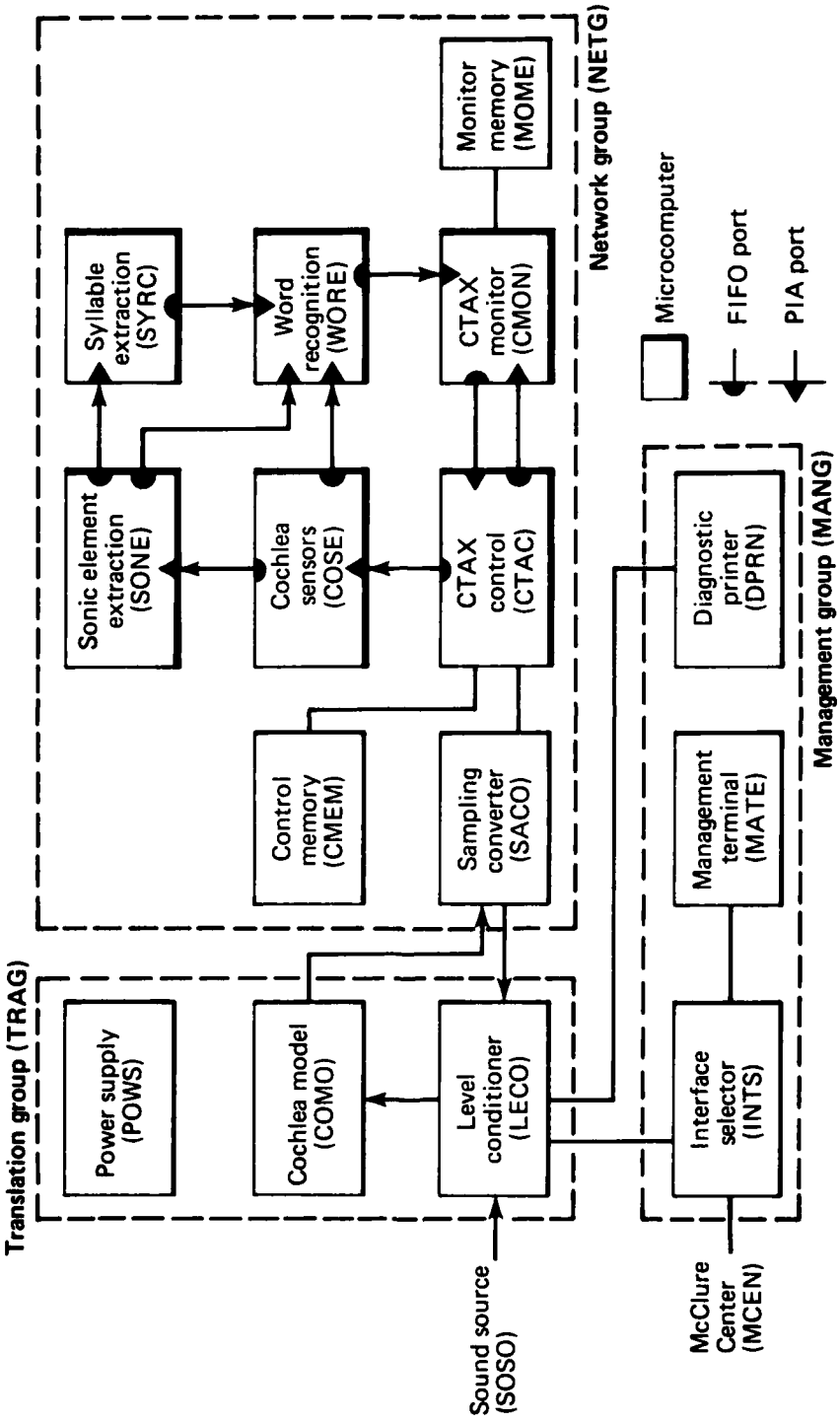

Fig. 1 Diagram of hardware elements.

off-the-shelf PL/M6800 evaluation kit. (Terms employed to identify the microcomputers reflect candidate future functions.) All nine network group elements are mounted in a 10-slot card cage containing a common interface bus. However, its control, address, and data lines have been strategically severed, creating separate partitions to avoid bus contention problems.

Data transfer between computers is accomplished by first-in-first-out (FIFO) buffers. The FIFO's augment the basic computer boards and interface to peripheral interface adapters (PIA's) that were included in the kit configuration.

The CTA control (CTAC) and CTAX monitor (CMON) boards are also modified to operate with 16 K-byte off-board memories (CTAX and monitor memories, CMFM and MOME). Monitor capabilities supplied with the kit do not support ASCII terminals so alternate monitors (Minibug 2 or 3, depending on desired capabilities) have been installed.

Each computer also contains an asynchronous communications interface adapter (ACIA) that is linked to two switches in the level conditioner (LECO). Thus, it is possible manually to connect either the interface selector (INTS) or the diagnostic printer (DPRN) to any of the six microcomputers.

The interface selector (INTS) is a switchbox that determines the role of the ASCII management terminal (MATE). It can be linked to the central computing facility (the McClure Center, MCEN) or to any one of the six microcomputers. In two other positions, terminal actions can initiate data transfers from MCEN to any of the microcomputers (e.g., loading programs) or in the reverse direction (e.g., transferring speech data to MCEN files).

The LECO element also includes a logarithmic amplifier and switches that permit its insertion between a signal source and the cochlea input. One input source option is sound from either a microphone or a recorder. Alternately, the source can be an analog test signal produced by the digital-to-analog output of the sampling converter responding to test software in CTAC.

Figure 2(a) depicts the cochlea model, and Figure 2(b) indicates its nominal response to a series of fixed frequency signals. Note that the response of any of the 15 taps is dependent upon the frequency of the signal applied to the input. However, recognize that for the intended application, the response to various speech sounds will be of central interest.

Two of the six microcomputers, which are required for initial experiments, have been fabricated. All other hardware is

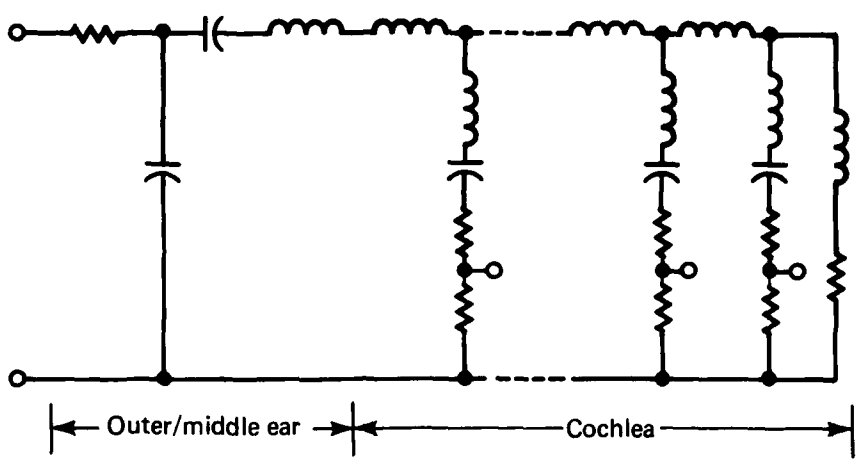

(a) Structure of model

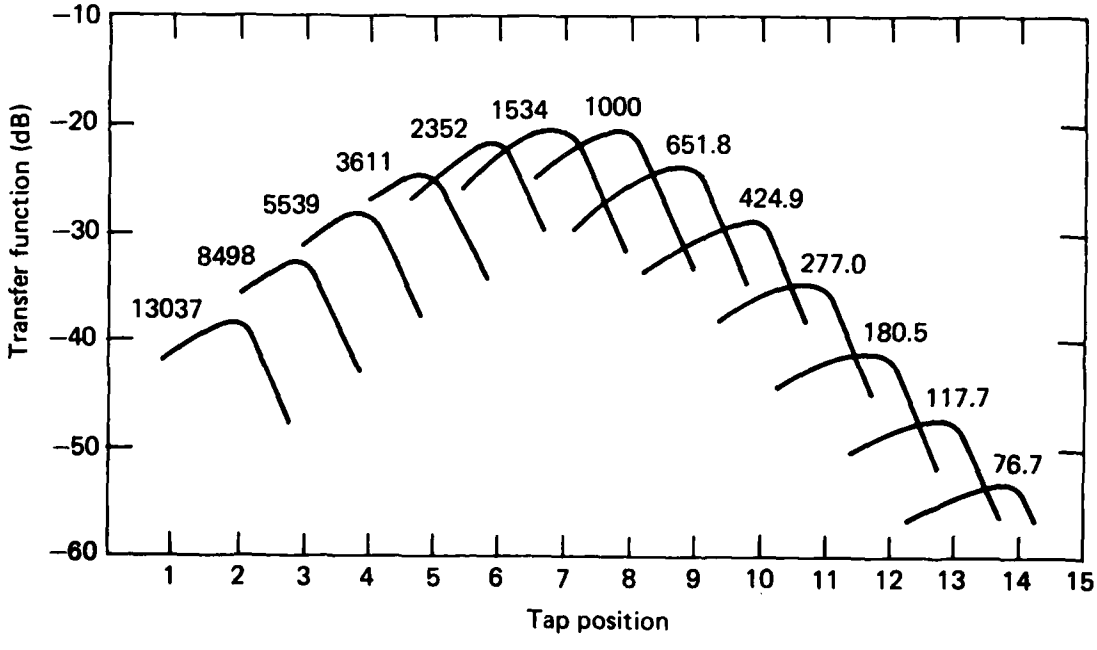

(b) Response

Fig. 2 Cochlea model and its nominal responses.

complete, and much utility software has been coded and debugged. Functions demonstrated to date include

1. Operator prompting and data entry via the terminal (MATE),
2. Program loading from the central computing facility (MCEN) after compiling PL/M6800 source code,
3. Data transfers from a microcomputer to the central computer, and
4. Data transfers via FIFO's between the microcomputers.

The last capability appears to confirm the effectiveness of the system initialization protocol for a FIFO-coupled pipeline network.

In summary, a flexible tool for the experimental investigation of speech characterizations by means of CTA's has been designed and placed into operation.

Principal Investigator: A. J. Cote, Jr., senior engineer, Space Systems Applications Group.

Reference

1. A. J. Cote, Jr., "Microprocessors and the Emulation Approach to Machine Intelligence," Computer, Vol. 11, No. 10, Oct 1978, pp. 75-76.

SES LASER PROFILER

A simple laser ranging system to meet or exceed Navy wave-profiling requirements for the surface effect ship SES-100A-1 has been conceived and demonstrated.

Problem

The Navy Surface Effect Ship (SES) Project Office is developing an oceangoing surface effect ship, the 3KSES, with a gross weight of about 3000 long tons, that rides on a cushion of air entrained by two hard sidewalls (keels) and flexible fore and aft air seals. The design is based on theoretical analyses, model tests, and operating data from two smaller manned test craft, the

SES-100A and the SES-100B, each weighing about 100 long tons. The SES-100A is being modified by the Navy to simulate the expected behavior of the much larger 3KSES; it is planned to test it in the Chesapeake Bay. An onboard real-time wave height profiler is required for the interpretation of these tests to validate theoretical predictions and model extrapolations.

Objective

The objective of the present project was to assemble a bench demonstration of a simple laser ranging system that would meet or exceed Navy wave-profiling requirements for the SES-100A-1 and that would serve as a basis for defining an onboard system. Navy requirements specify a maximum operating range of 25 ft altitude, a range accuracy of better than 0.5 in., and a frequency response better than 25 Hz.

The initial phase of the project has been to demonstrate the working principle of the optical altimeter in the laboratory. The design criteria for the onboard system have been tentatively established by testing the laboratory model.

Approach

Optical laser techniques for ocean surface profiling offer important advantages over microwave radar, primarily because optical wavelengths are short compared with the dimensions of relevant surface structures. Preliminary investigation established that a simple phase detection processor would easily permit range determiniation to better than 0.1 in. for ranges up to 25 ft and that achieving a frequency response at least as great as 25 Hz would not pose problems.

The demonstration system uses an amplitude-modulated technique with phase sensitive detection in order to accurately measure ranges at such uncharacteristically low altitudes as less than 10 m. The phases of the transmitted signal and the received signal are compared to determine range; that is, the phase difference is proportional to altitude or change in altitude by

$$d\phi = \frac{4\pi}{\lambda} \, dh \quad . \tag{1}$$

In order to avoid phase ambiguity for a single frequency system, that is, excursions in phase greater than $\pm\pi/2$, the wavelength must be matched to altitude such that the worst sea state will not vary the measured height by more than $\pm\lambda/4$.

The crux of the problem of laser altimetry against a water target rests on the sea surface characteristics that determine the spatial distribution of the return signal in a statistically accessible manner. If the field of view (FOV) of the receiver is matched to the beam divergence of the transmitter, the receiver will always see a signal return from some sample of the facets in the FOV. If either the beam divergence or the beamwidth is too small (so that the resulting footprint on the water is comparable to any single facet area), signal dropout will occur.

If beam divergence is made too large, a loss in accuracy results because different phases in the total return signal come from different altitudes that exist within a given footprint but the signal processor sees only the average of all return phases.

Progress

After appropriate analysis, a brassboard demonstration system was built and tested in the laboratory using both a retroreflective paper target and a water target. The design of the demonstration system and the test results are summarized below.

Signal Processing. The overall scheme of the feasibility demonstration system is shown in Fig. 1. Basically, the phase of the received signal is compared to the transmitter signal. This

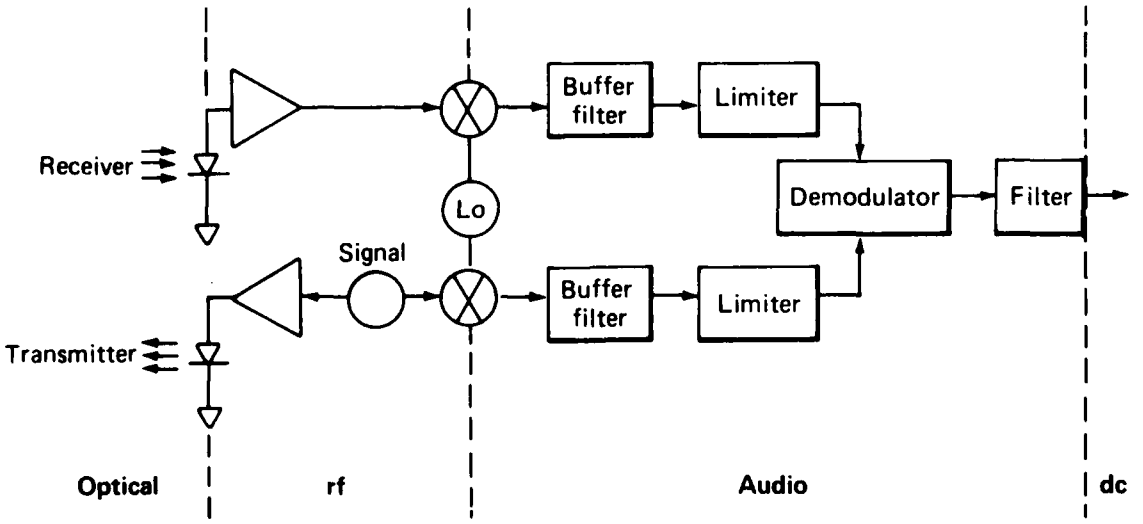

Fig. 1 Feasibility demonstration signal processing layout.

is accomplished by first beating down both the video-detected, rf-modulated, optically received signal and the pretransmitted rf signal with the same local oscillator. The signal processing is then done after both mixers are at audio frequencies (~ 10 kHz).

Transmitter. The laser source is a GaAlAs double heterojunction injection laser diode (RCA type C30127), dc biased in the forward direction and modulated at 30 MHz. Its operating wavelength is 0.82 μm.

Optics. The collimating optic for the transmitter is a symmetrical doublet of low combined f/number (f/0.77) that provides an elliptical beam with a major axis of ~ ½ in. when collimated. The altimeter optical train is essentially coaxial with the transmitter beam coming in at 90° to the principal axis and folding via a 45° diagonal mirror. The receiver collecting objective is an f/1.4 coated doublet of 5.5 cm aperture directly behind the diagonal mirror. At the back focal point of the objective is located the entrance aperture of the field lens doublet. A spectral bandpass filter ($\Delta\lambda$ = 20.0 nm) was placed between the symmetrical halves of the field lens where the rays are parallel. The field lens limits the FOV to ~ 0.4 rad.

Receiver. A two-stage preamplifier section is closely connected to the silicon pin photodiode (UDT type PIN 5-D), which is sensitive at 0.82 μm wavelength. The photodiode has a minimum risetime of 15 ns, responsitivity of ~ 0.5 A/W, and NEP of 5×10^{-13} $W/Hz^{\frac{1}{2}}$. The first stage of the receiver is a low-noise tuned FET voltage amplifier.

Test Results. The initial measurements were limited in accuracy primarily by if drift and inadequate forward gain rather than any fundamental limitation on the precision. A least squares analysis of the test data gives a 1σ altitude error of 0.51 in. and a peak altitude error of 1.22 in. These values were determined for the sample altitude range from 8.2 ft (2.5 m) to 12.14 ft (3.7 m), which corresponds to an altitude interval of 3.94 ft (1.2 m). The percentage 1σ error on altitude is then 1.08. Thus, these initial results are in close accord with the objective. However, significant improvement is possible because the bench system does not represent the state of the art for linear phase detectors. The altitude change measured (3.94 ft) corresponds very nearly to λ/8 (4.1 ft) for the 30 MHz modulation frequency used, which will accommodate sea state 3 conditions. Presently available commercial linear phase detectors have a guaranteed accuracy over ±90° of ±0.1° of phase shift. Therefore, the fundamental limit on altitude accuracy just in the linear detector is ±0.0045 ft (or ±0.054 in.).

Direct funding under Navy sponsorship resulted from these tests.

Principal Investigators: T. M. Rankin, senior engineer, and Dr. B. G. Boone, senior physicist, Control Technology Group of the Advanced Missiles Systems Branch.

Publications

1. B. G. Boone and T. M. Rankin, "Feasibility Demonstration of a Short-Range CW Laser Altimeter System," APL/JHU F1D(3)78-U-083, 27 Apr 1978.

2. T. M. Rankin and B. G. Boone, "Technical Program Plan — Laser Altimeter for Wave Profiling," APL/JHU F1D(1)78-U-117, 11 Apr 1978.

QUADRIFILAR ANTENNA

Techniques for broadbanding the quadrifilar helix antenna are being studied. The integration of a matching network into the balun and modifications to the radiating elements are both being considered.

Problem

The quadrifilar helix is a relatively small antenna that provides good circular polarization over wide beamwidths. By proper selection of the helix parameters, a wide range of beamwidths and beam shapes can be obtained. The problem addressed by this study is the narrow impedance bandwidth of this class of antenna, which in the past has limited its use to systems with bandwidths of a few percent or less.

Objective

The objective of the study is to develop techniques for broadband matching of the quadrifilar helix antenna. Impedance bandwidths on the order of 10 to 15% will make the attractive beam shaping characteristics of this antenna available to a wider class of applications.

Approach

Two broadbanding approaches are pursued. One is to integrate a broadband matching network into the cross-folded balun used to feed the antenna. The other is to modify the radiating elements themselves to lower the antenna Q.

Progress

The integration of a matching network into the feed balun requires the use of elements realized from a transmission line consisting of four closely spaced cylindrical conductors. The characteristic impedance of this geometry as a function of conductor spacing has been calculated using the moment method. This technique was also applied to the shielded four-conductor case. The results are given in Figs. 1 and 2.

Detailed data of impedance versus frequency of a hemispherical coverage 3/4 λ, 3/4 turn helix were taken. The result is given in Fig. 3. Similar data were taken on an antenna of the same geometry but with wide tape elements instead of wire, as shown in Fig. 4. In both cases, the impedance consists of a relatively constant real part and a rapidly varying imaginary part. The tape elements decreased both the real part and the frequency dependence of the imaginary part, resulting in a lower Q.

A design for a broadbanding network for the wire helix has been completed. The bandwidth over which a 2:1 VSWR is maintained is expected to be roughly doubled by the network.

Principal Investigator: R. K. Stilwell, associate engineer, Space Telecommunications Group of the Space Department.

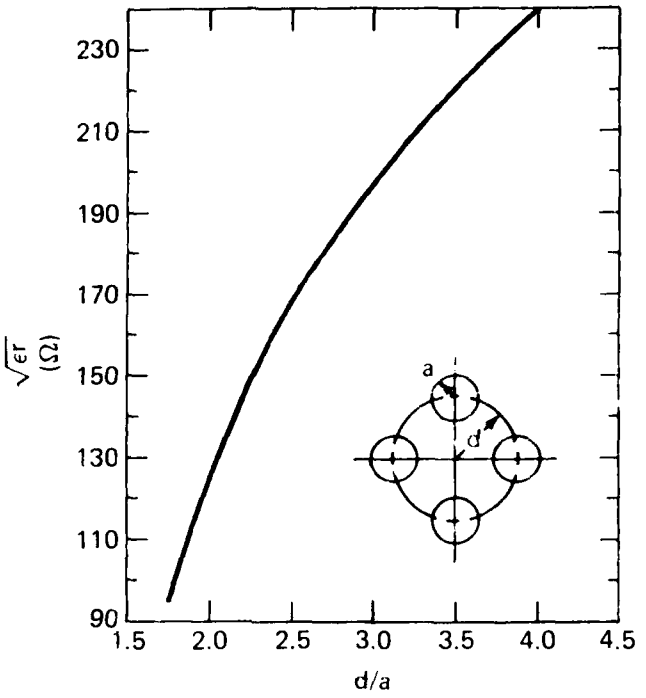

Fig. 1 Characteristic impedance of four-conductor transmission line.

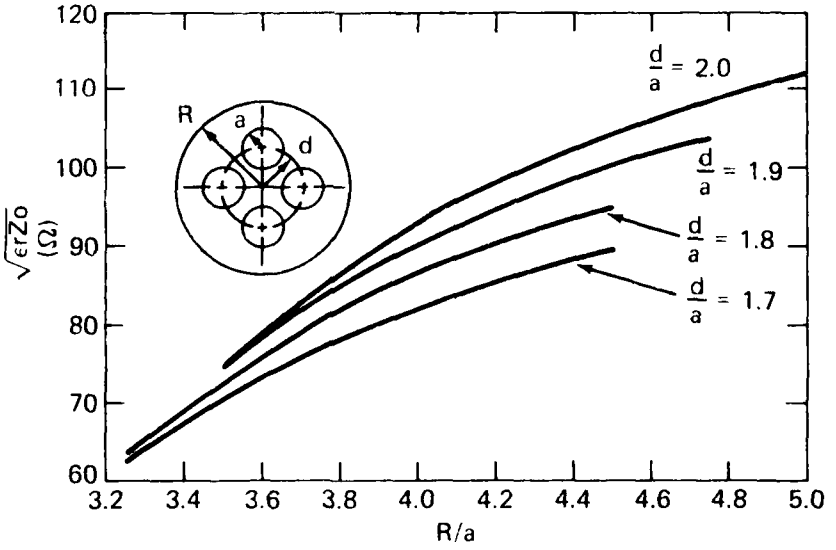

Fig. 2 Characteristic impedance of shielded four-conductor transmission line.

Impedance or admittance coordinates

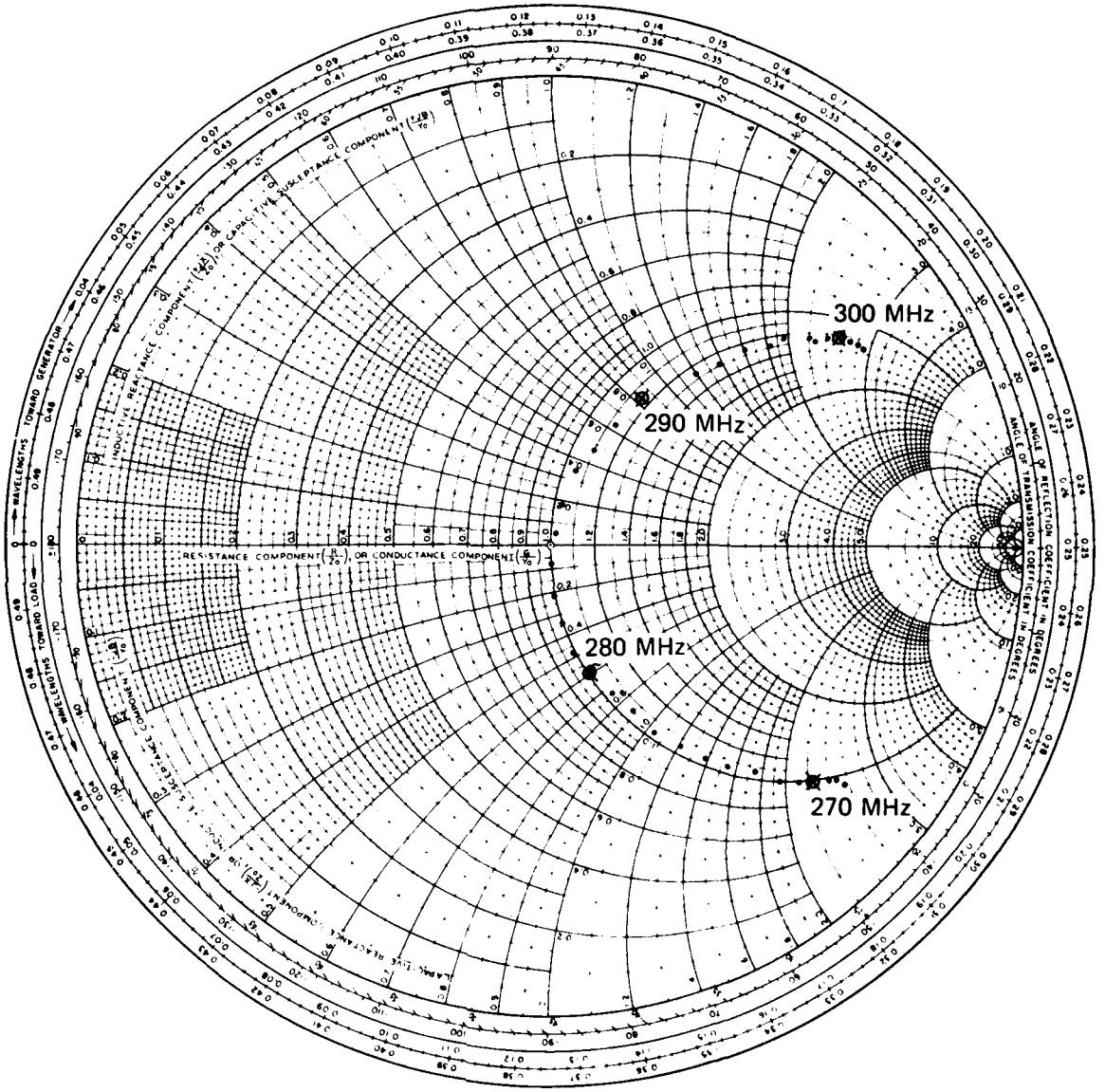

Fig. 3 Impedance of the experimental wire helix (normalized to 50 Ω).

Impedance or admittance coordinates

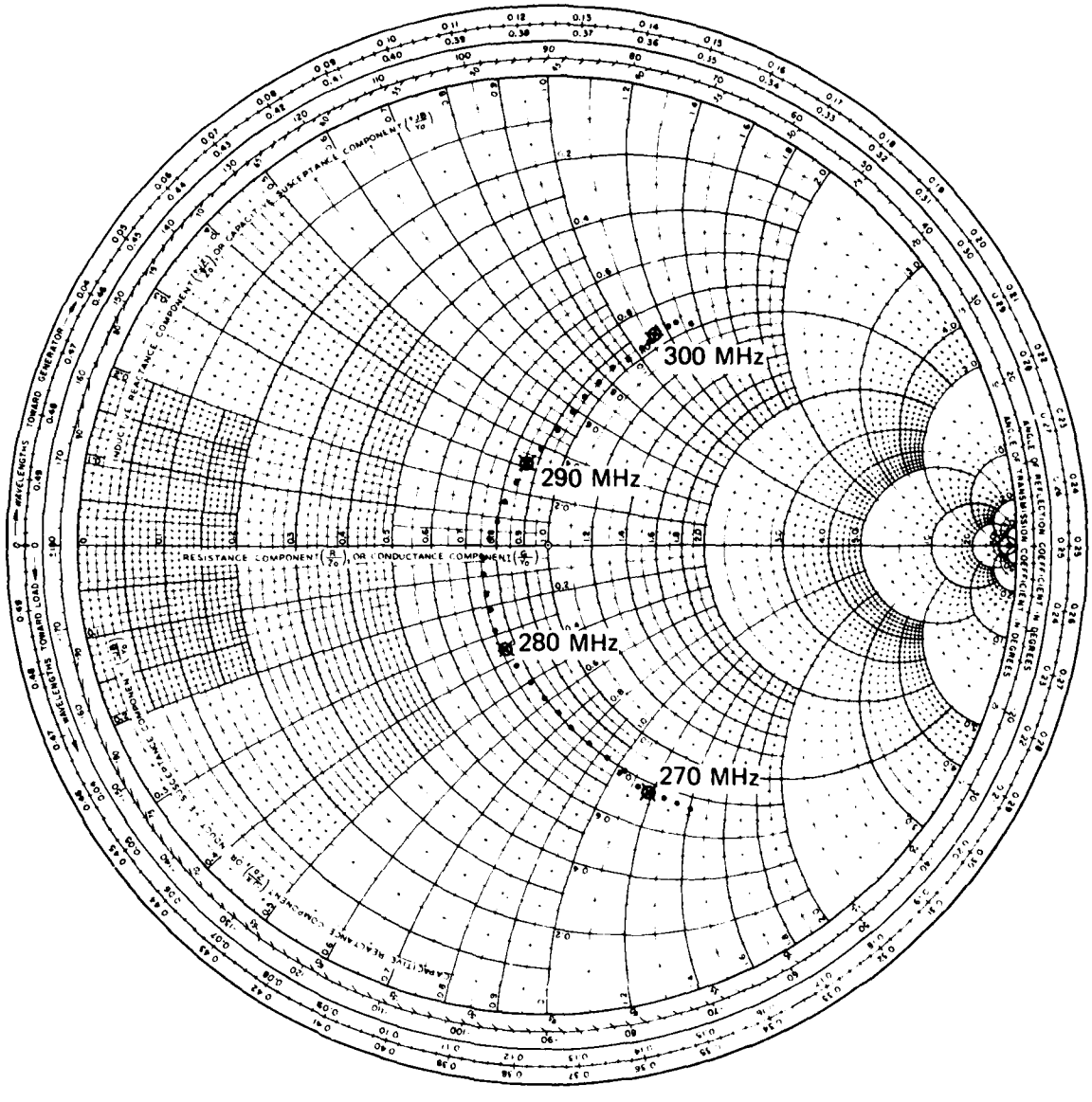

Fig. 4 Impedance of the experimental tape helix (normalized to 50 Ω).

THE JOHNS HOPKINS UNIVERSITY
APPLIED PHYSICS LABORATORY
LAUREL MARYLAND

CHARGE COUPLED DEVICE/ SURFACE ACOUSTIC WAVE DEVICE SURVEY

Charge Coupled Device (CCD) technology exhibits rapid growth in both the commercial and government-funded (NASA and DoD) areas. Commercial developments are primarily oriented toward audio delays, television imagers, and TV video storage devices. NASA programs are heavily weighted toward large-area imaging arrays for space telescopes. DoD programs cover a broad range from low-light level imagers to high-speed video storage devices. A fairly broad survey of the industrial and government-funded laboratories indicates that the commercial market will not provide off-the-shelf CCD's suitable for advanced radar signal processing, but that reliance on custom development will be necessary to apply this technology to the radar signal processor as a viable alternative to current techniques.

Problem

Recent advances in CCD technology and the appearance on the commercial market of moderate speed video CCD's for television use have indicated a potential application in radar signal processors. Experience to date, however, has indicated that the commercially available devices do not perform well enough to fulfill the requirements of advanced radar signal processing.

Objective

In order to assess the apparent potential of this technology for radar signal processing, it was necessary to determine the driving forces in both the civilian (commercial) sector and in the military laboratories that will contribute to the advancement of this technology. One of the prime concerns was to determine if growth in the commercial sector would result in the ready availability of standard integrated circuits suitable for sophisticated radar signal processing, much as happened with digital and analog integrated circuits, or whether reliance on custom design will be necessary as with surface acoustic wave (SAW) devices.

Approach

An APL task force of eight members, including the Project Engineer, was formed. Meetings with nine representatives of a broad spectrum of both military and industry laboratories were organized. The meetings were set up geographically so that, wherever possible, a single two-man team could cover a number of sources in a single trip. In addition to the meetings, one team was able to attend the Government Microcircuits Application Conference during the

same trip on which three industry representatives were interviewed. Each team was to write a detailed trip report to the task force, which would delineate its findings and serve as a baseline reference for the final report from the task force.

Progress

All interviews have been completed and reports on these trips received by the Project Engineer. The final report covering CCD's is being written at this time.

Indications are that, at least for the foreseeable future, the commercial sector will provide little in the way of standard CCD's suitable for anything more than limited-bandwidth, limited-delay radar video processing. This is because the main commercial application of video CCD's lies in television, with its limited bandwidth requirements. Two manufacturers have TV line store registers and one of these plans to introduce a TV frame store device within the next 12 to 18 months. Other commercially available devices include a chirp Z transform filter, a 32-bit tapped analog delay, and a dual addressable analog storage register. All the devices suffer from the common problem of limited bandwidth (less than 5 MHz).

A number of manufacturers are placing great emphasis on CCD imaging arrays. Fairchild and RCA are both deeply involved in developing solid-state television camera systems based on CCD imagers. RCA hopes to produce a $500 color camera for consumer use. Fairchild and Texas Instruments (TI) are likewise involved in large-scale imagers destined for both military and space applications. TI is currently producing an 800 × 800 array for the Galileo program. Here again, transfer rates (and as a result signal bandwidth capabilities) are limited; however, the development of area array fabrication techniques with high uniformity will provide spin-off benefits in area storage technology.

Of the commercial, non-military-funded organizations, only Fairchild indicated that it might be amenable to undertaking custom, high speed, wide bandwidth CCD development. Westinghouse Defense and Electronic Systems Center is currently working in this area (800 MHz sample rate) and indicated a willingness to undertake a development contract to produce a device suitable for a specific advanced radar signal processing task.

All of those interviewed indicated that the greatest effort is being expended in enhancing materials and fabrication techinques so as to improve critical parameters such as charge transfer efficiency (currently pushing 99.999%), fast interface and bulk charge

traps, and signal injection and extraction linearity. Of these, the first presents the greatest limitation to successful fabrication of long serial registers.

Other device organizations such as the serial-parallel-serial device, similar to an area imaging array without optical input, could, if properly designed, provide the large storage capacity required of many signal processor tasks without the severe limits imposed by current transfer inefficiencies. As an example, a 20 000 cell serial register with a 99.99% transfer efficiency will exhibit a charge dispersion so severe that the peak response will be 14 dB down with the pulse spread over 9 cells at the 10% points. On the other hand, a 100 × 200 array store will exhibit a peak only 0.5 dB down with a -25 dB trailing cell response. These effects are shown in Fig. 1.

With an array store organization, efforts could be concentrated on improving the other parameters so as to improve device linearity and signal-to-noise ratio. Concurrent with these efforts, improvements in device bandwidth and clock rates would have to be sought.

These goals do not seem to match those of the commercial organizations such as Fairchild or Reticon; however, they do seem to fit into the scheme of those organizations receiving DoD funding, such as Westinghouse.

TI is also working in the area of surface acoustic wave devices. Its efforts are directed toward custom-made monofunction devices matched to a particular task such as fixed or programmable transversal filters. Similarities in function exist for SAW's and CCD's, the prime differences being time delay, bandwidth, and the product of these two. The delineation of these functional areas is shown in Fig. 2. Indications are, however, that the T_d - BW product for CCD's may expand due to the work currently underway in area imagers that will impact advancement of area array storage CCD's. If this is the case, CCD's will encroach further on the area previously reserved for SAW devices.

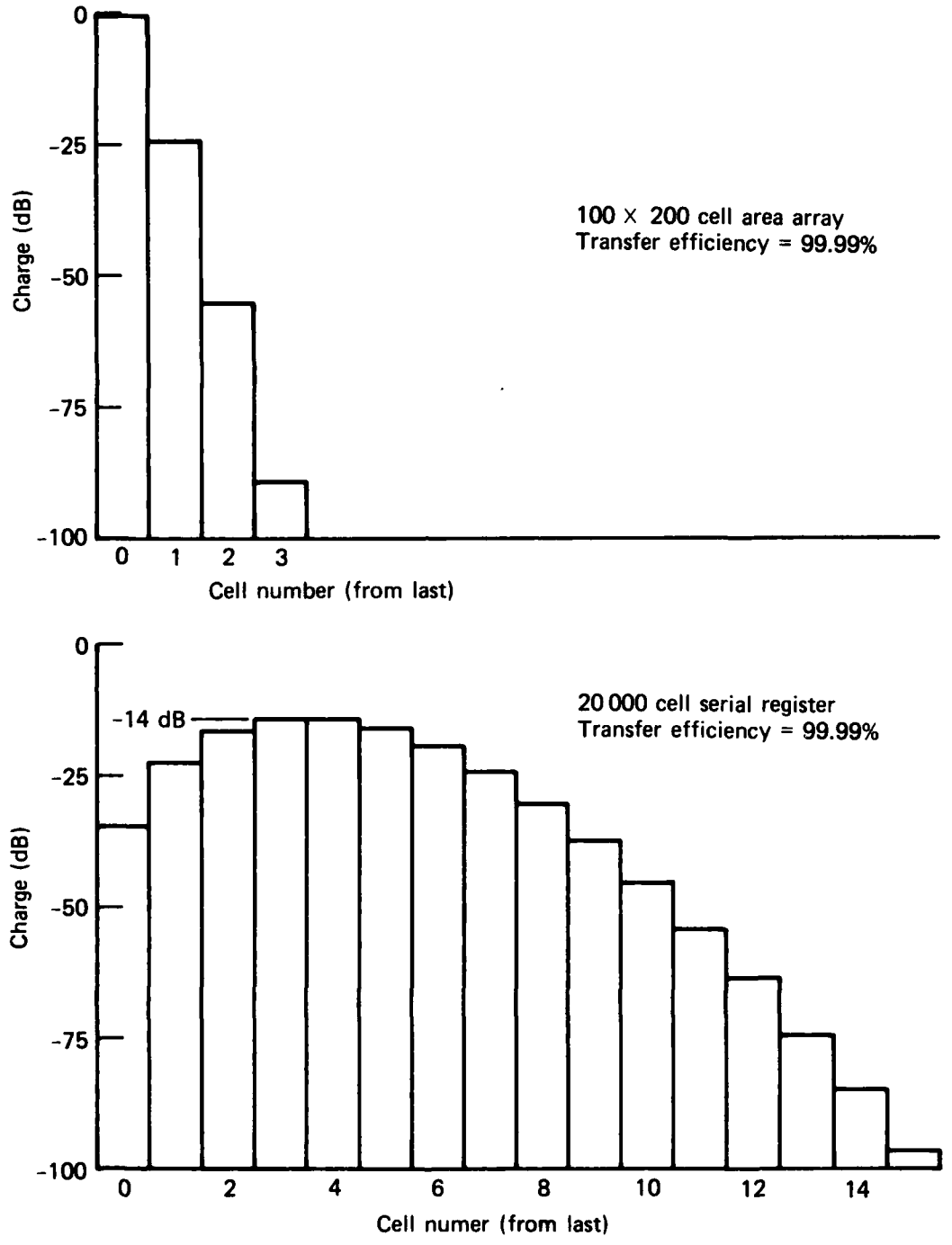

Fig. 1 CCD charge dispersion effects.

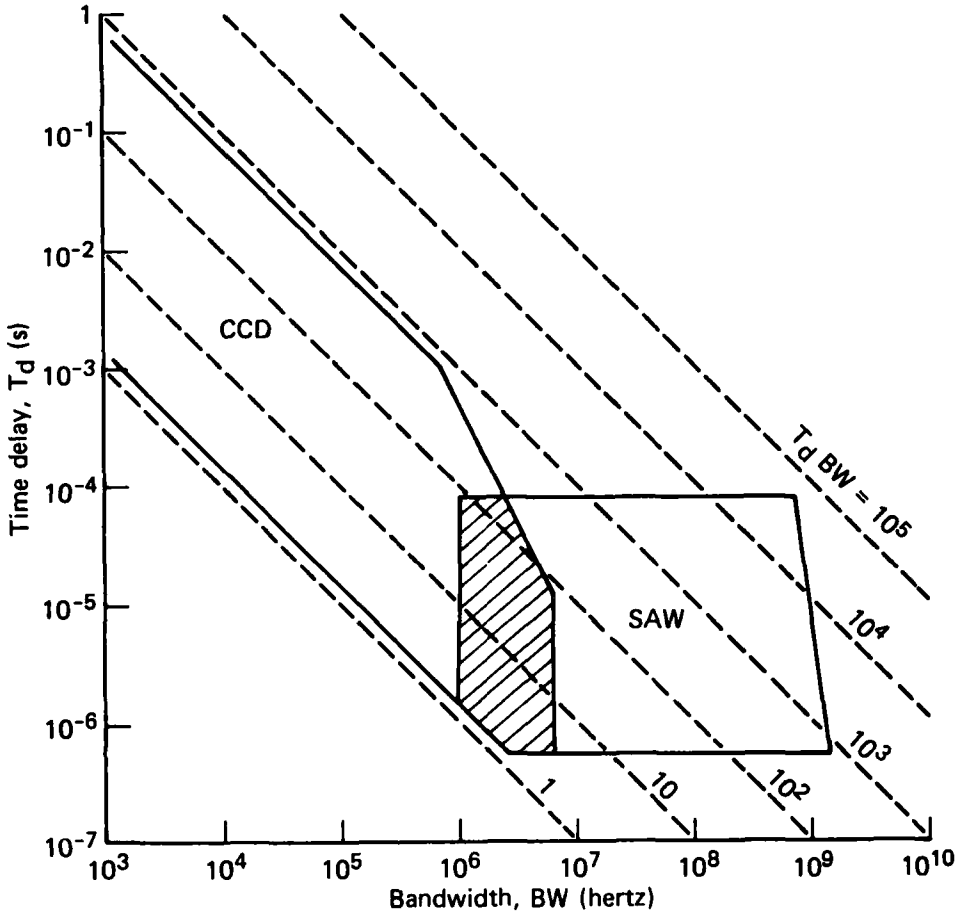

Fig. 2 CCD/SAW time bandwidth products.

Principal Investigator: W. H. Zinger, senior engineer, Radar Systems Group of the Fleet Systems Department.

THE JOHNS HOPKINS UNIVERSITY
APPLIED PHYSICS LABORATORY
LAUREL, MARYLAND

DISTRIBUTED PROCESSING SURVEY

A designer's handbook to aid the weapon system designer select advantageous distributed processing architectures is outlined. A distributed processing system model is proposed that promises to achieve high survivability at a cost substantially lower than conventional redundant designs without imposing burdensome software constraints.

Problem

So that the U.S. Navy may capitalize on the potentially beneficial attributes of a decentralized computing system, a design must be arrived at from a myriad of alternatives. Many decisions will have significant bearings on the cost, performance, maintainability, extensibility, and serviceability of the ultimate system.

Measures that permit system operation despite hardware failures in the decentralized computer system are of particular interest to the Navy. In large centralized computer complexes, hardware failures are typically accommodated by using software that reconfigures the system into the available hardware. A decentralized system, on the other hand, must rely on different principles to accommodate hardware failures since its level of control is distinctly different from that of a centralized system.

Objective

This project has two distinct goals. The first is to outline a handbook that will assist system designers in making intelligent, informed decisions about distributed processing alternatives. The second is to design an innovative distributed processing system that will use an autonomous series of master and backup microcomputers to achieve high survivability of its computing elements. This design will realize its survivability at a cost substantially lower than conventional redundant designs without imposing burdensome constraints on application software development. Thus, the first goal has a generalized focus to assist system designers, while the second has a narrower focus directed toward the Navy's need for high survivability.

Approach

In order to properly address the distinct features of the two objectives, two parallel tasks will be undertaken.

The first objective will be approached by surveying known alternatives and identifying those features that will affect that particular design. A variety of design factors will be discussed and analyzed, including: functional partitioning, geographical distribution, degree of coupling, system control, degree of resource sharing, topology of the computing and application elements, bus structures, communication schemes, computer architectures, and software architectures. Automated information retrieval will be used where applicable. The end product will be a collection of design guidelines in the form of a designer's handbook to aid the weapon system designer in selecting the most favorable architecture for his application. The handbook will contain an extensive checklist of viable alternatives. Representative examples of distributed processing will also be given in detail.

In meeting the second objective, the design concept relies on a series of master and backup fault-tolerant microcomputers, each having identical, autonomous system software. The near-term technical approach is to investigate and develop the computer system hardware and software mechanisms necessary for a hypothetical three-task distributed system that will be highly survivable with a minimum of constraints on the application software.

Progress

To meet the first objective of this project, known existing alternatives for distributed weapons system design have been surveyed and an annotated bibliography in machine-readable form has been developed with over 100 entries at present (Ref. 1). In addition, several handbook outlines have been prepared (Ref. 2).

To meet the second objective, a design summary of a hypothetical three-task system has been prepared (Ref. 3) and about one-third of the hardware design has been completed.

In brief, a hypothetical three-task distributed processing system has been developed consisting of six Z80-based microcomputers, each with simulated fault tolerance. The first level of survivability in this design is accomplished by dynamic designation of task and backup microcomputers. At all times, three task microcomputers are designated to perform each of three separate tasks and are required to be available periodically for a confidence test. The other microcomputers assume a backup role unless they have already failed. The backup microcomputers are responsible for detection and resolution of system failures and the resumption of task execution of a failed or failing microcomputer. This is

accomplished by several methods. The backup microcomputers selectively monitor all of the microcomputers in the system, a confidence test is performed periodically on each microcomputer, and the system buses are monitored by the backup microcomputers for discrepancies.

Each backup microcomputer aids in the detection of two kinds of failures: Category 1 and Category 2. A Category 1 failure occurs when a correctable failure, such as an internal Hamming code error, has been detected and corrected by a particular microcomputer. After the detection of the failure, the backup microcomputer takes over the task of the failing microcomputer at a prespecified breakpoint with little or no interruption of the specific task. The backup microcomputer performs the task take-over by changing the mode of the failing task microcomputer and transferring the memory contents of that unit to its own local memory through direct memory access. This active transfer of function is possible since Category 1 failures occur in microcomputers that are still executing proper results but have lost all additional error correction reserves and have an uncertain error-free lifetime.

A Category 2 failure is an uncorrectable failure in which the task must be started from task software stored in the system's secondary nonvolatile memory. Category 2 failures include: activation of a Category 2 manual switch simulating either an internal Hamming code error detection that cannot be corrected or a failure of an internal voting element that compares the results of redundant microprocessors in a fault-tolerant microcomputer; failure of a confidence test performed by a backup microcomputer; bus discrepancies caused by a specific microcomputer; and a statement from an "intelligent" task sensor/weapon that the microcomputer is no longer performing its function correctly. A Category 2 failure necessitates an interruption and the complete reinitialization of a specific task. In extreme failure cases, where a microcomputer is distorting or inhibiting the operation of other task microcomputers, the failed microcomputer may be electrically isolated from the system buses and designated "dead" by command of a backup microcomputer.

The distributed processing system consists of two main system buses. The input/output (I/O) bus is implemented to interface to all of the I/O devices and is connected in common to all of the microcomputers. Communication between sensor/weapons and microcomputers and between microcomputers takes place over this bus. The bus passes asynchronous communication without priority and is designed primarily as an expedient implementation while maintaining a reasonably high bandwidth. Each microcomputer of the distributed processing system will be addressed through the I/O bus by a virtual

address. The virtual address is unique for each microcomputer and depends on its current status and task. When a microcomputer changes from a backup to a task microcomputer, the virtual address will also change. Corresponding task I/O devices also have a unique virtual address.

The second system bus is the memory bus and is used for failure resolution, microcomputer status, task initialization, and microcomputer-to-microcomputer bulk memory transfer. It is through the memory bus that direct memory access occurs between a backup and a task microcomputer after a Category 1 failure has been detected. The status and control information of each microcomputer is passed through the memory bus and is held in a specially designated area called "shared local memory." Shared local memory is a 256-byte common addressed block of memory that can be broadcast-written over the memory bus and locally read by each microcomputer over internal buses. Additionally, initialization or restart of a task is accomplished by transferring the task software from system secondary nonvolatile memory, through the memory bus, to the requesting microcomputer. The microcomputers are selected with a logical address when accessed through the memory bus. The logical address of any specific microcomputer never changes regardless of status of task.

Principal Investigators: S. A. Kahn, associate engineer, Computer Systems Group, R. L. Trapp, associate engineer, Electronic Design Group, and M. E. Schmid, associate engineer, and A. E. Davidoff, senior mathematician, Advanced Systems Design Group; all in the Fleet Systems Department.

References

1. S. A. Kahn, "Distributed Processing Bibliography," APL/JHU F3C-1-372, 21 Dec 1978.

2. S. A. Kahn, "Distributed Processing Outlines," APL/JHU F3C-1-382, 6 Feb 1979.

3. R. L. Trapp, M. E. Schmid, and A. E. Davidoff, "Exploratory Development Status: A Highly Survivable Distributed Processing Systems," APL/JHU F2F-2-220, 5 Feb 1979.

THE JOHNS HOPKINS UNIVERSITY
APPLIED PHYSICS LABORATORY
LAUREL MARYLAND

ENERGY CONVERSION

ULTRASONIC REMOVAL OF BIOFOULING

State-of-the-art technology for ultrasonic removal of biofouling accumulations is examined in the special context of heat exchangers. Experiments are defined to provide data prerequisites to the design of ultrasonic cleaning systems. Field data collected from a DOE project indicate that the method has merit. However, quantitative data on the cleaning mechanism for surface deposit removal are needed to permit design, cost, life, and damage factors to be evaluated.

Problem

This project supports the development of technology directed toward providing Navy, DoD, DOE, and civilian facilities with new energy sources, energy conversion devices (specifically including ocean thermal), and means for reducing energy usage (cf., e.g., Navy Energy Technology Task Area F57-571, YF54.593.012).

The basic problem is to determine a practical method for the removal of biofouling from the evaporators and condensers in Ocean Thermal Energy Conversion (OTEC) plant ships. These heat exchangers have large surface areas over which seawater flows to transfer heat from small temperature differences (4 to 7°C) between warm surface water and the working fluid in the evaporators or between cold seawater (drawn from 900 m depths) and the working fluid in the condensers. The heat exchanger surfaces are difficult to reach with mechanical cleaners. Ultrasonic cleaning appears desirable because of its simplicity, efficiency, and convenience. Since a significant degradation in heat transfer occurs in two to six weeks due to biofouling, in situ cleaning is necessary.

Objective

The specific objective is to explore the merits of the removal of biofouling from a model heat exchanger by ultrasonic radiation. The required radiation intensity (W/cm^2), exposure duration (15 to 30 s), and frequency (weekly or biweekly) of application to maintain a suitable seawater-side heat transfer coefficient are to be determined. Intensity is expected to be one to three times the cavitation threshold for a planar acoustic wave.

Approach

The use of ultrasonic radiation to clean biofouling from heat exchangers may provide a means of efficiently and economically

keeping large and complicated submerged heat transfer structures clear of biofouling. The application, however, requires an understanding of the mechanism of removal of surface contamination.

Progress

A rudimentary device was obtained at minimum cost from Alpha Ultrasonics and Electronics Corp. in the form of a 0.1 m^2 × 22 mm thick planar assembly of 12 disk-type piezoelectric elements, with a generator-oscillator supplying power at a frequency near 20 kHz. The output was just marginal in producing cavitation near the radiating surface, and it was anticipated that effective cleaning would occur over only the adjacent tube surfaces, as shown in Fig. 1. Measurements of the acoustic output and its operation are given in Ref. 1. This unit was used on the OTEC heat transfer model setup at Keahole Point, Hawaii, where water pumped from the ocean was allowed to flow continuously over the 0.1-m-OD aluminum tubes of the model. Heat transfer through the cylindrical aluminum walls was measured at one to three week intervals before and after application of the ultrasonic cleaner. In addition, aluminum samples were set out in Chesapeake Bay and Florida coastal waters to accumulate biofouling for laboratory studies of cleaning action.

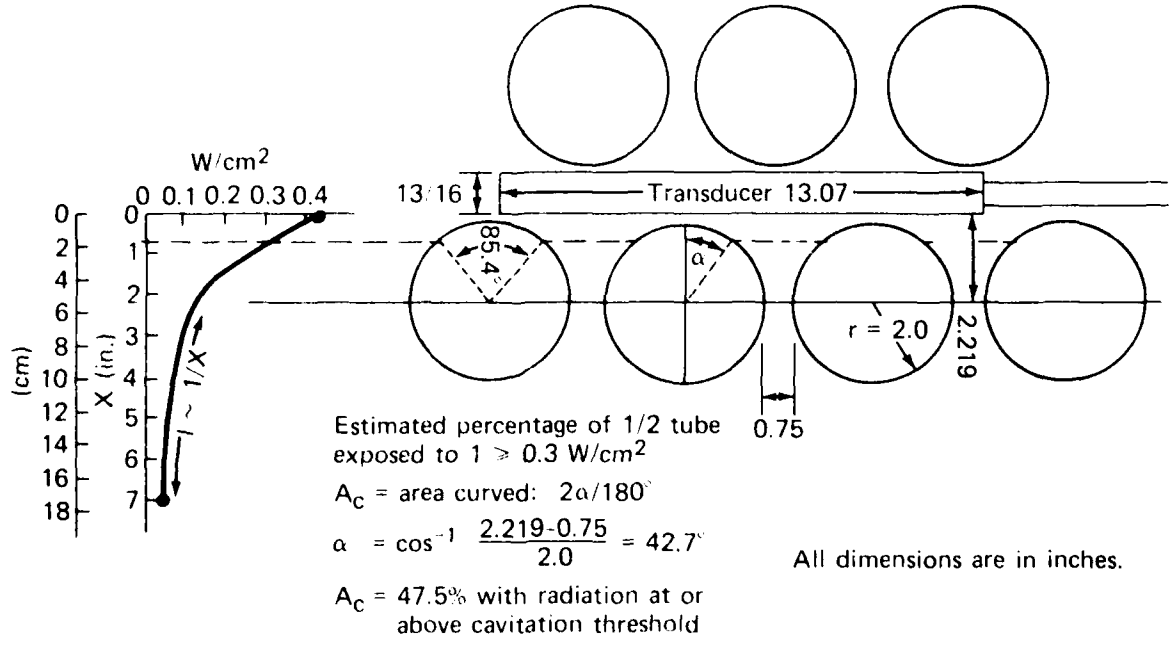

Fig. 1 Geometry of ultrasonic cleaning device inserted into tube bank.

Results from the application of the cleaner at Keahole Point indicate that a resistance coefficient of 0.0002 to 0.0003 Btu^{-1} hr ft^2 °F (4 - 6 × 10^5 W^{-1} m^2 °C) was maintained over an 82 day test period.

Analysis of the biofouling specimens accumulated over periods of two to three weeks in the Chesapeake Bay showed that they had green filamentary biofouling, including some slime and in one case some scale, a barnacle, and some worms. All the material was cleaned in a small tank capable of producing ~ 0.5 W/cm^2 at 42 kHz; the slime and filamentary biofouling were removed in 15 to 30 s, up to 2 min was required to remove the scale and worms, and the barnacle was not removed.

In brief, the use of ultrasonic cleaning was found to have potential merit. A more definitive assessment will require obtaining more extensive biofouling samples and using a wider range of intensities for the cavitational flows to determine as precisely as possible the requirements for biofouling removal. The cleaning process must be tested and analyzed in more detail to determine the mechanism by which collapse of cavitation bubbles is effective with this kind of organic surface accumulation. Much higher intensities for short periods are feasible, which may provide a means to remove chemically bonded layers. Equipment providing a wider range of acoustic intensities and calibrated surface contamination indexes are needed to quantify and compare results.

Principal Investigator: Dr. F. K. Hill, Supervisor, Fluid Mechanics Group of the Aeronautics Division.

Reference

1. F. K. Hill, "Ultrasonic Cleaner for Biofouling Cleaning at Keahole Point, Hawaii," APL/JHU BFM-1077, 2 Oct 1978.

THE JOHNS HOPKINS UNIVERSITY
APPLIED PHYSICS LABORATORY
LAUREL, MARYLAND

AIRBREATHING COMBUSTION

NONINTRUSIVE INSTRUMENTATION

Nonintrusive optical techniques for measuring velocity, temperature, species concentration, and soot particle size are examined and developed for use in the analysis of hot, reacting, fuel-rich ramjet combustor exhaust flow. A computer evaluation of light transmission and scattering techniques for particle sizing indicates that a two-angle, perpendicularly polarized light-scattering method will give reasonable accuracy for particulate sizes up to approximately 10 μm.

Problem

New diagnostic measurement techniques are required to define more completely the aerothermochemical flowfields in the combustors and exit nozzles of advanced airbreathing propulsion systems. Some of the new combustion systems to be developed will include mixed cycles in which very fuel-rich flows may be generated for subsequent burning to completion with additional air in supersonic flowfields. A thorough understanding of the character and properties of such flows (i.e., species concentration, temperature, and velocity) is required to know how to alter engine design to solve problems that may arise and thereby to meet cycle performance and structural integrity objectives. Nonintrusive optical techniques have been developed under controlled laboratory conditions to make these measurements, but the techniques must be adapted to the harsh nonlaboratory environment of the engine test stand.

Objective

The objective is to outline a program to develop nonintrusive measurement techniques that can be used in the development of sophisticated high-speed air-breathing engines. This will include both the adaptation of techniques now used in laboratory experiments to the typical engine test cell environment and the development of data acquisition and reduction procedures consistent with either on-line or quick-turn-around requirements inherent in engine development testing.

Approach

Flow parameters of particular interest include the identity, number density, velocity, and temperature of the species. In principle, all of these characteristics may be determined by nonintrusive optical methods. Candidate techniques to identify the combustion products include laser absorption and light scattering, and visible emission measurements. The first question that must be answered is what is the number density and size distribution of

particles produced by the combustion process. If the number density is found to be sufficiently small, the particles will be of little apparent importance in subsequent experiments and in the interpretation of the results. Conversely, if large numbers of particles occur, light scattering from them may interfere with other potential diagnostic methods. Accordingly, initial experiments must be planned to ascertain the number density and size of particulates as well as the identity of certain molecular species.

After these studies have provided an initial picture of the milieu, appropriate instrumentation methods must be evaluated to measure velocity, temperature, and more detailed species information.

Progress

A two-phase program has been developed. In phase I, to be discussed below, a small-scale combustion apparatus will be fabricated and installed at the Propulsion Research Laboratory at APL to provide an initial picture of the milieu, and new diagnostic measurement techniques will be evaluated. In phase II, the appropriate techniques would be applied to the full scale integral-rocket dual-combustion ramjet (IRDCR) combustor apparatus.

The small-scale combustion apparatus is illustrated in Fig. 1. Atmospheric air will be heated in a nickel storage heater to temperatures as high as 1500°F before passing into the small subsonic combustion chamber. Fuel will be supplied by a simple system consisting of a fuel tank pressurized by instrument air, a flowmeter, and pintle nozzles. A sonic blast tube attached to the combustor will provide a flow that simulates the gas generator discharge in an IRDCR engine. The initial testing and evaluation of the nonintrusive instrumentation will be made downstream of the sonic discharge in the optical test section (see Fig. 1).

The first question to be answered concerns the importance of light scattering from particulates. Computer assessment of the light transmission and scattering methods for determining particle size and concentration was carried out based on the Mie theory of light scattering from spherical particles with complex refractive index, m. The values of m for particles generated by JP-5 and Shelldyne-H fuels are not yet known. However, for these computational studies it was assumed the unknown value falls within the known values of hydrocarbon/air flames shown in Table 1. Studies were made of the two-wavelength transmission technique, the perpendicular polarized light-scattering technique, and the two-angle light-scattering technique.

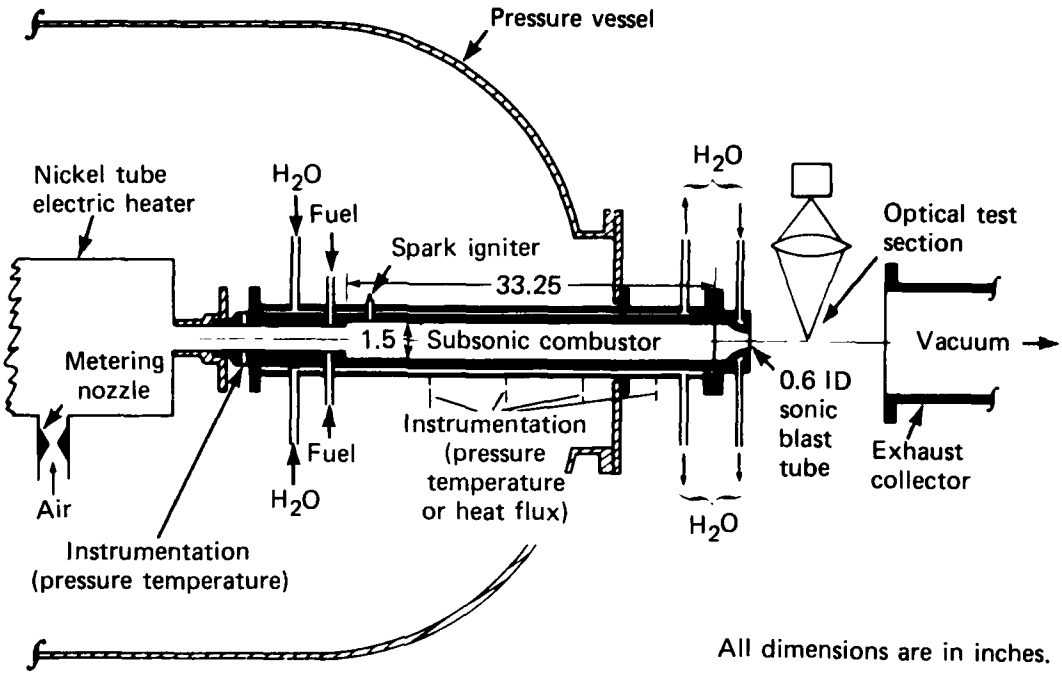

Fig. 1 Test apparatus for nonintrusive diagnostic instrumentation.

Table 1

Soot characteristics.

Reference	Flow	Particle diameter (μm)	Refractive index (i)
1	Air-hydrocarbon mixture (primarily C_4H_{10})	0.12 - 0.2	1.91 - 0.675 (assumed)
2	Air-propane	0.1	1.9 - 0.35 1.6 - 0.6
	Air-acetylene	0.013 - 0.025	2.0 - 0.5

In the two-wavelength transmission technique, the ratio of light transmission at two wavelengths, λ_1 and λ_2, can be related to the scattering efficiency factor, Q_λ, to define particle diameter, D_p, for a defined m. It was found that, for the range of m values of interest, only particles having $D_p \leq 0.4$ μm could be resolved without ambiguity (i.e., without having multiple values of D_p for a given $Q_{\lambda_1}/Q_{\lambda_2}$).

The second technique for determining D_p is based on the measurement of the parallel and perpendicular polarized intensities, $I_{||}$ and $I_{\perp}$, of a laser light at selected scattering angle, θ. For certain ranges of D_p, the ratio of $I_{||}/I_{\perp}$ can determine the actual value of D_p, but sensitivity and ambiguity remain as problems. However, analysis demonstrates that the ratio of intensities of perpendicularly polarized light at different scattering angles, $I_{\perp}\theta_2/I_{\perp}\theta_1$, can be used to resolve D_p. Figure 2 shows this ratio for four sets of angles as a function of $\alpha = \pi D_p/\lambda$ and, in turn, of D_p for three laser sources. In general, ambiguity exists at large α's if θ is large, but the curve for $I_{\perp}8°/I_{\perp}4°$ suggests that this technique may be quite attractive to use to determine D_p.

A second set of preliminary experiments will be direct spectral measurements of visible and infrared emission. Spectral measurements will be made in real time using an optical multichannel analyzer, borrowed from the Research Center. The experiments should allow identification of the presence of certain species, such as C_2, CN, CH, NH, and NO, and give a qualitative measure of their concentration. Aside from species identification, the measurements will be important in determining spectral regions where the background emission may interfere with other techniques such as Raman or laser fluorescence. An important element of these tests will be the comparison of these species with those obtained from the instream probes and off-line analysis by gas chromatography.

After these studies have provided an initial picture of the medium, it should be possible to instrument the system to measure velocity, temperature, and more detailed species information. In principle, the velocity associated with the combustion product can be measured by standard laser doppler velocimetry methods. However, the effectiveness of this technique will depend on the optical

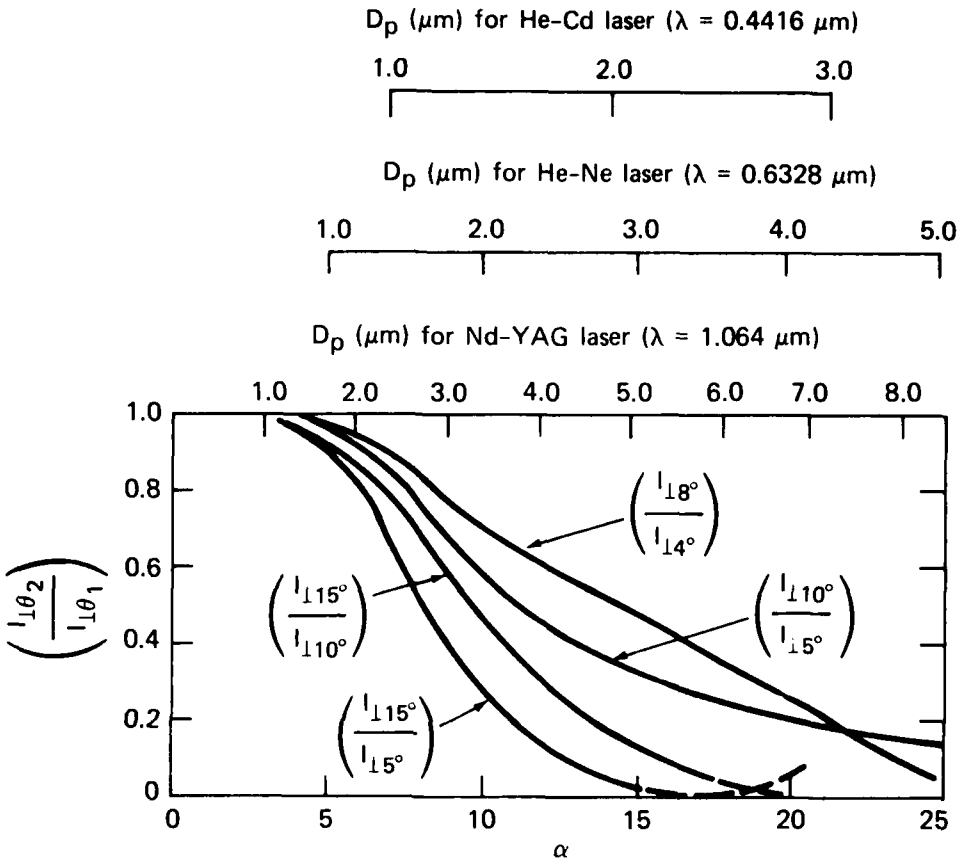

Fig. 2 Ratios of intensities of perpendicularly polarized light for four combinations of scattering angles.

quality of the medium; for example, nonuniformities caused by temperature, concentration gradient, and/or turbulence could present serious problems. The significance of these factors will be evaluated during the preliminary experiment.

Both temperature and detailed species information can be obtained using laser Raman techniques. The temperature measurements could be conducted using either spontaneous Raman or coherent anti-stokes Raman (CARS) methods. Spontaneous Raman scattering may be a desirable approach if particulate levels are low and background emission does not interfere. CARS may be an important alternative for major species concentrations, although its sensitivity is expected to be inadequate for measurement of low concentration species. Of course, the dephasing effects of turbulence will have to be evaluated.

The small-scale combustor setup shown in Fig. 1 is currently being assembled in test cell 5 at the Propulsion Research Laboratory. To permit safe "hands-on" operation of the diagnostic instrumentation, the pressurized portion of the system is enclosed in a pressure vessel. After completing the setup, several check-out tests of the combustor must be made to define its operating envelope and to ascertain its performance in attaining equivalence ratios between 1 and 4.5. This would then be followed by the basic optical experiments described previously to arrive at the most feasible diagnostic instruments for the large-scale hypersonic ramjet combustor flow studies.

Principal Investigators: Dr. F. S. Billig, Assistant Division Supervisor, and Dr. R. E. Lee, senior engineer, Aeronautics Division.

References

1. M. Kunugi and H. Jinna, "Determination of Size and Concentration of Soot Particles in Diffusion Flames by a Light-Scattering Technique," 11th International Symposium on Combustion, Combustion Institute, 1966, pp. 257-266.

2. S. Chippett and W. A. Gray, "The Size and Optical Properties of Soot Particles," Comb. Flame, Vol. 31, 1978, pp. 149-159.

THE JOHNS HOPKINS UNIVERSITY
APPLIED PHYSICS LABORATORY
LAUREL MARYLAND

SPACE TECHNOLOGY

MAGSAT II

The advent of the space shuttle opens up the possibility of orbiting drag-free satellites that can operate at extremely low altitudes (as low as is permitted by thermal considerations). Such satellites have many applications and can perform a variety of scientific missions. The possibilities are shown to be sufficiently attractive to warrant a design and cost study to consider this specific alternative in future mission planning. The work outlined here is described in more detail in two other documents (Refs. 1 and 2). Further work is now sponsored by NASA.

Problem

Drag-free satellites orbiting at very low altitudes could provide data unobtainable with present satellites that would greatly improve knowledge of the earth's atmosphere and crust. Until now, however, low orbiting drag-free satellites were not considered feasible because of the large propellant requirements. This study examines the utility and advantages of very-low-altitude DISCOS-equipped satellites in view of the impending availability of the space shuttle.

Objective

The objective of this work then is to explore the use and advantages of the drag-free technique for substantially lowering the minimum altitude that can be considered practicable for satellite orbits. Such low orbits would minimize launch costs and provide low-altitude observations of the earth's surface or of subjects in close proximity to the earth's surface.

Approach

In 1972, the Triad satellite, designed by APL with the assistance of Stanford University, fully demonstrated the operability and practicality of the drag-free satellite subsystem DISCOS (disturbance compensation system). This system provided controlled propulsion to precisely counteract the effects of drag and radiation pressure, resulting in a purely ballistic trajectory. Because of very large propellant requirements, the use of such a system at extremely low altitudes had not been seriously contemplated. Since the space shuttle is ideally suited for launching extremely heavy payloads, very-low-altitude orbits for DISCOS will soon become feasible and cost effective. Thus, a conceptual design study of the use and advantages of DISCOS on very-low-altitude satellites is appropriate.

Progress

There are two quite different reasons for using very-low-altitude satellites. The first is that the choice of a lower altitude allows an increase in satellite weight and completeness of the experiment that can be carried. The second reason is to obtain observations by the satellites of the earth's surface or things in close proximity to the earth's surface (e.g., the atmosphere or the earth's crust). Thus, Air Force classified surveillance satellites, which are concerned with photographic observation of the earth's surface, are flown at very low altitudes.

Figure 1 shows how the accuracy of gravity field measurements improves as altitude decreases. The curves were computed for a gravity satellite system comprised of two low-orbiting, DISCOS-equipped satellites. Table 1 summarizes some of the potential applications for satellites at very low altitudes.

Table 1

Applications of very-low-altitude satellites.

Discipline	Some objectives
Geodesy	Improved gravity field model Refined gravity anomaly measurement
Oceanography	Sea surface topography
Geomagnetism	Improved geomagnetic field model Refined magnetic anomaly measurement Updated and improved magnetic charts
Aeronomy	Upper atmosphere and ionosphere density and composition Ozone measurements (drag mechanisms)
Meteorology	Cloud height measurements
Geology	Stereoscopic photography

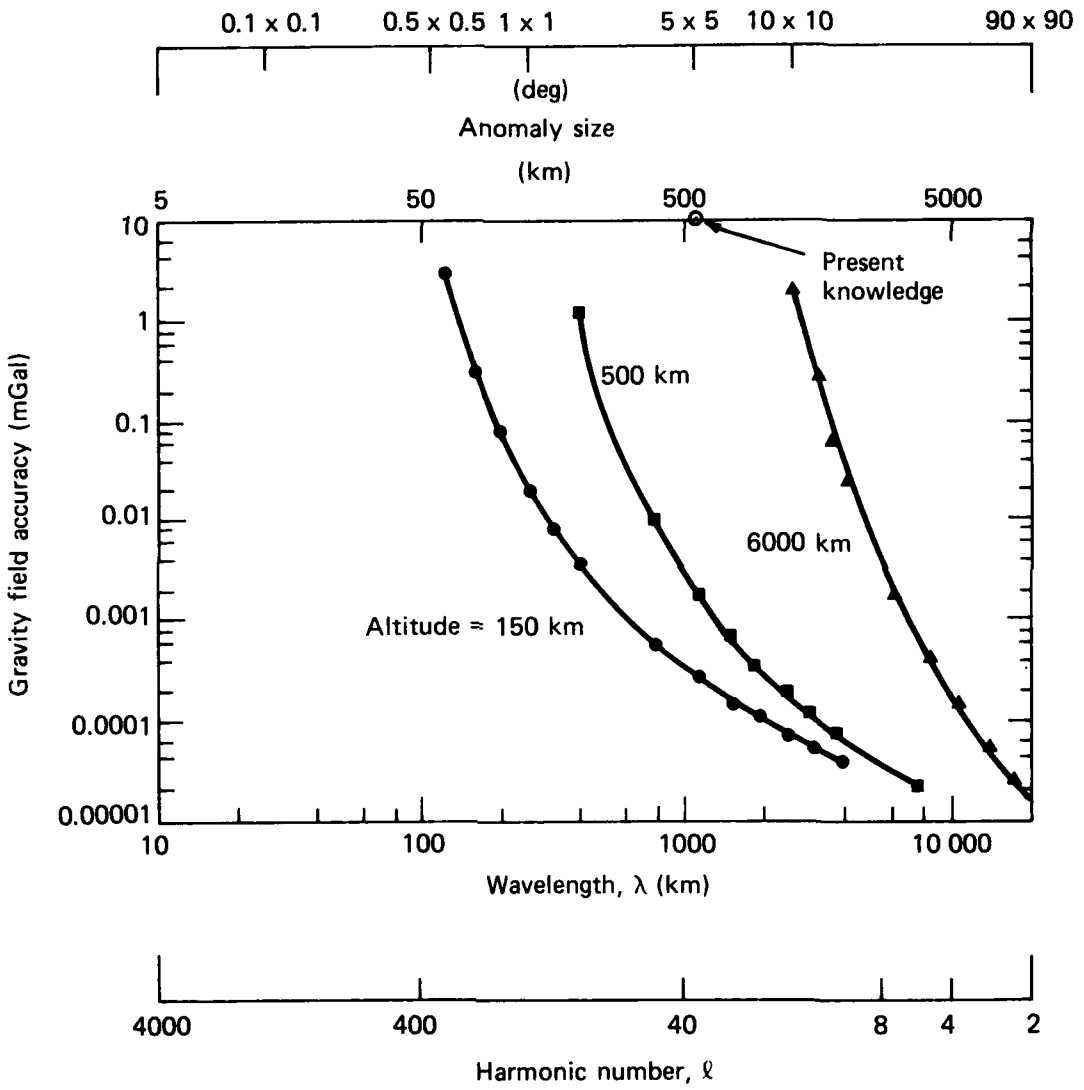

Fig. 1 Anticipated accuracy for recovery of the gravity field by a gravity satellite system comprised of two low-orbiting DISCOS satellites.

The shuttle can place DISCOS satellites in extremely low-altitude orbits. The lower limit on altitude appears to be set by thermal considerations. Figure 2 shows the stagnation temperature that must be withstood by a heat shield for prolonged periods as a function of altitude. It would appear that an altitude of 125 km would result in stagnation temperatures of about 300°C at the air density resulting from solar maximum. It might not be too difficult to design an appropriate heat shield to make 125 km practicable. Increasing the altitude to 150 km reduces this temperature to the neighborhood of a relatively comfortable 100°C, which is unquestionably practicable. Thus, the feasibility of a DISCOS is considered for operation at the low-altitude limits of 125 to 150 km. It is seen from Fig. 3 that the propellant weight (hydrazine) lies in the range of 200 to 1000 kg/mon/m^2 of satellite cross section. A selection of a preferred configuration would, of course, require a detailed design study that we have not yet carried out, but a conceptual design of a shuttle-compatible low-altitude DISCOS satellite clearly indicates its feasibility.

Attitude stabilization has been chosen to be earth-pointing, since the primary reason for using a very-low-altitude orbit is observation of the earth or something closely tied to the earth (e.g., the magnetic field). However, gravity gradient stabilization, which is frequently preferred for earth-pointing satellites, has not been adopted since it usually results in a high drag configuration. Instead, we assume the type of momentum wheel stabilization used in the earth-pointing mode of SAS-C and adopted for Magsat. This allows horizontal spacecraft flight to achieve minimum drag.

The conceptual design (Fig. 4) shows two fuel tanks symmetrically displaced with respect to the DISCOS sensor. This makes it possible for the DISCOS sensor to remain at the center of gravity of the spacecraft as the fuel is used in equal quantities from each tank. Provision is made for an altimeter dish to provide a follow-on for SEASAT and for an extendible boom to carry instruments (such as magnetometers) that must be distant from the main spacecraft (follow-on Magsat mission). The configuration shown provides for 2000 kg of hydrazine, providing 2 1/2 months of performance at 125 km altitude or 20 months at 150 km. The spacecraft could readily be designed to permit refueling from later shuttle flights. As seen in Fig. 5, a pair of such satellites would constitute only a modest fraction of a shuttle payload.

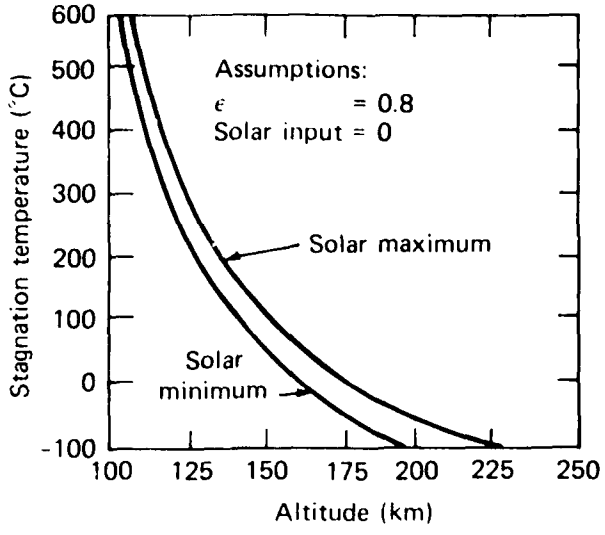

Fig. 2 Effect of altitude on stagnation temperatures.

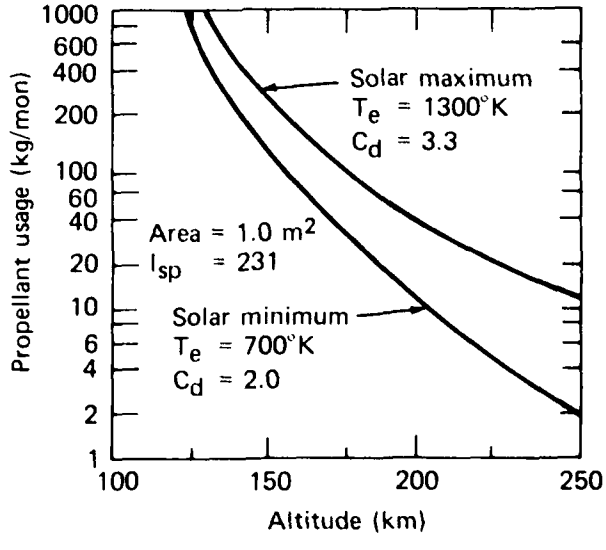

Fig. 3 Propellant usage for satellites at very low altitude.

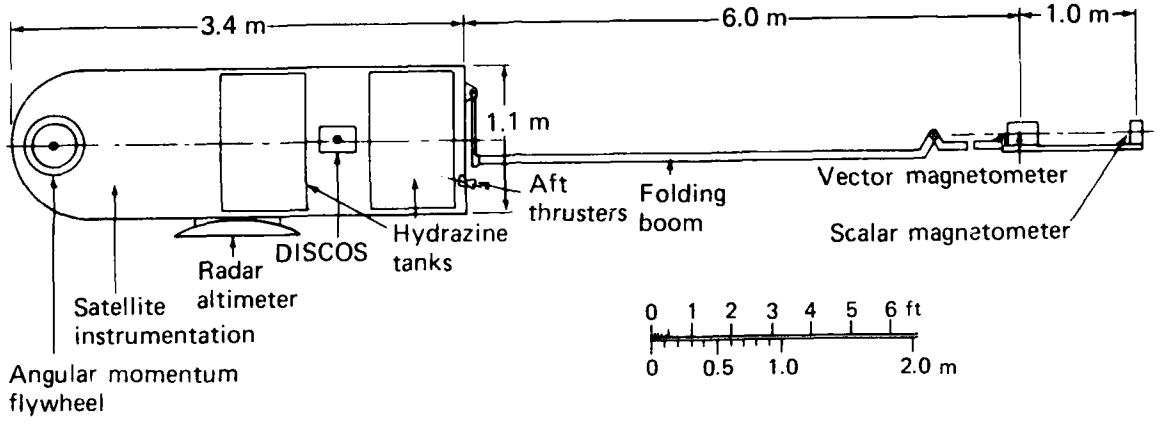

Fig. 4 Geodetic mapping satellite (GEOMAPSAT) conceptual design.

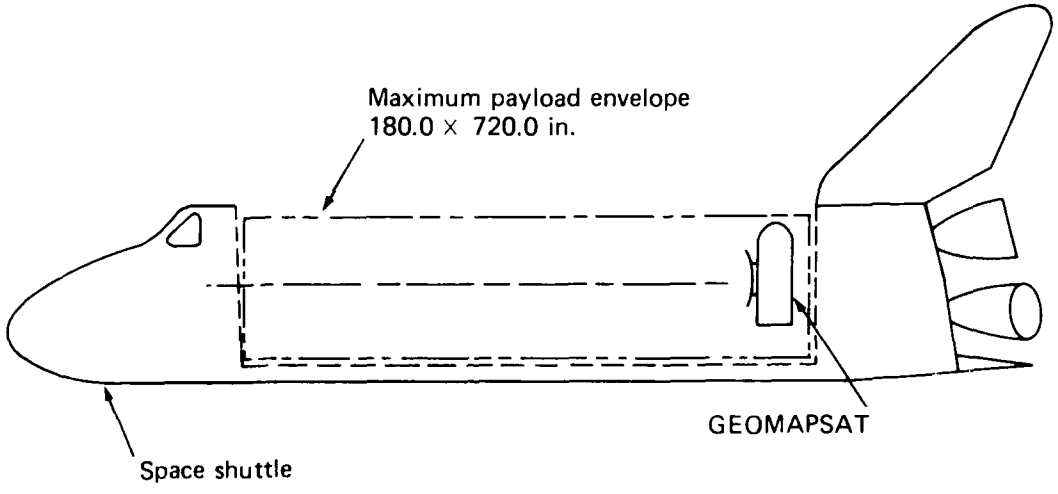

Fig. 5 Space shuttle launch configuration for GEOMAPSAT.

THE JOHNS HOPKINS UNIVERSITY
APPLIED PHYSICS LABORATORY
LAUREL, MARYLAND

Principal Investigators: R. E. Fischell, Chief Engineer and Assistant Space Department Head, Dr. V. L. Pisacane, Assistant Branch Supervisor, Space Department Space Sciences Branch, and Dr. R. B. Kershner, Space Department Head and Assistant Director of the Laboratory.

Publications

1. R. E. Fischell and R. B. Kershner, "Very Low Altitude Drag-free Satellites," APL/JHU CP 065, Jan 1979.

2. R. E. Fischell and V. L. Pisacane, "New Satellite Techniques for the Determination of the Gravity Field," Proceedings, 9th GEOP Conference, Ohio State University, 4 Oct 1975 (to be published).

SEASAT SYNTHETIC APERTURE RADAR IMAGING

APL is among three early recipients of SEASAT synthetic aperture radar (SAR) data. To evaluate the performance of the system, we seek to derive image quality descriptors from the information inherent in the images themselves. Preliminary results confirm the half-power resolution of 25 m in range and 15 m in azimuth expected for multilook imagery with an averaged value of 2.5 images. The results also show a dynamic range at least 20 dB on the second generation films delivered to us.

Problem

To be scientifically useful, SEASAT imagery must be of known quality. That is, its resolution, modulation transfer function, dynamic range, linearity, noise level, and scattering statistics must be known. Nominally, these descriptors should be known from the overall system model used in the design. However, due to uncertainties, and possible aging, the system must be examined independently in actual operation. One way of doing this is to compare images with known ground truth information to derive system degradation and response directly. This is, however, expensive, and ground truth measurements are often difficult to interpret in terms of radar scattering properties.

Objective

Since the SAR imagery contains inherent information concerning system performance, our goal is to extract this information to infer system performance parameters from it. The descriptors we wish to derive include: resolution in range and azimuth, dynamic range, linearity, noise level, and scattering statistics.

Approach

Resolution and modulation transfer function can be determined in two ways, first, by studying the two-dimensional autocorrelation function of imagery from uniform scattering or sharp feature areas and, second, by locating simple known features, such as edges and linear patterns, in the imagery and integrating the image intensity parallel to them so as to form a one-dimensional cross section normal to them.

Scattering statistics can be studied by forming histograms of intensity from uniformly scattering regions and fitting hypothesized probability distributions. Deviations from the fitted distribution indicate nonlinearities, dynamic range, and noise level.

Progress

Preliminary results confirm the expected 25 m resolution in range and 15 m in azimuth. An autocorrelation function computed from imagery of a uniformly scattering area of the Salton Sea shows this directly in Fig. 1. This is confirmed by edge and line resolution studies, such as the one shown in Fig. 2 for the edge between two agricultural fields near the Salton Sea. The edge lies roughly parallel to the satellite track, so that the 25-m half power resolution in the range direction is displayed.

Figure 3 is a histogram study of coherent scattering from the Salton Sea. A Rayleigh distribution is shown for comparison. A dynamic range of about 20 dB is indicated in the early phases of this investigation.

Further evaluation of the SEASAT SAR system is needed, using a larger imagery data base. Resolution should be further evaluated by correlation studies of images of the corner reflector array in Goldstone, California, and the recovery and enhancement of ocean waves should be investigated.

Principal Investigator: Dr. A. D. Goldfinger, senior physicist, Space Analysis and Computation Group of the Space Department.

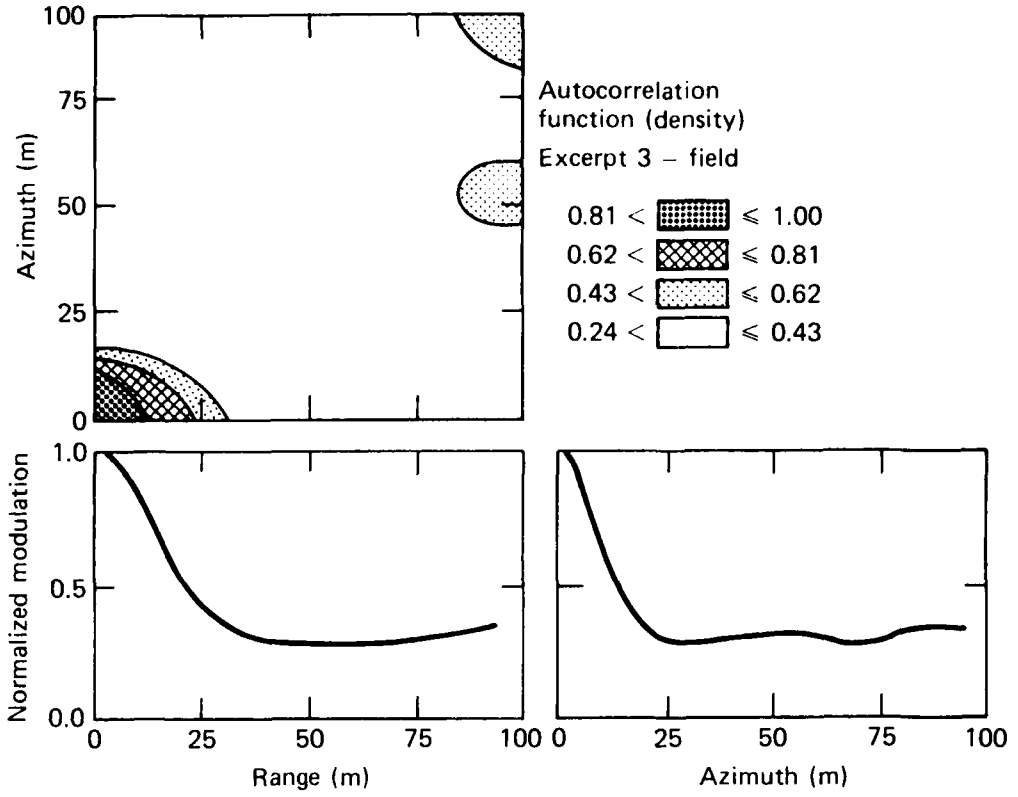

Fig. 1 Measured autocorrelation function from SEASAT-A SAR, Salton Sea (7 Jul 1978).

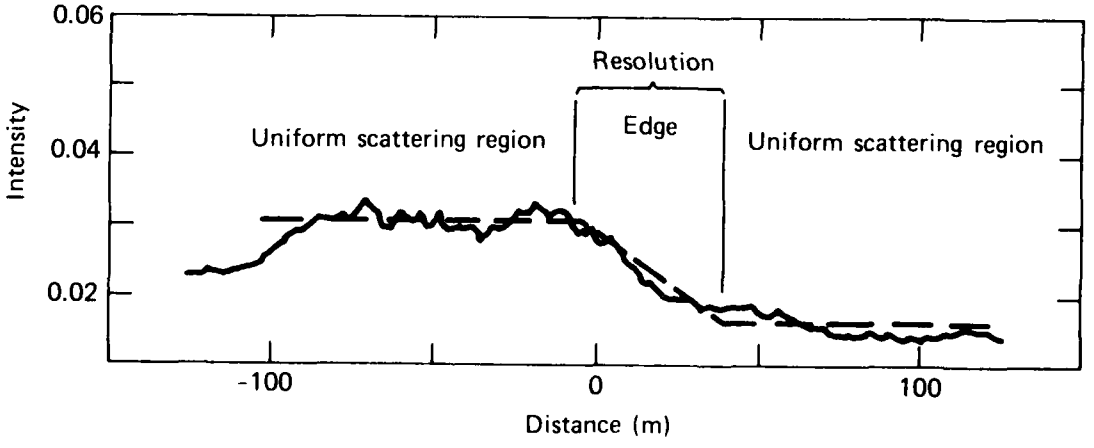

Fig. 2 Edge resolution study (agricultural area).

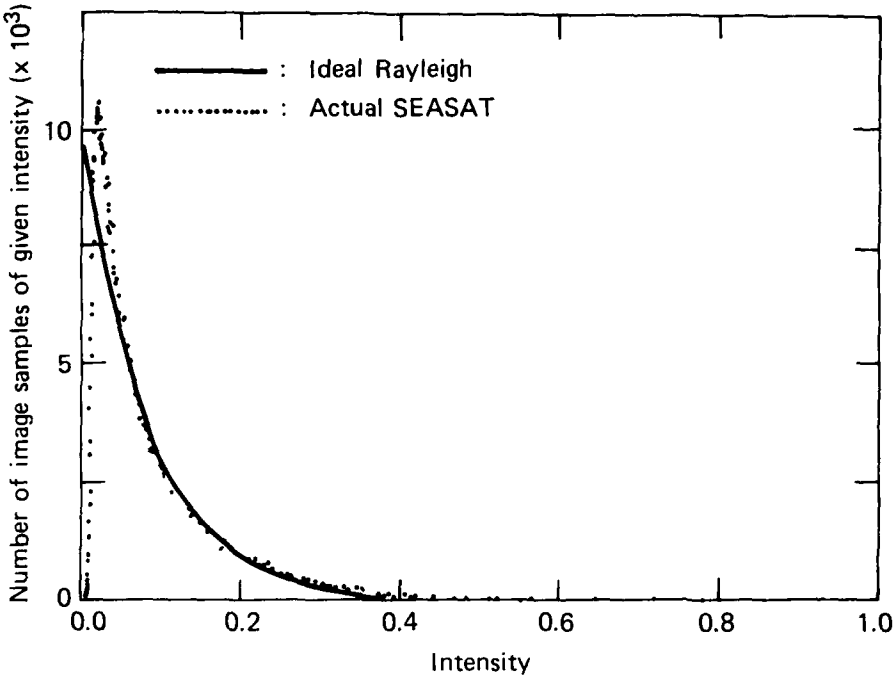

Fig. 3 Salton Sea dynamic range study, Excerpt 1.

INITIAL DISTRIBUTION EXTERNAL TO THE APPLIED PHYSICS LABORATORY*

The work reported in SR 79-2 was done under Task X8 of Contract N00024-78-C-5384 with the Department of the Navy.

ORGANIZATION	LOCATION	ATTENTION	No. of Copies
DEPARTMENT OF DEFENSE			
Harry Diamond Lab.	Washington, DC 20438	A. Renner, 1040	1
DDC	Alexandria, VA 22314		12
Department of the Navy			
Assistant Secretary, R&D	Washington, DC 20350		1
Office of Assistant Secretary, R&D	Washington, DC 20350	Dr. R. Hoglund	2
		Dr. T. Jacobs	1
Director of Navy Technology	Washington, DC 20360	Dr. J. Probus	1
Commands			
NAVMATCOM	Washington, DC 20360	Dr. T. Horwath	1
NAVSEASYSCOM			
Commander	Washington, DC 20360	SEA-00	1
Assistant Deputy Dir./Tech. Dir. R&T	Washington, DC 20360	SEA-003	1
Chief Engineer	Washington, DC 20362	SEA-00E	1
	Washington, DC 20360	SEA-62	1
	Washington, DC 20360	SEA-0253W	1
	Washington, DC 20360	SEA-61R/62R	1
	Washington, DC 20360	SEA-06	1
NAVAIRSYSCOM	Washington, DC 20360	AIR-310B	1
Offices			
Naval Research	800 N. Quincy St.	ONR-420	1
	Arlington, VA 22217	ONR-470	1
NAVPRO	Laurel, MD 20810		1
Defense Contract Audit Agency	Laurel, MD 20810		1
Laboratories			
Naval Research Lab.	Washington, DC 20390	NRL-6000	1
Naval Surface Weapons Center	White Oak, MD 20910	Commanding Officer	1
Naval Weapons Center	China Lake, CA 93556	Commanding Officer	1
Naval Ocean Systems Center	San Diego, CA 92152	Commanding Officer	1
Naval Underwater Systems Center	New London, CT 06920	Commanding Officer	1
Naval Coastal Systems Laboratory	Panama City, FL 32401	Commanding Officer	1
Naval Air Development Center	Johnsville, PA 18974	Commanding Officer	1
Department of the Army			
USA Electronics Command	Ft. Monmouth, NJ 07703	Proj. Mgr., NAVCON	1
USA Research Office	Physics Dept. Box CM, Duke Station Durham, NC 27706	Dr. C. Boghosian	1
Department of the Air Force			
Deputy Chief of Staff, R&D	Washington, DC 20330	LGEN A. D. Slay	1
Office of Scientific Research	Washington, DC 20330	Dr. Max Swerdlow	1
HQ ASD	Wright-Patterson AFB	C. H. Marshall, ASD/RWDE	1
Avionics Lab., Guid. and Nav. Anal. Office	Wright-Patterson AFB		
L. G. Hanscom Field	Dayton, OH Bedford, MA 01730	J. W. Chin, NVA/666A L. Higginbotham, ESD/DCL Stop 43	1 1
AFOSR	Bolling AFB Washington, DC 20338	Dr. W. Lehmann	1

Requests for copies of this report from DoD activities and contractors should be directed to DDC, Cameron Station, Alexandria, Virginia 22314 using DDC Form 1 and, if necessary, DDC Form 55.

*Initial distribution of this document within the Applied Physics Laboratory has been made in accordance with a list on file in the APL Technical Publications Group.

INITIAL DISTRIBUTION EXTERNAL TO THE APPLIED PHYSICS LABORATORY*

ORGANIZATION	LOCATION	ATTENTION	No. of Copies
U.S. GOVERNMENT AGENCIES			
Department of Transportation			
US Coast Guard	Washington, DC	GD/TP 53	1
NASA	Washington, DC 20546	Code RRC	1
		Code RT-6, Res. & Tech.	1
National Science Foundation	1800 G St., N.W.	Dr. R. Silberglitt	1
	Washington, DC 20550	Dr. H. W. Etzel	1
		Dr. W. E. Wright	1
		Dr. T. Kitchens	1
EPA	Research Triangle Park Durham, NC 27711	Dr. D. Cahill	1
UNIVERSITIES			
JHU Center for Metro. Planning and Research	Shriver Hall Baltimore, MD 21218	J. Fischer, Dir.	1
CONTRACTORS			
Woods Hole Oceanographic Institution	Woods Hole, MA 02543	Paul Fye, Dir.	1

*Initial distribution of this document within the Applied Physics Laboratory has been made in accordance with a list on file in the APL Technical Publications Group.

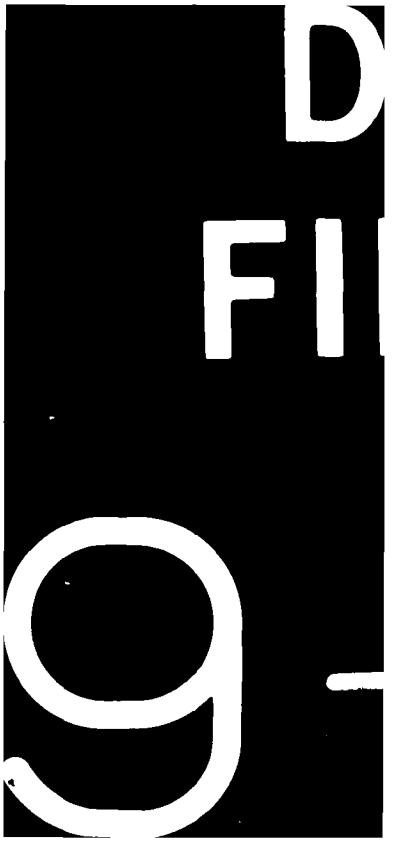
D
FI
9